Red Cedar River, Menomonie, WI

CE-QUAL-W2 – Water Quality Model

July 2019

US Army Corps of Engineers ®

Prepared by:
U.S. Army Corps of Engineers
St. Paul District
180 Fifth Street East, Suite 700
St. Paul, Minnesota 55101-1678

Table of Contents

1 Introduction 6
2 Background (Red Cedar River, Tainter Lake and Lake Menomin) 6
2.1 Study site 6
2.2 Objectives 8
3 CE-QUAL-W2 Model Development 8
3.1 CE-QUAL-W2 Model Background 8
3.2 Model Bathymetry 9
3.3 Dam Outlet Structures (Menomonie Hydroelectric Project and Cedar Falls Hydroelectric Project) 14
3.3.1 Cedar Falls Hydroelectric Project 14
3.3.2 Menomonie Hydroelectric Project 15
3.4 Boundary Conditions 16
3.4.1 Flow 16
3.4.2 Temperature 18
3.4.3 Water Quality 20
3.4.4 Meteorological Data 31
4 CE-QUAL-W2 Model Performance 31
4.1 In-Pool Data 31
4.2 Model Calibration / Validation Approach 32
4.2.1 Flow/Water Surface Elevation 34
4.2.2 Water Temperature 35
4.2.3 Water Quality Calibration 44
5 Limitations 71
6 Conclusions 71
7 Acknowledgements 71
8 References 72

Table of Figures

Figure 1. Station locations. HR = Hay River at Wheeler, WI, RCRin = Red Cedar River at Colfax, WI, RCRout = Red Cedar River at Menomonie, WI, TL = Tainter Lake, ML = Menomin Lake. 7
Figure 2. Red Cedar River CE-QUAL-W2 Segments overlaid on 2008 USDA Farm Service Agency Imagery for Dunn County, WI 10
Figure 3 Red Cedar River Segments 11

Figure 4 CE-QUAL-W2 layers for Tainter Lake (Branches 1 and 2, Normal Pool elevation in blue - 265.8 m, USGS Datum) 12
Figure 5. Tainter Lake Volume-Depth Curves, Model vs. Observed (Courtesy of Sean Hartnett, Univ. of Wisconsin, Eau Claire) 12
Figure 6. CE-QUAL-W2 layers for Lake Menomin (Branches 3 and 4, Normal Pool elevation in blue - 248.11 m, USGS Datum) 13
Figure 7. Lake Menomin Volume-Depth Curves, Model vs. Observed (Courtesy of Sean Hartnett, Univ. of Wisconsin, Eau Claire) 13
Figure 8. Cedar Falls Hydroelectric Project. 14
Figure 9. Menomonie Hydroelectric Project. Picture downloaded on 4.17.2019 at https://mapio.net/pic/p-89858029/ 15
Figure 10. 2014-2018 Average Monthly Discharge vs. period of record at Red Cedar River at Menomonie, WI. Monthly mean in ft3/s (Calculation Period: 1907-07-01 -> 2018-05-31). 2018 data may still be considered provisional by the USGS. 16
Figure 11. Branch 1 inflows (yellow line) - Red Cedar River near Colfax, WI (05367500), branch 2 inflows (blue line) - Hay River near Wheeler, WI, (05368000), intervening flows (red line), Cedar Falls and Menomonie Dam releases (green line) - Red Cedar River at Menomonie (0536900) 17
Figure 12. Estimated discharge from Cedar Falls Dam separated into penstock discharge (red) and tainter gate discharge (blue) 18
Figure 13. Estimated discharge from Menomonie Dam separated into penstock discharge (red) and tainter gate discharge (blue). 18
Figure 14. Observed Red Cedar River (05367500) temperatures (blue) and estimated daily temperature input file (red) for branch 1. 19
Figure 15. Observed Hay River (05368000) temperature (blue) and estimated daily temperature input file (red) for branch 2. 20
Figure 16. Bioavailable phosphorus concentration input time-series used for branch 1 compared to observed SRP measurements at Red Cedar River near Colfax, WI, (05367500). 21
Figure 17. Bioavailable phosphorus concentration input time-series used for branch 2 compared to observed SRP measurements at Hay River near Wheeler, WI, (05368000). 21
Figure 18. Ammonium concentration input time-series used for branch 1 compared to observed NHx measurements at Red Cedar River near Colfax, WI, (05367500). 22
Figure 19. Ammonium concentration input time-series used for branch 2 compared to observed NHx measurements at Hay River near Wheeler, WI, (05368000). 23
Figure 20. Nitrate-nitrite concentration input time-series used for branch 1 compared to observed NOx measurements at Red Cedar River near Colfax, WI, (05367500). 23
Figure 21. Nitrate-nitrite concentration input time-series used for branch 2 compared to observed NOx measurements at Hay River near Wheeler, WI, (05368000). 24
Figure 22. Observed and predicted DO concentrations using 86% saturated DO concentration assumption at Hay River near Wheeler, WI, (05368000). 25
Figure 23. Dissolved Oxygen concentration input time-series used for branch 1 compared to observed DO measurements at Red Cedar River near Colfax, WI, (05367500). 26
Figure 24. Dissolved Oxygen concentration input time-series used for branch 2 compared to observed DO measurements at Hay River near Wheeler, WI, (05368000). 26

Figure 25. TDS concentration input time-series used for branch 1 compared to observed conductivity X 0.67 at Red Cedar River near Colfax, WI, (05367500). 27
Figure 26. TDS concentration input time-series used for branch 2 compared to observed conductivity X 0.67 at Hay River near Wheeler, WI, (05368000). 27
Figure 27 Organic matter (LDOM, RDOM, LPOM and RPOM) concentration input time-series used for branch 1 at Red Cedar River near Colfax, WI, (05367500). 29
Figure 28. Organic matter (LDOM, RDOM, LPOM and RPOM) concentration input time-series used for branch 2 at Hay River near Wheeler, WI, (05368000). 29
Figure 29. Total algal biomass (diatoms, green algae, and blue-green algae) concentration input time-series used for branch 1 at Red Cedar River near Colfax, WI, (05367500) compared to chlorophyll a (mg/l x 30). 30
Figure 30. Total algal biomass (diatoms, green algae, and blue-green algae) concentration input time-series used for branch 2 at Hay River near Wheeler, WI, (05368000) compared to chlorophyll a (mg/l x 30). 30
Figure 31. 2014-2018 Hourly Air Temperature (blue), Dew Point Temperature(red) and Shortwave Radiation (green)reported from Menomonie Municipal Airport-Score Field (KLUM). 31
Figure 32. Observed (blue) and computed (red) water surface elevations for Tainter Lake. Mean absolute error (MAE) = ... 0.06 m, Percent bias (PBIAS) = 0.0071, Relative % Error (Rel%Err) = 0.0071 and Count = 41328 34
Figure 33. Observed (blue) and computed (red) water surface elevations for Tainter Lake. Mean absolute error (MAE) = ... 0.013 m, Percent bias (PBIAS) = -0.0001, Relative % Error (Rel%Err) -0.0001and Count = 41328 35
Figure 34. Modeled residence times for Tainter Lake (red) and Tainter Lake + Lake Menomin (blue). 35
Figure 35. Computed versus observed temperatures at station TL5 37
Figure 36 Computed versus observed temperatures at station TL5. Cont. 38
Figure 37 Computed versus observed temperatures at station TL5. Cont. 39
Figure 38 Computed versus observed temperatures at station TL5. Cont. 40
Figure 39 Computed versus observed temperatures at station TL5. Cont. 41
Figure 40. Computed versus observed surface temperatures at station ML1, MAE = 0.91, PBIAS = 2.3, Rel%Err = 2.1. 41
Figure 41 Computed versus observed temperatures at station ML5 – surface 42
Figure 42 Computed versus observed temperatures at station ML5 – 1m 42
Figure 43 Computed versus observed temperatures at station ML5 – 2m 42
Figure 44 Computed versus observed temperatures at station ML5 – 3m 43
Figure 45 Computed versus observed temperatures at station ML5 – 4m 43
Figure 46 Computed versus observed temperatures at station ML5 – 5m 43
Figure 47. Surface observed algal biomass versus modeled algal biomass at station TL5 45
Figure 48. Surface observed algal biomass versus modeled algal biomass at station ML5. 45
Figure 49. Tainter Lake 1-m observed chlorophyll a (red) versus model chlorophyll a (blue) based on estimated chlorophyll a to algal biomass ratios (ALCHLA). 49
Figure 50. Lake Menomin 1-m observed chlorophyll a (red) versus model chlorophyll a (blue) based on estimated chlorophyll a to algal biomass ratios (ALCHLA). 50
Figure 51. Tainter Lake (TL5) 1-m phosphate calibration, model (blue) vs. observed SRP (red). 53
Figure 52. Lake Menomin (ML5) 1-m phosphate calibration, model (blue) vs. observed SRP (red). 54

Figure 53. Tainter Lake (TL5) 1-m total phosphorus (TP) calibration, model (blue) vs. observed (red). 55
Figure 54. Lake Menomin (ML5) 1-m total phosphorus (TP) calibration, model (blue) vs. observed (red). 56
Figure 55. Tainter Lake (TL5) 1-m ammonium (NH4) calibration, model (blue) vs. observed (red). 57
Figure 56. Lake Menomin (ML5) 1-m ammonium (NH4) calibration, model (blue) vs. observed (red). 58
Figure 57. Tainter Lake (TL5) 1-m nitrate/nitrite (NO3/NO2) calibration, model (blue) vs. observed (red). 59
Figure 58. Lake Menomin (ML5) 1-m nitrate/nitrite (NO3/NO2) calibration, model (blue) vs. observed (red). 60
Figure 59. Tainter Lake (TL5) 1-m total kjeldahl nitrogen (TKN) calibration, model (blue) vs. observed (red). 61
Figure 60. Lake Menomin (ML5) 1-m total kjeldahl nitrogen (TKN) calibration, model (blue) vs. observed (red). 62
Figure 61. Tainter Lake (TL5) 1-m total organic carbon (TOC) calibration, model (blue) vs. observed (red). 63
Figure 62. Lake Menomin (ML5) total organic carbon (TOC) calibration, model (blue) vs. observed (red). 64
Figure 63. Observed (blue) vs model (red) dissolved oxygen profiles at TL5. 65
Figure 64. Observed (blue) vs model (red) dissolved oxygen profiles at TL5.Cont. 66
Figure 65. Observed (blue) vs model (red) dissolved oxygen profiles at TL5.Cont. 67
Figure 66. Observed (blue) vs model (red) dissolved oxygen profiles at TL5.Cont. 68
Figure 67. Observed (red) vs model (blue) dissolved oxygen at ML1 (1-m). 69
Figure 68. Observed (red) vs model (blue) dissolved oxygen at ML5. 70

Table of Tables

Table 1 Morphometric characteristics of Tainter and Menomin Lakes. 7
Table 2. Tainter and Menomin Lake sampling stations and water chemistry variable list. AlkPAct = alkaline phosphatase activity. 32
Table 3 Calibration Targets for Model State Variables 33
Table 4. Temperature calibration values 36
Table 5. Mean absolute error (MAE) for temperature 36
Table 6. Water quality calibration coefficients 46
Table 7. Organic matter calibration coefficients 47
Table 8. Nutrients calibration coefficients 47
Table 9. Sediment calibration coefficients 48
Table 10. Chlorophyll a calibration statistics. 48
Table 11. Calibration statistics for nutrients. 51
Table 12. Dissolved Oxygen MAE statistics for Tainter Lake and Lake Menomin. 52

1 Introduction

The Red Cedar River CE-QUAL-W2 (W2) model water quality assessment is summarized in this appendix. This appendix is meant to be a companion document to the Draft Limnological Conditions in Tainter and Menomin Reservoirs: Interim Report 2018, (Ref.1). This combined limnological and modeling study is part of a basin-wide project led by the West Central Wisconsin Regional Planning Commission (WCWRPC) to evaluate the significance of various social, economic and water quality aspects of the Red Cedar River to the surrounding region. Funding for this project is through a joint Wisconsin Department of Natural Resources' (WDNR) Lake Protection Grant and an US Army Corps of Engineers' (USACE) Section 22, planning assistance to states cost share agreement.

The central focus of this W2 model is to assist the Wisconsin Department of Natural Resources with refining phosphorus loading reduction scenarios for the Tainter Lake and Lake Menomin Phosphorus TMDL (Ref. 2) 1), which can be downloaded from the WDNR website at: https://dnr.wi.gov/water/wsSWIMSDocument.ashx?documentSeqNo=73903997.

Originally, the TMDL predicted flowage responses to reduce phosphorus loading with a 1-D trophic response model (USACE BATHTUB model, Ref.2) However, due to the unique dynamic relationships between hydrology, constituent loading, and cyanobacterial bloom development in the Tainter-Menomin system, a W2 model, which is developed specifically for reservoirs, was determined to be needed to more accurately predict current limnological conditions and project future responses to loading reduction. As a result, the modeling phase of this study was tasked to:

1. Develop a 2-D, laterally-averaged, CE-QUAL-W2 model for the Red Cedar River system from Tainter Lake to the outflow of Lake Menomin.
2. Calibrate the model to current loading and limnological conditions found in the monitoring phase of the study (2014-2018), and
3. Forecast river and reservoir responses to loading reducing scenarios that are needed to refine TMDL goals.

2 Background (Red Cedar River, Tainter Lake and Lake Menomin)

2.1 Study site

Tainter and Menomin Lakes are hypereutrophic impoundments of the Red Cedar River (Figure 1) and usually exhibit periods of massive cyanobacterial blooms during summer. Major tributary inputs to Tainter Lake include the Red Cedar River and the Hay River. Tainter Lake discharge and Wilson Creek flow into Menomin Lake. Hydraulic residence time is short at ~ 6 d and ~ 4 d for Tainter and Menomin Lake, respectively. Watershed land use is forest (51%), croplands (28%), grass-pasture (19%), and urban (2%). Tainter and Menomin dams are managed by Xcel Energy for hydropower and are operated as run-of-the-river (ROR) hydroelectricity with a maximum pool operation range of only 0.5 ft (Ref. 2). Morphometric characteristics are shown in Table 1.

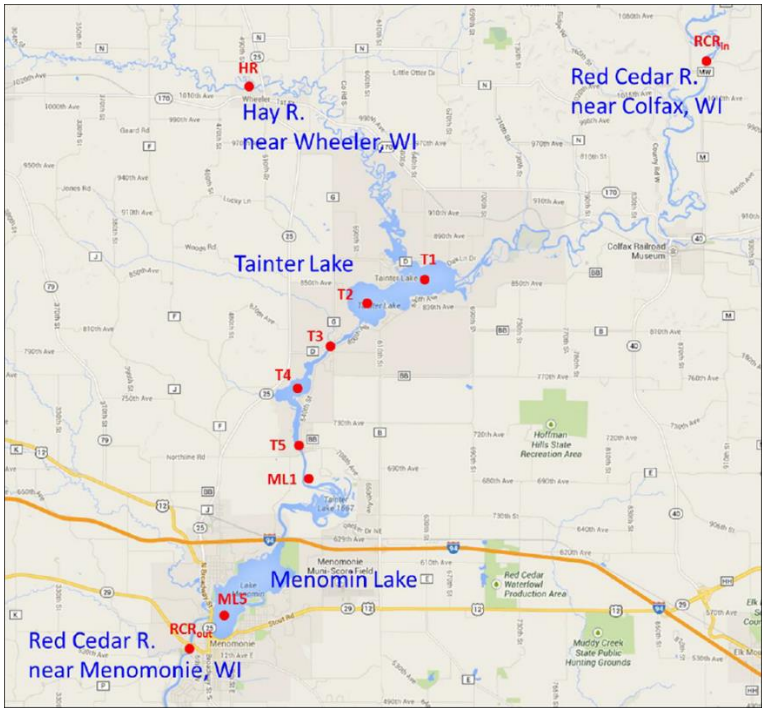

Figure 1. Station locations. HR = Hay River at Wheeler, WI, RCRin = Red Cedar River at Colfax, WI, RCRout = Red Cedar River at Menomonie, WI, TL = Tainter Lake, ML = Menomin Lake.

Substantiated by several years of monitoring (2014-2018) and analysis by this document's companion study (Ref.1), phytoplankton dynamics appears to be regulated in large part by high soluble P inputs from the watershed and hydrological advection. Periods of high watershed inflow results in rapid reservoir flushing and discharge of algae coupled with the input of high concentrations of soluble P (directly available for cyanobacterial uptake and growth). As inflows subsides and residence times increase, chlorophyll concentrations increase substantially in conjunction with declines in soluble P, suggesting cyanobacterial nutrient assimilation for growth. Soluble P appears to be driving cyanobacterial growth versus dissolved inorganic N in 2014-18. However, these summers were characterized by frequent periods of summer inflow and rapid flushing. More information is needed during periods of extended summer drought to better understand to role of available N and P on cyanobacterial blooms in these reservoirs (Ref.1).

Table 1 Morphometric characteristics of Tainter and Menomin Lakes.

Morphometric	English			Metric		
Variable	Tainter	Menomin	Unit	Tainter	Menomin	Unit
Surface area	1,608.2	1,325.4	ac	6,508,160	5,363,708	m^2
Volume	20,242.0	14,183.7	ac-ft	24,968,102	17,495,310	m^3
Mean depth	12.6	10.7	ft	3.84	3.26	m
Max depth	36.0	30.0	ft	10.97	9.14	m
Shoreline length	24.4	26.7	mi	39.30	42.97	km

2.2 Objectives

Tainter and Menomin Lakes are hypereutrophic impoundments located near the mouth of the Red Cedar River Watershed in Dunn County, WI. More information is needed to better understand and manage nutrient loading and reduce cyanobacteria blooms. The objectives of the Limnological research (Ref. 1) and the development of the W2 model were to:

• Examine interrelationships between hydrology, advection (horizontal water movement), residence time and riverine nutrient (primarily phosphorus) delivery on cyanobacteria dynamics and potential cyanotoxicity in wet versus dry years. Cyanobacterial bloom development in these reservoirs is driven by seasonal variations in nutrient loadings, bioavailability, and hydraulic residence time in relation to cell doubling time. High precipitation years provide abundant phosphorus loading but low hydraulic residence time, which can result in discharge of cyanobacteria before they can divide. Severe bloom development is reduced under this scenario. During lower flow years, summer nutrient loads followed by drought and longer hydraulic residence time sets the stage for severe bloom development because soluble phosphorus concentrations are high and cellular doubling time exceeds discharge rate. Nutrient loading stoichiometry (i.e., bioavailable nitrogen versus phosphorus) can also regulate growth limitation and cyanotoxicity. Long-term monitoring information is needed to better understand these interrelationships and predict the severity of blooms and potential cyanotoxicity.

• Determine Red Cedar and Hay River soluble phosphorus (bioavailable to algae) loading and concentration as a function of storm and base flow. Recent research on bedrock geology and groundwater in wells and has suggested that soluble phosphorus concentrations could be relatively high during base flow conditions in the Red Cedar River basin. A better understanding of soluble phosphorus dynamics and loading during base flow and storm flow conditions is needed to assess the significance of soluble phosphorus derived from surface runoff on agriculturally-managed land cover versus groundwater recharge through bedrock and soils naturally high in phosphorus. This information is needed to refine the TMDL and better target best management practices for remediation.

• Examine soluble P loading in relation to the TMDL. High soluble P loading and reservoir flushing complicate the original management goals. The primary objective has been to drive cyanobacteria toward phosphorus-limited growth. A better understanding of when cyanobacteria growth becomes limited by advection versus phosphorus or other nutrients is needed to refine TMDL goals.

A comprehensive research program was developed to examine nutrient and chlorophyll dynamics in Tainter and Menomin Lakes to address the above knowledge gaps and gain a better understanding of factors regulating cyanobacterial growth.

3 CE-QUAL-W2 Model Development

3.1 CE-QUAL-W2 Model Background

CE-QUAL-W2 (Ref.3) is a two-dimensional, longitudinal/vertical, hydrodynamic and water quality model for rivers, estuaries, lakes, reservoirs and river basin systems. Some of the model capabilities are hydrodynamic modeling, water quality, long term simulations, head boundary conditions, multiple branches, multiple water bodies, variable grid spacing, coupled water quality with hydrodynamics, auto stepping, restart provision, layer/segment addition and subtraction, multiple inflows and outflows, ice cover calculations, selective withdrawal calculations, and time-varying boundary conditions. The governing equations are laterally averaged which may be inappropriate for large water bodies exhibiting significant lateral variations in water quality.

CE-QUAL-W2 was originally developed in the 1970s as a hydrodynamic model, the Laterally Averaged Reservoir Model (Ref.10). Over the last several decades, the development of the model has been led by the USACE and Portland State University (PSU). CE-QUAL-W2 Version 4.1, released by PSU, was used in this project to model Tainter Lake and Lake Menomin.

Data requirements for successful application of the W2 model depends on the what parameters are simulated. At a minimum for flow and temperature models, data required includes: geometric data (bathymetric x-y-z data), initial conditions and boundary conditions (temperature and flow), hydraulic parameters, kinetic parameters, meteorological data and calibration data. Meteorological data includes: air temperature, dew point temperature (or relative humidity), wind speed and direction, cloud cover and/or solar radiation. If the model contains hydraulic structures, flow rates and locations of outflows are needed, including structure details for any dams, rating curves for the spillways, and water surface elevation data. For modeling water quality, all of the above data plus parameters involved with the fate and transport of the parameter(s) of interest is/are necessary. For this study, where the focus is on the interrelationships of certain reservoir characteristics (nutrient availability, residence time and temperature) with the dynamics of cyanobacteria blooms, boundary and calibration data of chlorophyll a, dissolved oxygen, organic matter and nutrients (e.g., NH_4, NO_3, and PO_4) were required.

3.2 Model Bathymetry

The model bathymetry files for Lake Menomin and Tainter Lake were developed from one meter GRID files with UTM projection created from 2005-2007 bathymetric surveys done by the University of Wisconsin, Eau Claire. The grid files were converted to 5-meter DEMs and combined into one TIN file that was loaded into Watershed Modeling System (WMS) v10.1 (Ref.9). Using the CE-QUAL-W2 WMS interface, the model computational grid was divided into two waterbodies (Tainter Lake and Lake Menomin) with two branches in each waterbody. Branch #1 represents the main branch in Tainter Lake from the upstream boundary of the Red Cedar River inflows down to the outlet of Tainter Lake at Cedar Falls Hydroelectric Dam. Branch #2 represents the lower section of the Hay River as it enters Tainter Lake. Branch #3 is the main branch of Lake Menomin from the outfall of Cedar Falls Hydroelectric Dam to the Menomonie Hydroelectric dam. Branch #4 represents the lower portion of Lake Menomin that is south of the reservoir's outlet. In total, there are 34 user-defined longitudinal segments of varying lengths (~100-1000m) in the model's computational grid, as shown in Figure 2 and Figure 3.

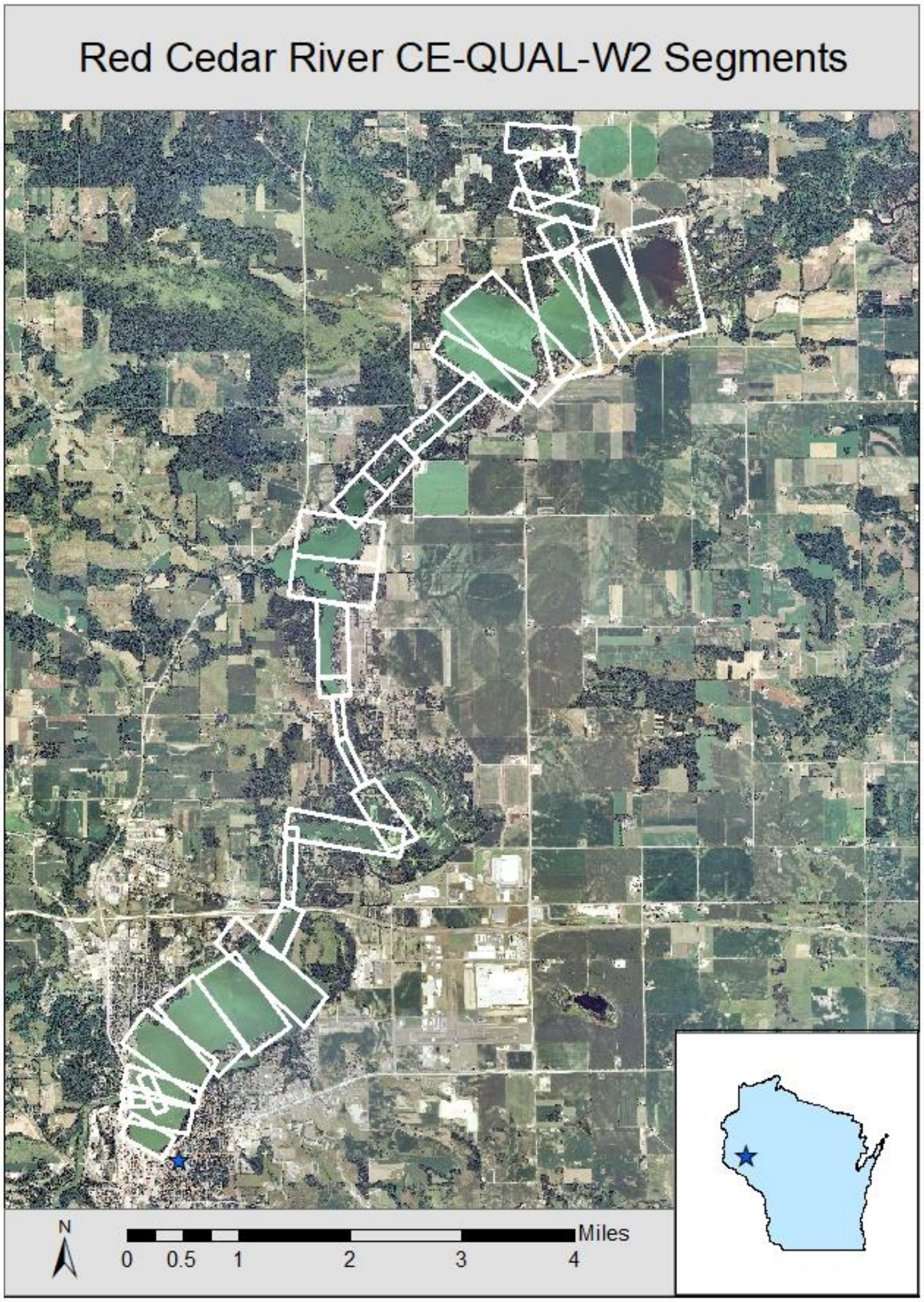

Figure 2. Red Cedar River CE-QUAL-W2 Segments overlaid on 2008 USDA Farm Service Agency Imagery for Dunn County, WI

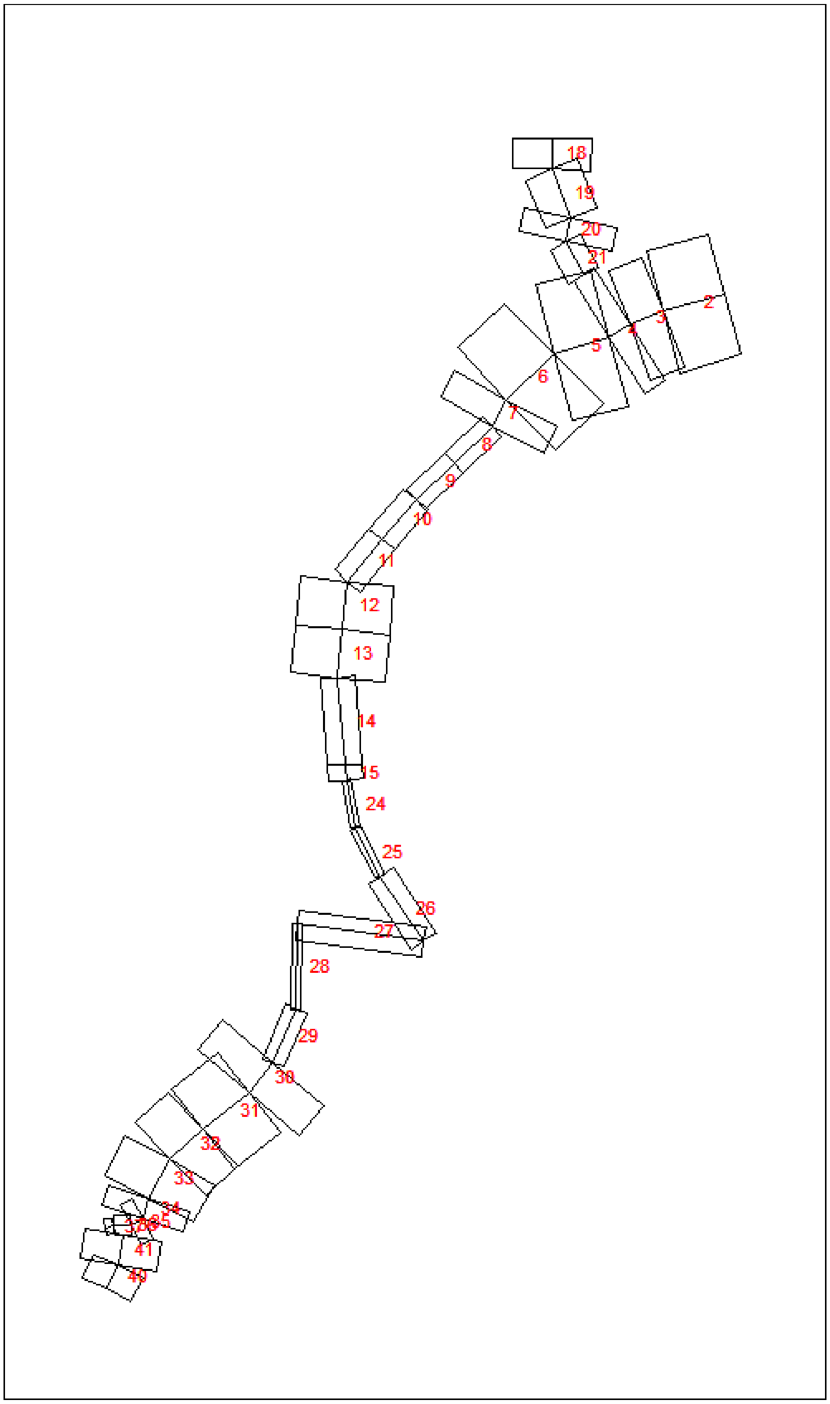

Figure 3 Red Cedar River Segments

Vertically, the model was split into 25 layers that span Tainter Lake's maximum depth of 11 meters and Lake Menomin's maximum depth of 9.5 meters (0.48 m/layer for Tainter Lake and 0.39 m/layer for Lake Menomin. Figure 4 depicts the layers of the Tainter Lake's 18 segments and Figure 5 shows the matching comparison of the depth volume curves generated by the model vs. what was calculated from the 2005 Tainter Lake bathymetric survey.

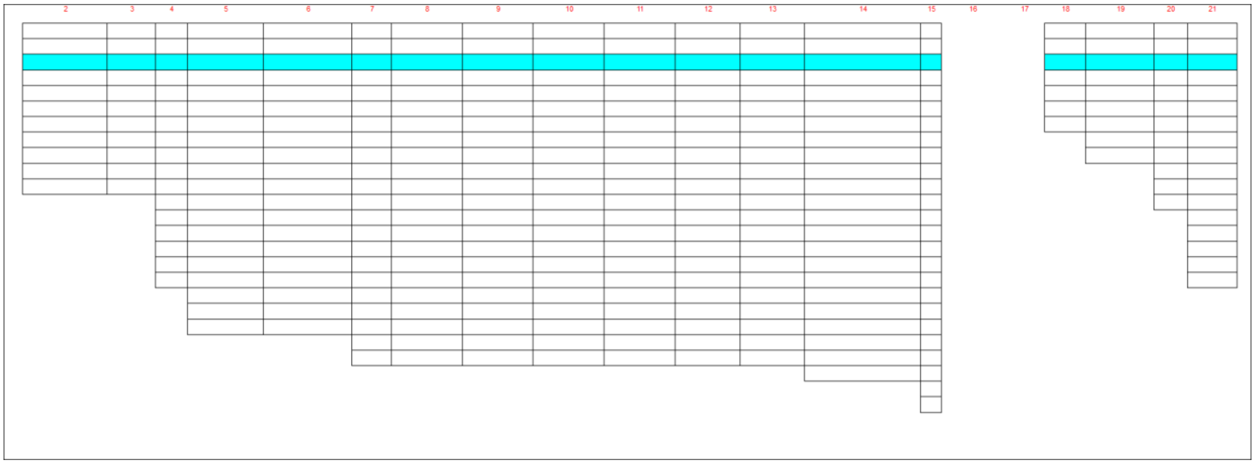

Figure 4 CE-QUAL-W2 layers for Tainter Lake (Branches 1 and 2, Normal Pool elevation in blue - 265.8 m, USGS Datum)

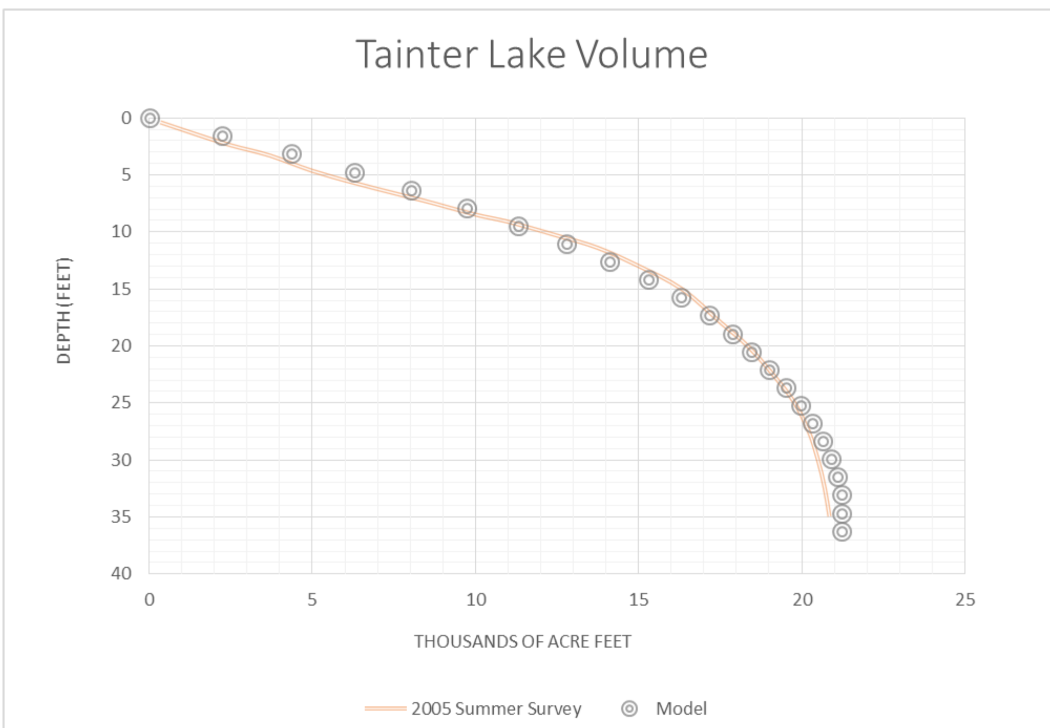

Figure 5. Tainter Lake Volume-Depth Curves, Model vs. Observed (Courtesy of Sean Hartnett, Univ. of Wisconsin, Eau Claire)

Likewise, Figure 6 depicts the model layers that represents Lake Menomin's 16 segments and Figure 7 validates the depth volume curves generated by the model vs. what was calculated from the 2006-2007 Lake Menomin bathymetric survey.

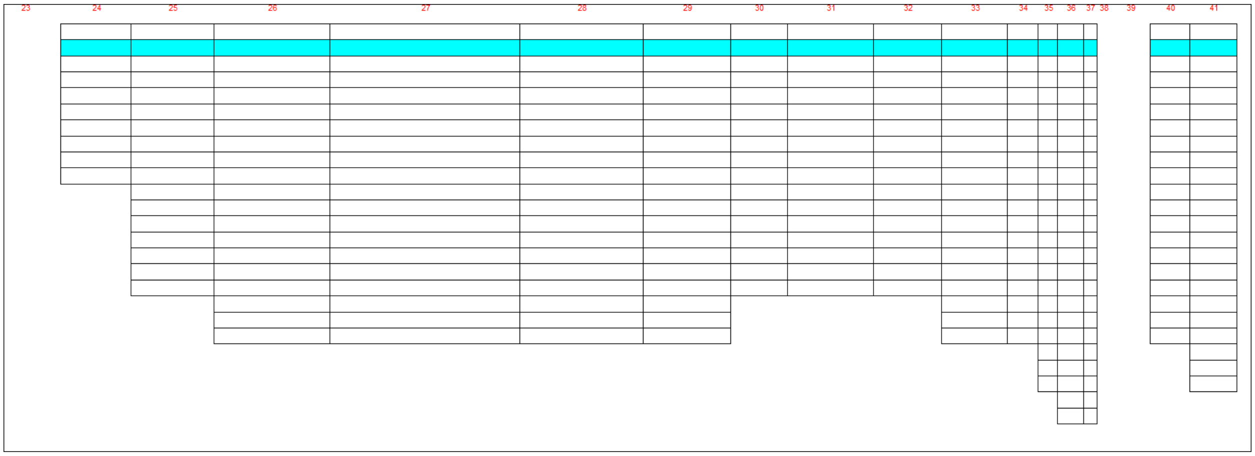

Figure 6. CE-QUAL-W2 layers for Lake Menomin (Branches 3 and 4, Normal Pool elevation in blue - 248.11 m, USGS Datum)

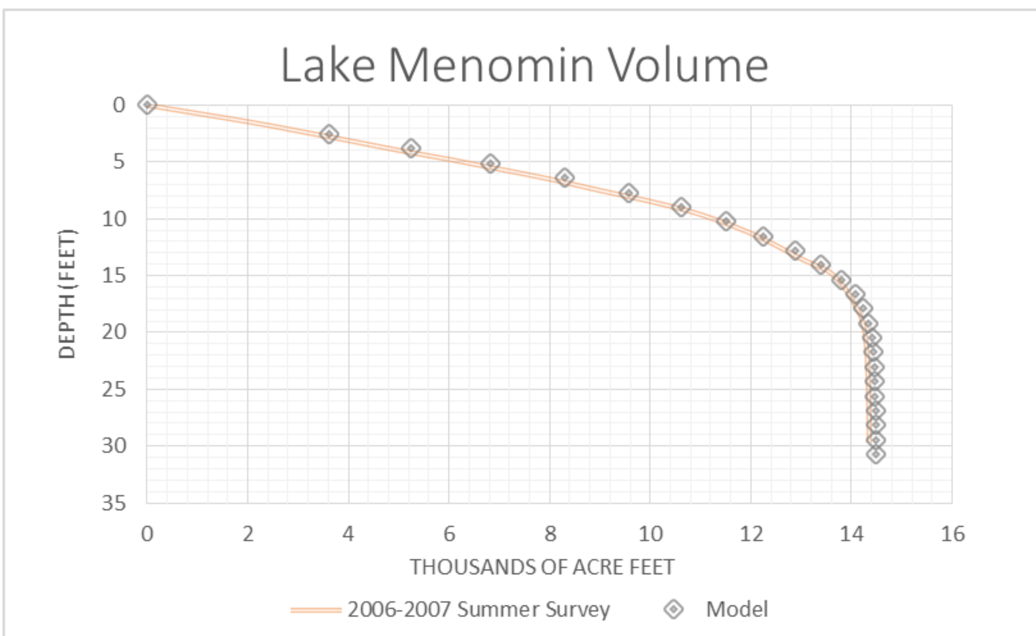

Figure 7. Lake Menomin Volume-Depth Curves, Model vs. Observed (Courtesy of Sean Hartnett, Univ. of Wisconsin, Eau Claire)

3.3 Dam Outlet Structures (Menomonie Hydroelectric Project and Cedar Falls Hydroelectric Project)

Both dams are managed within a limited range of daily hydropower peaking and their Federal Energy Regulatory Commission licenses (FERC Projects 2181-014 and 2697-014) do not allow significant seasonal storage. The impoundments have a maximum pool operation range of 0.5 feet. As a result, daily average flows delivered by the watershed are not likely affected by dam operation and potential for impact on water quality would be identical to a non-hydropower dam were inflow equals outflow on a daily basis. Operators are at the plants daily, Monday through Friday. In addition, the plants are monitored and operated remotely by staff at Xcel's Wissota Hydro facility near Chippewa Falls, Wisconsin. Headwater and tailwater levels and their rates of change are monitored in addition to several operation conditions.

3.3.1 Cedar Falls Hydroelectric Project

The Cedar Falls Hydroelectric Project is comprised of reinforced concrete structures founded on bedrock. The site consists listed in order from upstream to downstream and right to left across the dam (facing downstream) of an upstream reservoir; overflow and tainter gate spillway sections; non-overflow dam; powerhouse; abutment walls; downstream retaining walls; and a downstream river channel (Figure 8).

Figure 8. Cedar Falls Hydroelectric Project.

For modeling purposes, the elevation of the normal water surface elevation of 265.8 meters (872.2 feet (NGVD 29)) was used as the starting elevation for Tainter Lake and all discharge from the reservoir at the dam for power generation were placed at the centerline of the penstock inlet at 260.9 meters (855.8 feet). At periods when the discharge from the dam exceeded the powerhouse's capacity or when turbines were off-line, excess flow was placed at the crest of the regulating tainter gate, which has a sill elevation of 264.4 meters (867.4 feet).

3.3.2 Menomonie Hydroelectric Project

The Menomonie Hydroelectric Project structures (Figure 9) are comprised of reinforced concrete founded on bedrock. Listed in order from upstream to downstream and right to left across the dam (facing downstream) the project features consist of the upstream reservoir; an earthen embankment supporting a substation on the right bank; a concrete non-overflow gravity dam; a concrete powerhouse; a tainter gate spillway section comprised of mass concrete rollway, concrete piers and operators bridges, six steel tainter gates; a concrete non-overflow dam; an earthen embankment/abutment on the left bank, and a downstream river channel.

Figure 9. Menomonie Hydroelectric Project. Picture downloaded on 4.17.2019 at https://mapio.net/pic/p-89858029/

For modeling purposes, the elevation of the normal water surface elevation of 248.1 meters (814.0 feet (NGVD)) was used as the starting elevation for Lake Menomin and all discharge from the reservoir at the dam for power generation were placed at the centerline of the penstock inlet at 240.3 meters (788.4 feet). At periods when the discharge from the dam exceeded the powerhouse's capacity or when turbines were off-line, excess flow was placed at the crest of the regulating tainter gate, which measures 7.6 meters wide and 2.7 meters high with a sill elevation of 245.36 meters (805.0 feet) and is equipped with a cable drum hoist.

3.4 Boundary Conditions

3.4.1 Flow

Existing US Geological Survey flow gaging stations on the Hay River near Wheeler, WI, (05368000), Red Cedar River near Colfax, WI (05367500), and Red Cedar River at Menomonie, WI (05369000) were used to generate the model's 2014-2018 daily inflows and outflows (Figure 1). Unfortunately, the 2014-2018 observed flow conditions during the prime growing season for cyanobacteria (late summer- early fall) were predominately above historic monthly average flows (Figure 10). Ideally, the model would be calibrated to a mix of low, average and high flows to maximize confidence of any scenario results.

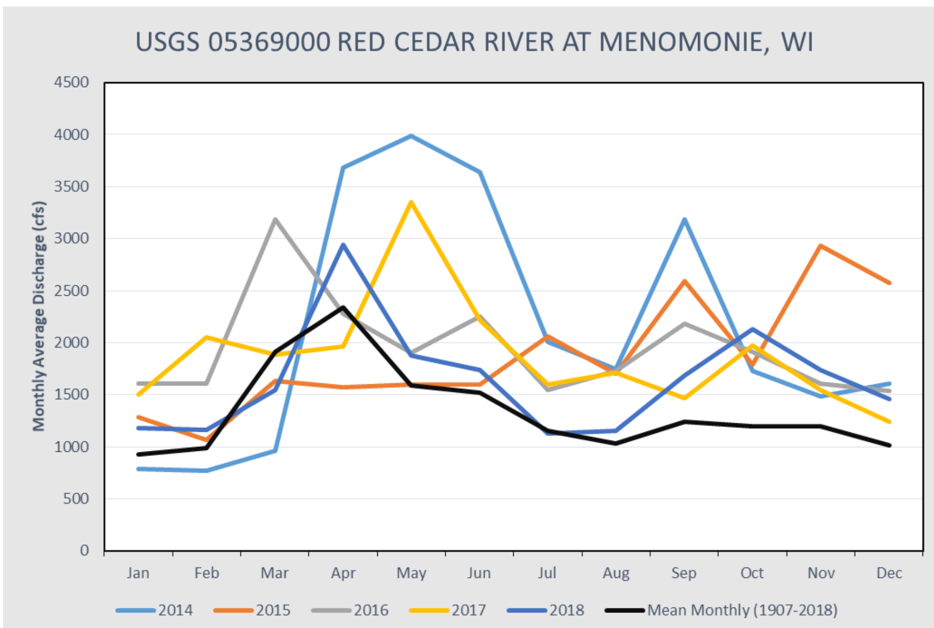

Figure 10. 2014-2018 Average Monthly Discharge vs. period of record at Red Cedar River at Menomonie, WI. Monthly mean in ft3/s (Calculation Period: 1907-07-01 -> 2018-05-31). 2018 data may still be considered provisional by the USGS.

Daily mean flows recorded at USGS gages upstream of Tainter Lake on the Hay River (05368000) and Red Cedar River (05367500) were used as inflows to the model. Because of the relatively short residence times and small but flashy elevation changes for Tainter Lake and Lake Menomin (Ref. 11), hourly flow data would have been preferred, but daily flows were found acceptable. In reconstructing the water budget for the model, the determining factors were the two main inflows to Tainter Lake (05368000 and 05367500), the changes in reservoir storage and the observed flow recorded about a half-mile below Menomonie Dam (05369000). Once calculated, it was evident that around a 5 percent shortfall was needed to balance the budget. These unaccounted for flows were likely due to some combination of ground water, precipitation and ungagged tributaries minus evaporation. Because the upstream gaging stations on the Hay and Red Cedar rivers were several miles from the model boundary and littered with many small unnamed tributaries, it was assumed for modeling purposes that all of the missing flows came from this upper intervening drainage area. Figure 11 shows the three gaged flow records and an estimate of the unaccounted intervening flows that were incorporated into branch 2 of the model as a distributed tributary. The flows for the distributed tributary were estimated by calculating a 9-day center moving average of the difference between downstream mean daily flows (05369000) and the upstream mean daily flows (05368000+ 05367500). A 9-day centered moving average was selected to prevent the use of unrealistic negative flows.

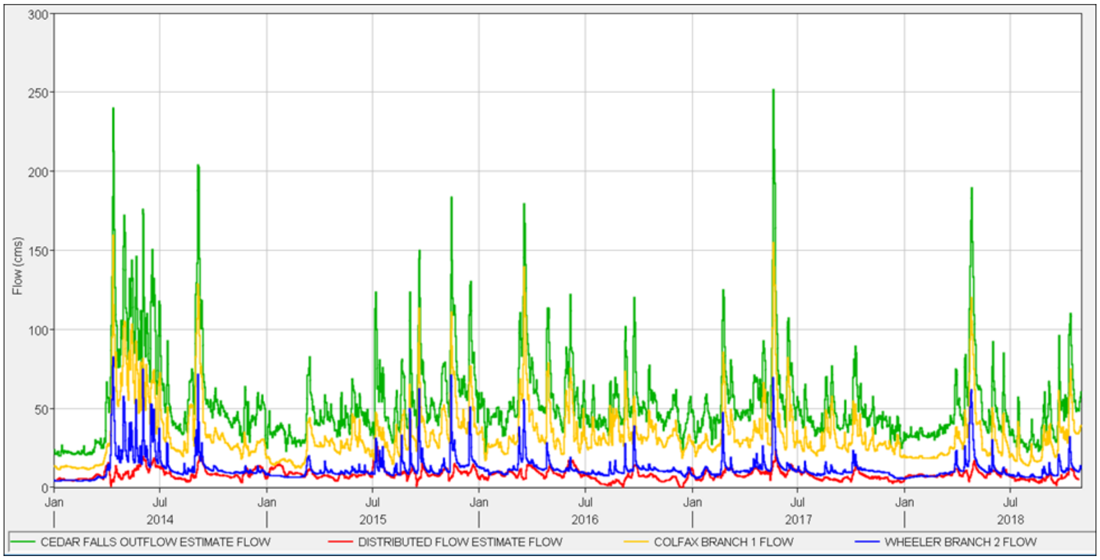

Figure 11. Branch 1 inflows (yellow line) - Red Cedar River near Colfax, WI (05367500), branch 2 inflows (blue line) - Hay River near Wheeler, WI, (05368000), intervening flows (red line), Cedar Falls and Menomonie Dam releases (green line) - Red Cedar River at Menomonie (0536900)

During model calibration, acceptable temperature and water quality concentrations selected to represent the missing flows were found obtainable using the Red Cedar River at Colfax data.

Discharge records for Tainter Lake and Lake Menomin were not available for this study and not routinely measured by Xcel energy or any other resource agency. In lieu of observed structure outflow data, Red Cedar River at Menomonie, WI (05369000) daily average flows were used as outflow time-series for both Cedar Falls Dam and Menomonie Dam. In consultation with Xcel energy (Ref. 11), outflows at each dam were separated into penstock flow and tainter gate releases (Figure 12 and Figure 13). Cedar Falls Hydroelectric Project utilizes three turbines with similar capacity that have a combined flow capacity of around 70.79 cms (2500 cfs). Menomonie Hydroelectric Project utilizes two similar sized turbines that have a combined flow capacity of around 76.46 cms (2700 cfs). As a general operational rule, all flow through the dams went through the turbines via the penstocks up to the maximum flow capacity of the turbines and then all excess flow was discharged from the regulating tainter gates. At times of turbine maintenance, affected turbines would divert any flow above their reduced capacity through the tainter gates. To account for the maintenance outages, the model relied on monthly records that were kept for each turbine. As a consequence, the model only uses a monthly average for individual turbine capacity that spreads out the effect of any significant change in outflows from the penstocks. Fortunately, these maintenance incidences were very minimal for Menomonie Dam; and for Cedar Falls Dam, besides 2015, they rarely coincided with higher flows that exceeded the capacity of the remaining operational turbines or occurred during winter months, which were outside of the time period of interest for this study.

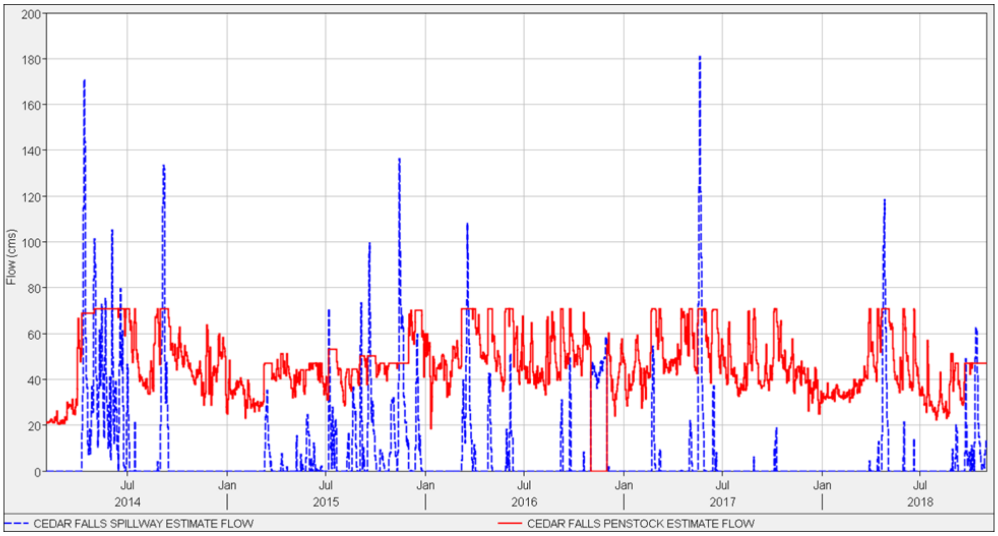

Figure 12. Estimated discharge from Cedar Falls Dam separated into penstock discharge (red) and tainter gate discharge (blue).

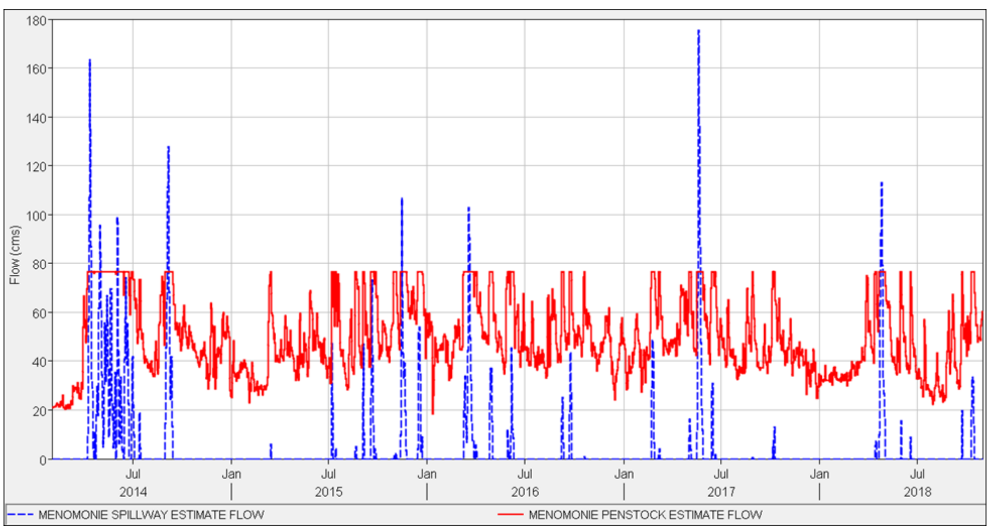

Figure 13. Estimated discharge from Menomonie Dam separated into penstock discharge (red) and tainter gate discharge (blue).

3.4.2 Temperature

Water temperature is of primary importance in the W2 model because of its influence on almost all aspects of water quality simulations. For instance, water temperature is critical in surface and sediment heat exchange, density functions that control water column stratification, temperature rate multipliers for chemical reactions, and algal growth cycle, etc. Moreover, the use of temperature profiles is often used to test the adequacy of the hydrodynamic regime instead of relying on more costly dye studies.

Daily temperature time-series for model input representing branch 1 (Red Cedar River) and branch 2 (Hay River) were developed using estimated values (rTemp model) calibrated with observed data. The observed data were collected (2016-2018) on a roughly one week interval during the growing season at USGS gages upstream of Tainter Lake on the Hay River (05368000) and Red Cedar River (05367500).

However, during model calibration, it became clear for just branch 1 that inserting a simple linearly interpolated time-series between observed values improved temperature calibration downstream in Tainter Lake and Lake Menomin. Interestingly, this simple linearly interpolated method was counterproductive for branch 2 and was not used.

Response Temperature: a simple model of water temperature (rTemp) is a spreadsheet model developed by the Washington State Department of Ecology (WSDE) (Ref. 12). Based on the work by Edinger et al. (Ref. 13), rTemp program expands the response temperature concept to include stream bed, groundwater, and hyphorheic zone heat fluxes. To calibrate the rTemp model to observed temperatures only the groundwater inflow and temperature options were used. The rTemp program calculates surface heat exchange using air temperature, dewpoint temperature, wind speed, cloud cover and shortwave solar radiation. Figure 1Figure 14 and Figure 15 shows the model inflow temperatures (branch 1 and branch 2) and observed temperatures for the Red Cedar River (05367500) and Hay River (05368000) gages, respectively.

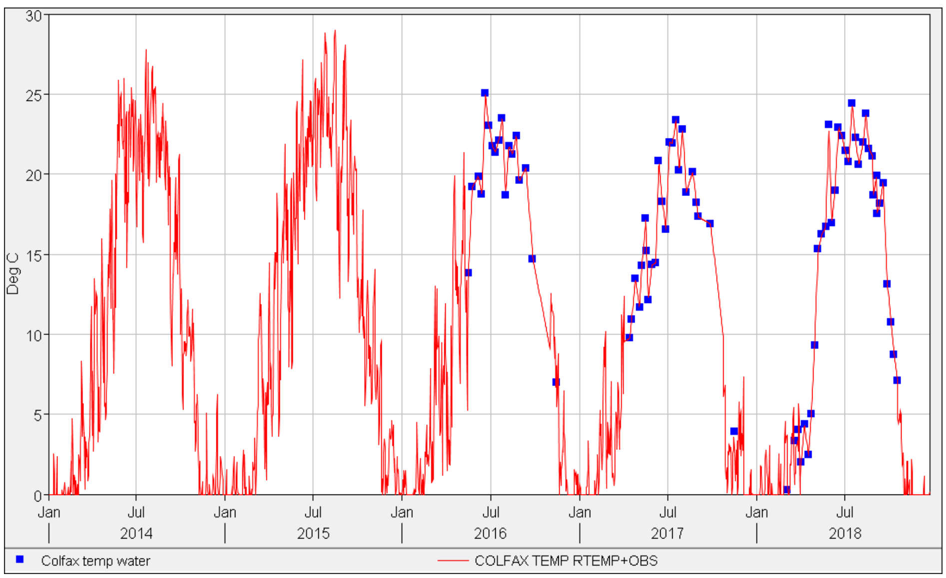

Figure 14. Observed Red Cedar River (05367500) temperatures (blue) and estimated daily temperature input file (red) for branch 1.

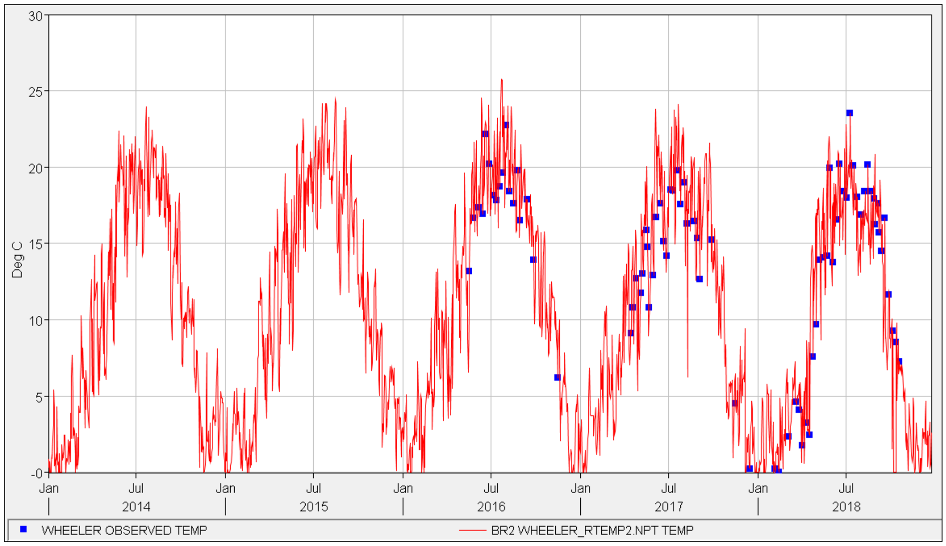

Figure 15. Observed Hay River (05368000) temperature (blue) and estimated daily temperature input file (red) for branch 2.

3.4.3 Water Quality

Water grab samples were collected at the Hay River near Wheeler, WI, (05368000), Red Cedar River near Colfax, WI (05367500), and Red Cedar River at Menomonie, WI (05369000) weekly to monthly intervals in 2015-18 and less frequently in 2014 according to the methods outlined in this report's companion document (Ref.1). The samples collected at the upstream sites, 05368000 and 05367500, were used to develop input water quality concentration files for branch 1 and branch 2, respectively. The samples collected at the downstream site (05369000) were used to compare model outflow concentrations throughout the calibration process. Constituents measured include: total organic carbon (TOC), dissolved organic carbon (DOC), total kjeldahl nitrogen (TKN), ammonium-N (NHx), nitrate-nitrite-N (NOx), total phosphorus (TP), soluble reactive phosphorus (SRP) and chlorophyll (CHLA). Annual and seasonal loadings (kg/y or kg/d) were estimated using the computer program FLUX (Ref.14). Daily concentrations of each constituent were back calculated from the loading estimates using mean daily flow.

Water quality state variables used in the Red Cedar W2 simulations included: bio-available phosphorus/phosphate (PO4), ammonium (NHx), nitrate-nitrite (NOx), total dissolved solids (TDS), labile and refractory forms of dissolved and particulate organic matter, 3 groups of algae (diatoms, "greens" and bluegreens), and dissolved oxygen (DO).

3.4.3.1 Bioavailable Phosphorus

Phosphorus serves as one of the primary nutrients for phytoplankton growth and in many fresh waters phosphorus is considered to be the limiting nutrient for maximum production of phytoplankton biomass (Refs. 16)+ 17). Phosphorus input to model is in the form of orthophosphate (PO4), which is assumed to be completely available for uptake by phytoplankton. As a proxy for PO4, measurements of soluble reactive phosphorus were used. Using the methods described above, daily time-series for bioavailable phosphorus were estimated for branch 1 and branch 2 from observed soluble reactive phosphorus measurements. Figure 16 compares the PO4 daily time-series used for branch 1 with the observed SRP measurements collected at Red Cedar River near Colfax, WI, (05367500). Figure 17 compares the PO4 daily time-series used for branch 2 with the observed SRP measurements collected at Hay River near Wheeler, WI, (05368000).

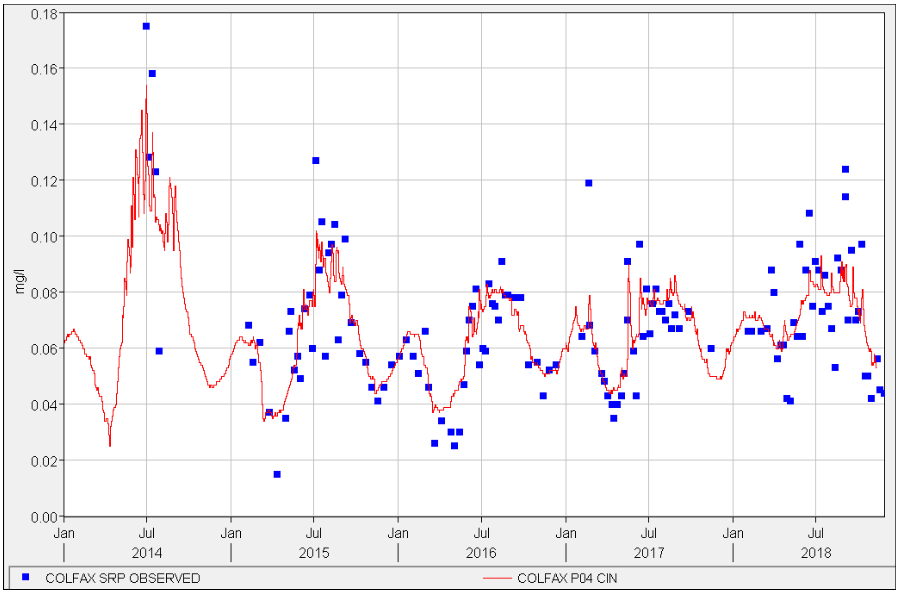

Figure 16. Bioavailable phosphorus concentration input time-series used for branch 1 compared to observed SRP measurements at Red Cedar River near Colfax, WI, (05367500).

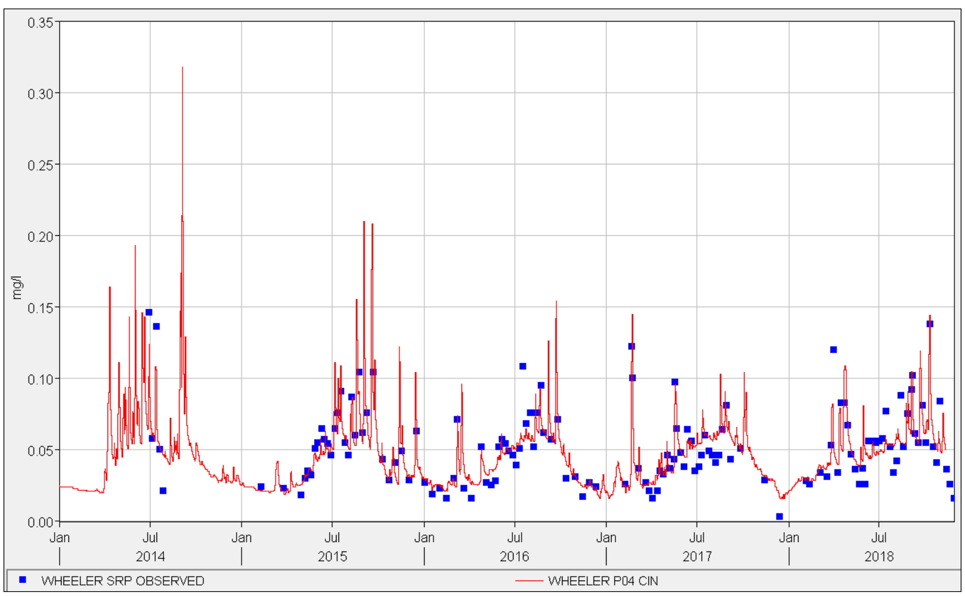

Figure 17. Bioavailable phosphorus concentration input time-series used for branch 2 compared to observed SRP measurements at Hay River near Wheeler, WI, (05368000).

3.4.3.2 Ammonium

Algae use ammonium during photosynthesis to form proteins. Ammonium was measured from grab samples that were collected during the summers of 2016 and 2017 at the upstream USGS gages on the Red Cedar River (05367500) and Hay River (05368000). These samples were used to calculate annual loadings and estimate daily inflow concentrations for branch 1 (Red Cedar River) and branch 2 (Hay River). Figure 18 Figure 19 compare the daily time-series used for ammonium concentrations with the observed samples for inflows of branch 1 and branch 2, respectively.

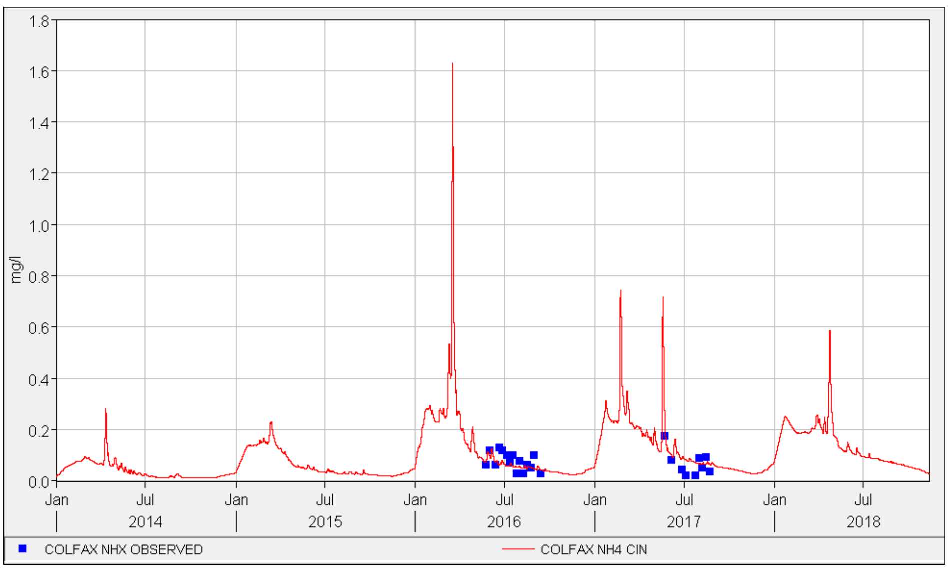

Figure 18. Ammonium concentration input time-series used for branch 1 compared to observed NHx measurements at Red Cedar River near Colfax, WI, (05367500).

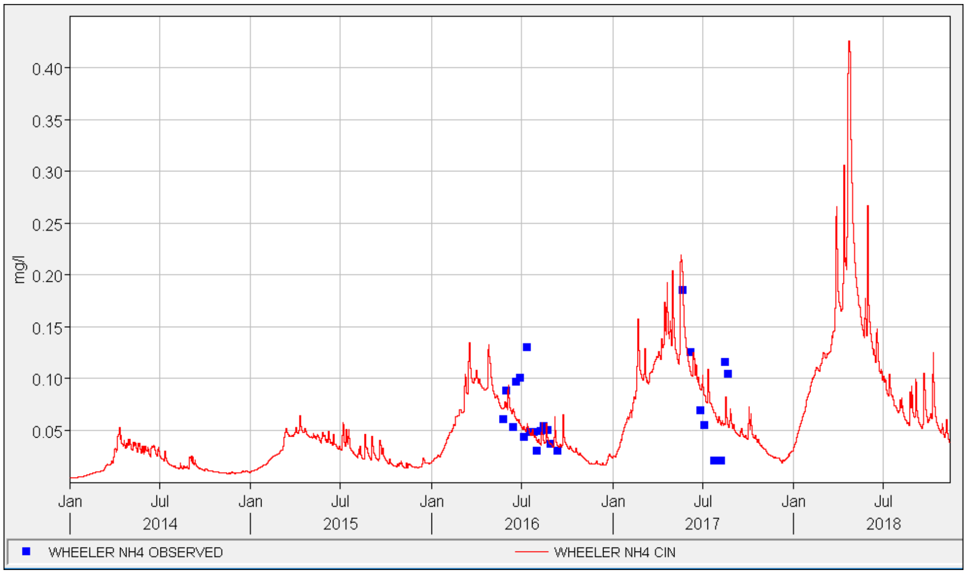

Figure 19. Ammonium concentration input time-series used for branch 2 compared to observed NHx measurements at Hay River near Wheeler, WI, (05368000).

3.4.3.3 Nitrate-Nitrite

Nitrite is an intermediate product in nitrification between ammonium and nitrate. Nitrate is used as a source of nitrogen for algae during photosynthesis. Likewise to ammonium, nitrate-nitrite was measured from grab samples that were collected during the summers of 2016 and 2017 at the upstream USGS gages on the Red Cedar River (05367500) and Hay River (05368000). Figure 20 and Figure 21 compare the daily time-series used for nitrate-nitrite concentrations with the observed samples for inflows of branch 1 and branch 2, respectively.

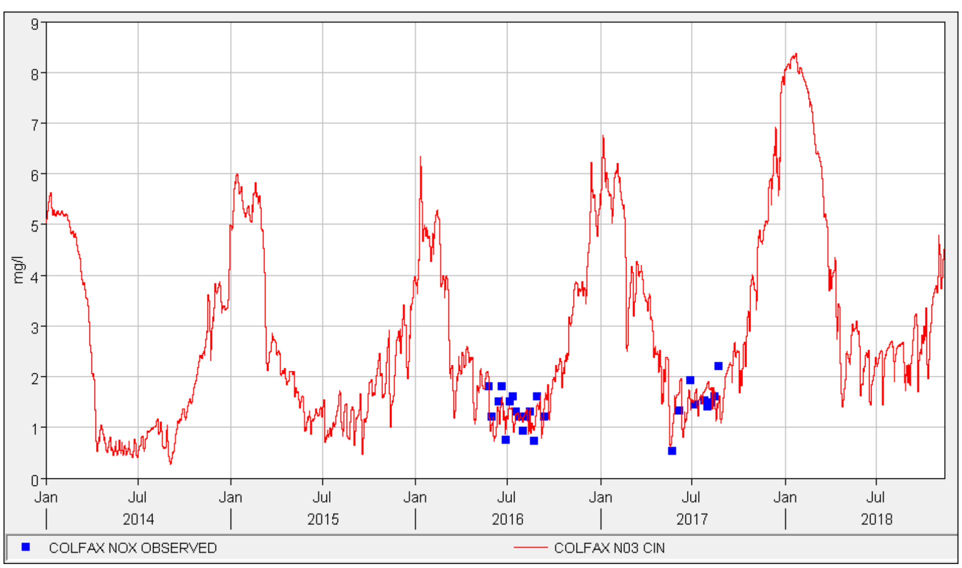

Figure 20. Nitrate-nitrite concentration input time-series used for branch 1 compared to observed NOx measurements at Red Cedar River near Colfax, WI, (05367500).

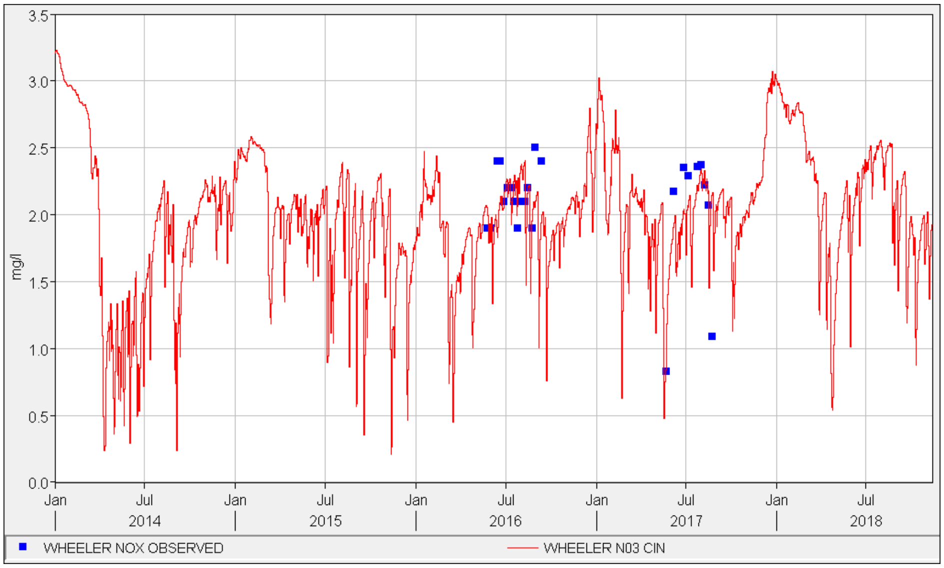

Figure 21. Nitrate-nitrite concentration input time-series used for branch 2 compared to observed NOx measurements at Hay River near Wheeler, WI, (05368000).

3.4.3.4 Dissolved Oxygen

Oxygen is one of the most important elements in aquatic ecosystems. It is essential for higher forms of life, controls many chemical reactions through oxidation, and is a surrogate variable indicating the general health of aquatic systems. Dissolved oxygen (DO) measurements at the upstream USGS gages on the Red Cedar River (05367500) and Hay River (05368000) were made with samples collected during the growing seasons of 2016 through 2018. During the time-periods were DO were measured, a simple linearly interpolated daily time-series was used for branch 1 and branch 2 model input. For time-periods not covered by observed data, DO concentrations were developed assuming 90% and 86% of the saturated DO concentrations for the Red Cedar River (05367500) and Hay River (05368000), respectively. The calculation of the dissolved oxygen concentration is performed using the equation (Ref. 15) below, where temperature is represented by T [°C] , O_p is the dissolved oxygen saturation [%], O_M [mg/l] and O_U [µmol/l] represent dissolved oxygen concentrations.

$$O_M = \frac{O_p}{100} \times O_2 \times 1.42903$$

$$O_U = \frac{O_p}{100} \times O_2 \times 44.660$$

$$T_s = 273.15 \times T$$

$$lnO_2 = A_1 + A_2 \times \frac{100}{T_s} \times A_3\, ln\left(\frac{T_s}{100}\right) + A_4 \times \frac{T_s}{100} + S\left\{B_1 + B_2 \times \frac{T_s}{100} + B_3 \times \left(\frac{T_s}{100}\right)^2\right\}$$

$$A_1 = -173.4292 \qquad A_2 = 249.6339 \qquad A_3 = 143.3483 \qquad A_4 = -21.8492$$

$$B_1 = -0.033096 \qquad B_2 = 0.014259 \qquad B_3 = -0.0017$$

The 90% saturated assumption for Red Cedar River and 86% saturated assumption for Hay River were based on observed data. The equation shown above was also corrected for salinity (S) and atmospheric pressure based on average observed specific conductivity and elevation at the two gages. Simulated water temperatures from the rTemp program were used in the approximation. Growing season inflow DO concentrations were verified for Hay River and had an absolute mean error of 0.52 mg/l (Figure 22). Observed and simulated DO concentrations are shown in Figure 23 Figure 24 for Red Cedar River (05367500) and Hay River (05368000), respectively.

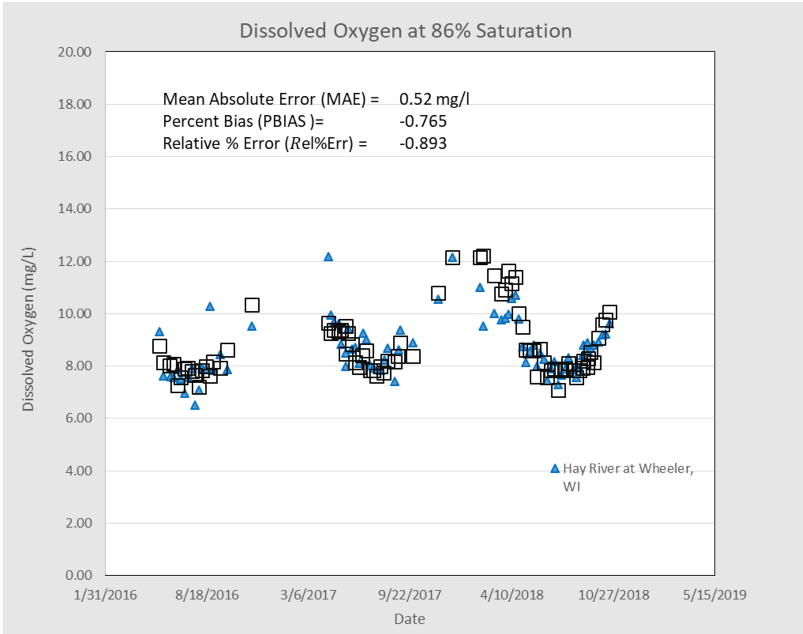

Figure 22. Observed and predicted DO concentrations using 86% saturated DO concentration assumption at Hay River near Wheeler, WI, (05368000).

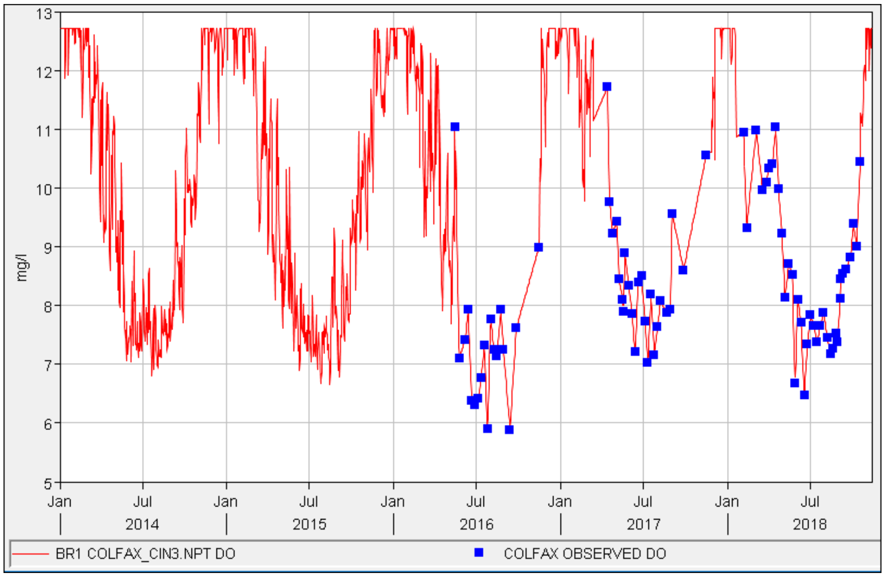

Figure 23. Dissolved Oxygen concentration input time-series used for branch 1 compared to observed DO measurements at Red Cedar River near Colfax, WI, (05367500).

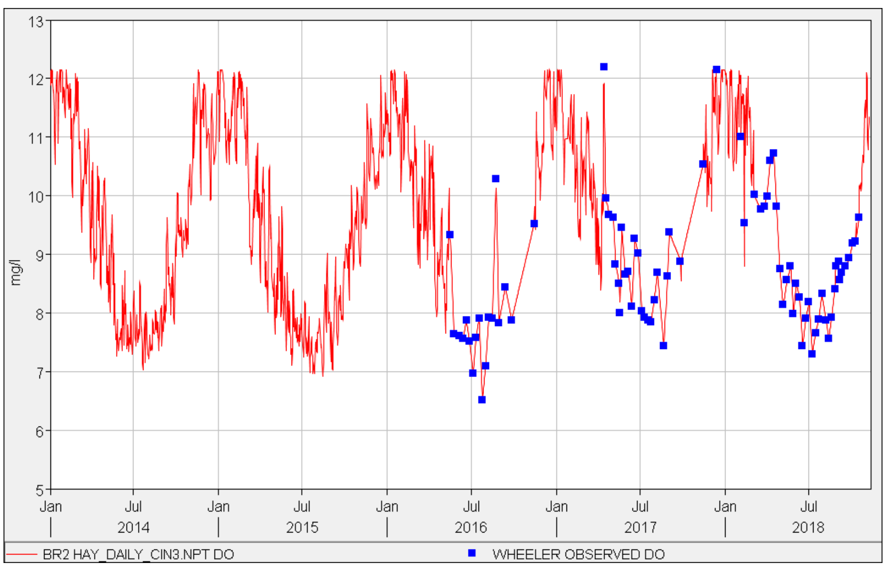

Figure 24. Dissolved Oxygen concentration input time-series used for branch 2 compared to observed DO measurements at Hay River near Wheeler, WI, (05368000).

3.4.3.5 TDS

Total dissolved solids (TDS) affect water density and ionic strength. Total dissolved solids were not measured directly at the upstream USGS gages on the Red Cedar River (05367500) and Hay River (05368000); instead, the 2016-2018 daily time-series of TDS was roughly estimated by linearly interpolating between observed specific conductivity (EC25) readings and then adjusting the values using the following equation, which is fairly accurate for most natural waters:

$$\text{TDS (mg/L)} = 0.67 \times \text{EC25 (uS/cm)}$$

To fill-in the 2014-2015 TDS values, the 2016-2018 pattern was repeated. Observed EC25 x 0.67 readings and branch 1 and branch 2 concentration time-series are shown in Figure 25 and Figure 26 for Red Cedar River (05367500) and Hay River (05368000), respectively.

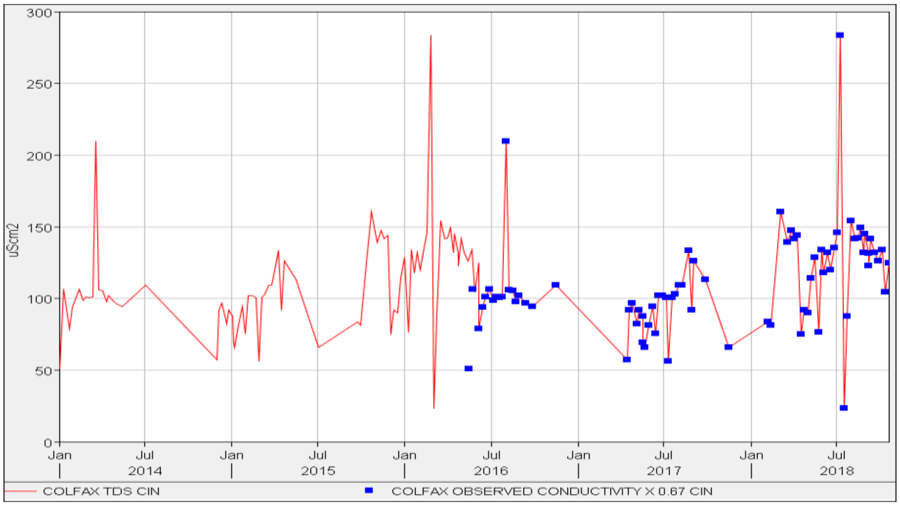

Figure 25. TDS concentration input time-series used for branch 1 compared to observed conductivity X 0.67 at Red Cedar River near Colfax, WI, (05367500).

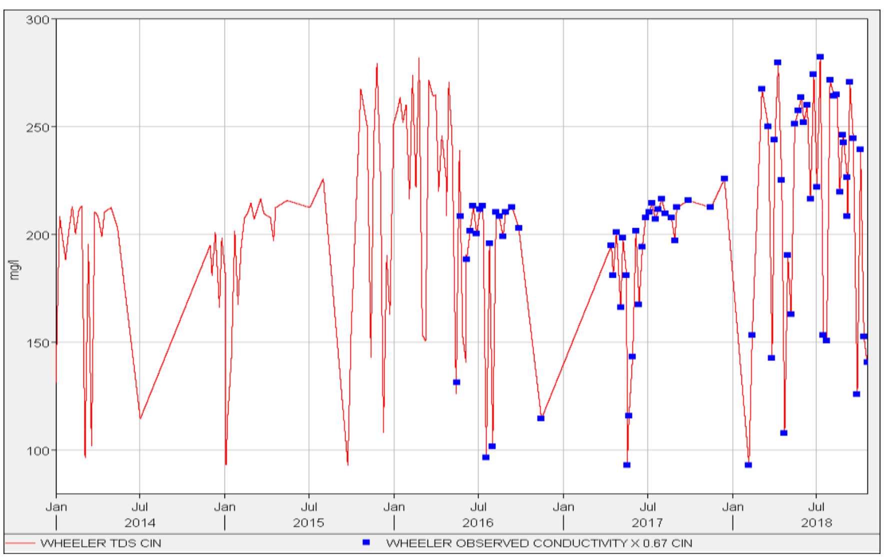

Figure 26. TDS concentration input time-series used for branch 2 compared to observed conductivity X 0.67 at Hay River near Wheeler, WI, (05368000).

3.4.3.6 Organic Matter

The decay of organic matter in the water column and sediments of reservoirs are important internal sources of nutrients and internal sinks for dissolved oxygen. Organic matter loadings to the system are either in the form of allochthonous organic matter (produced outside the system), and autochthonous organic matter (produced within the system) mainly due to phytoplankton production. Unfortunately, boundary condition data to adequately represent allochthonous organic matter are not routinely measured. For the Red Cedar W2 model, the four state variables describing organic matter: labile dissolved organic matter (LDOM), refractory dissolved organic matter (RDOM), labile particulate organic matter (LPOM), and refractory particulate organic matter (RPOM), were not directly measured, but estimated from total organic carbon (TOC). Labile DOM and labile POM decay at a faster rate than refractory OM, which is product of labile OM decay. Settling POM contributes to the lake sediment oxygen demand. DOM and POM are produced by algal mortality and excretion.

Listed below are the equations (Ref. 19) used in estimating the allochthonous loadings of these constituents from TOC.

LDOM= ((TOC -algae)* 0.75) * 0.30

RDOM= ((TOC-algae) * 0.75) * 0.70

LPOM = ((TOC-algae) * 0.25) * 0.30

RPOM = ((TOC - algae) * 0.25) * 0.70

Inflow algal concentrations were estimated from chlorophyll a data using the following conversion (Ref. 19).

$$\frac{ug\ chl\ a}{l} \times \frac{mg}{10^3 ug} \times \frac{gm}{10^3 mg} \times \frac{10^3 l}{m^3} \times 65\ \frac{gm\ OM}{gm\ chl\ a} = \frac{0.065\ gm\ OM}{m^3}$$

Estimated organic matter inputs to branch 1 and branch 2 are shown in Figure 27 and Figure 28 for Red Cedar River (05367500) and Hay River (05368000), respectively.

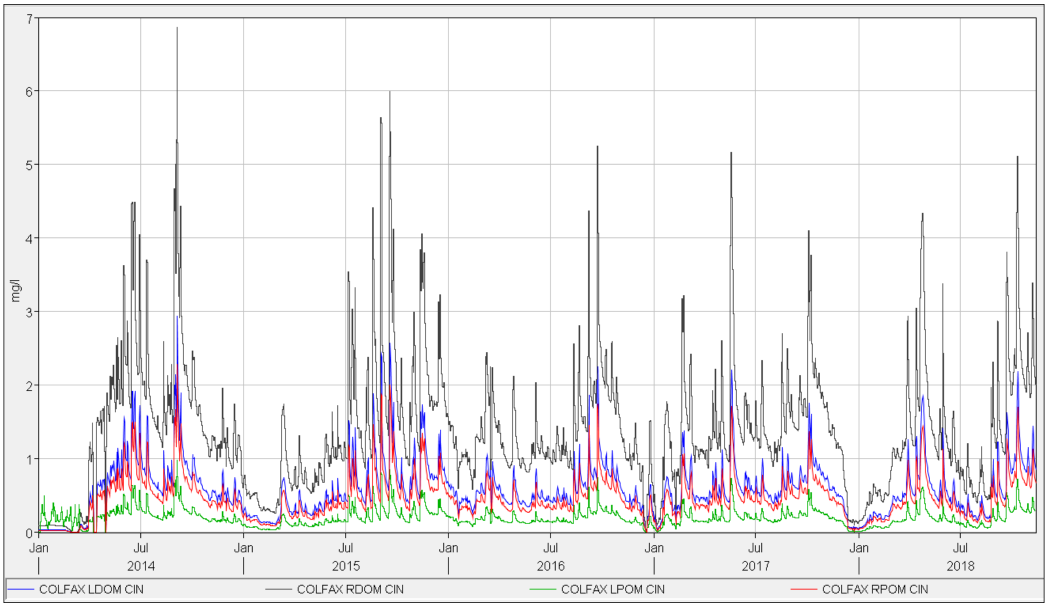

Figure 27 Organic matter (LDOM, RDOM, LPOM and RPOM) concentration input time-series used for branch 1 at Red Cedar River near Colfax, WI, (05367500).

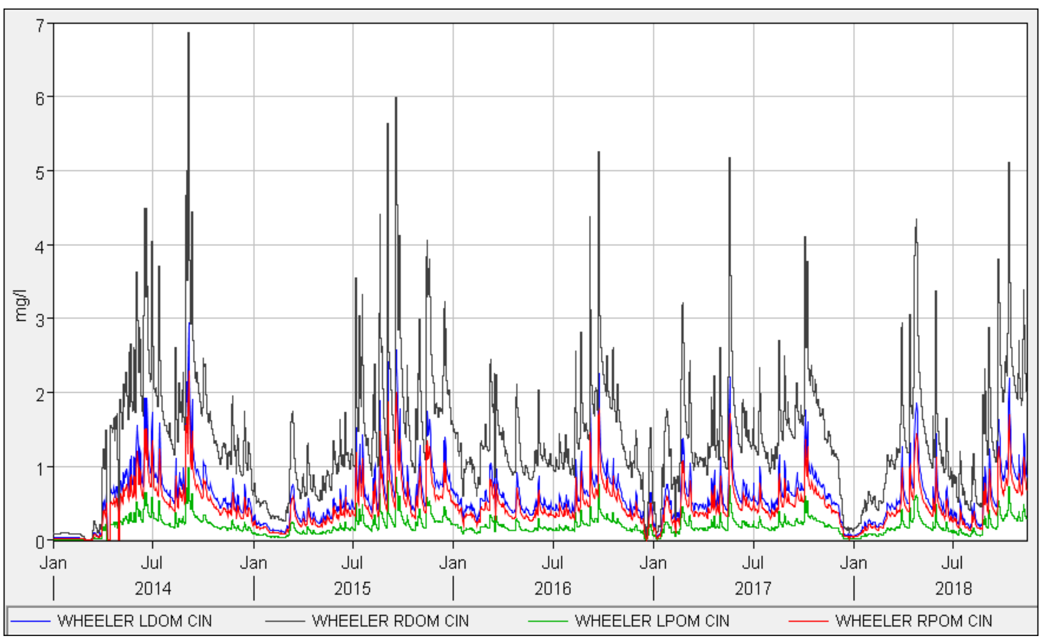

Figure 28. Organic matter (LDOM, RDOM, LPOM and RPOM) concentration input time-series used for branch 2 at Hay River near Wheeler, WI, (05368000).

3.4.3.7 Algae

Three different algal groups are included in the model to represent different types of algae: diatoms, green algae, and blue-green algae. Algae are important in nutrient and DO dynamics by utilizing nutrients and producing DO during photosynthesis and then consuming DO during respiration. Algal mortality and excretion produces DOM and POM which eventually decay and further deplete DO.

Chlorophyll a (Chl a) concentrations measured at the upstream gages at Red Cedar River (05367500) and Hay River (05368000) were used for estimating the algal biomass. Without taxonomic information, the estimated biomass was assumed to be divided between diatoms (45%), green algae (45%), and blue-green algae (10%). Figure 29 and Figure 30 presents the total algal biomass time-series used for branch 1 and branch 2, respectively. A ratio of 30/1 between chlorophyll a and algal biomass in terms of ug chl a/mg algae was used for comparison purposes.

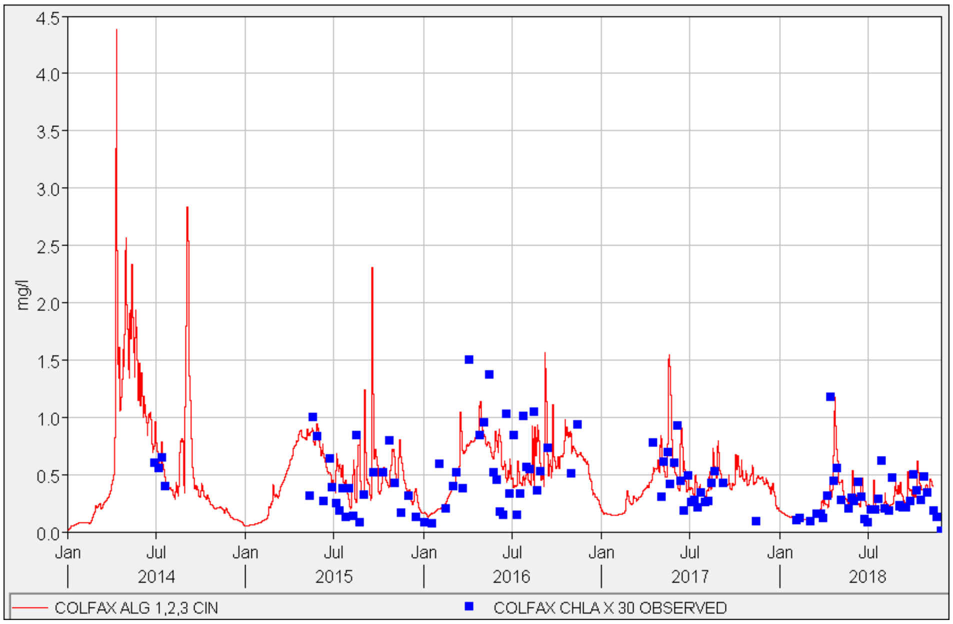

Figure 29. Total algal biomass (diatoms, green algae, and blue-green algae) concentration input time-series used for branch 1 at Red Cedar River near Colfax, WI, (05367500) compared to chlorophyll a (mg/l x 30).

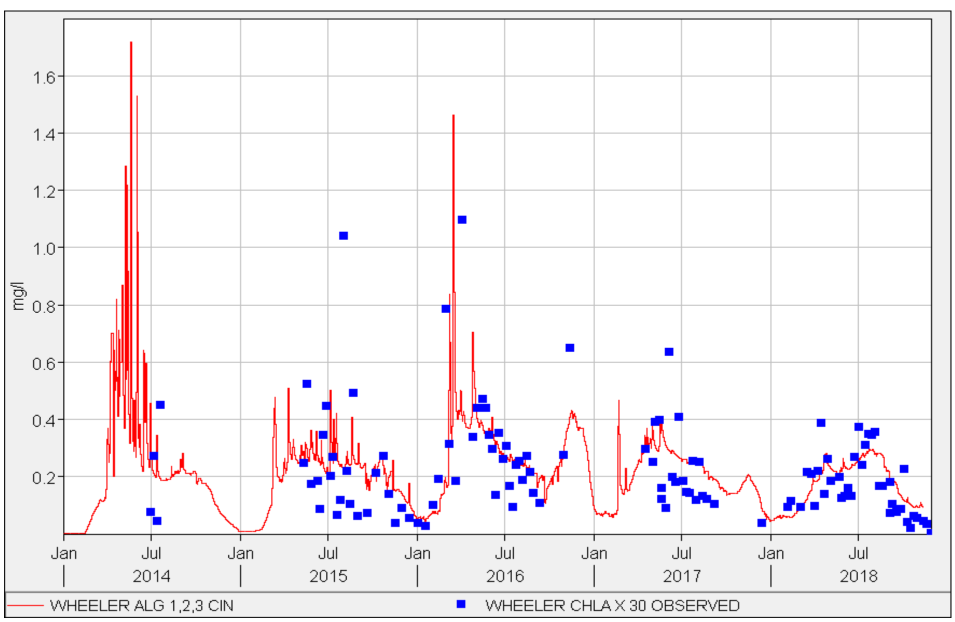

Figure 30. Total algal biomass (diatoms, green algae, and blue-green algae) concentration input time-series used for branch 2 at Hay River near Wheeler, WI, (05368000) compared to chlorophyll a (mg/l x 30).

3.4.4 Meteorological Data

Input files of the meteorological forcing in the appropriate units and format were prepared using hourly air temperature, dew point temperature, wind speed, wind direction, cloud cover and solar radiation reported from Menomonie Municipal Airport-Score Field (KLUM), located about a half-mile east of Lake Menomin. Figure 31 shows the large periodic range of air temperature, dew point temperature and solar radiation typical of Wisconsin's continental location.

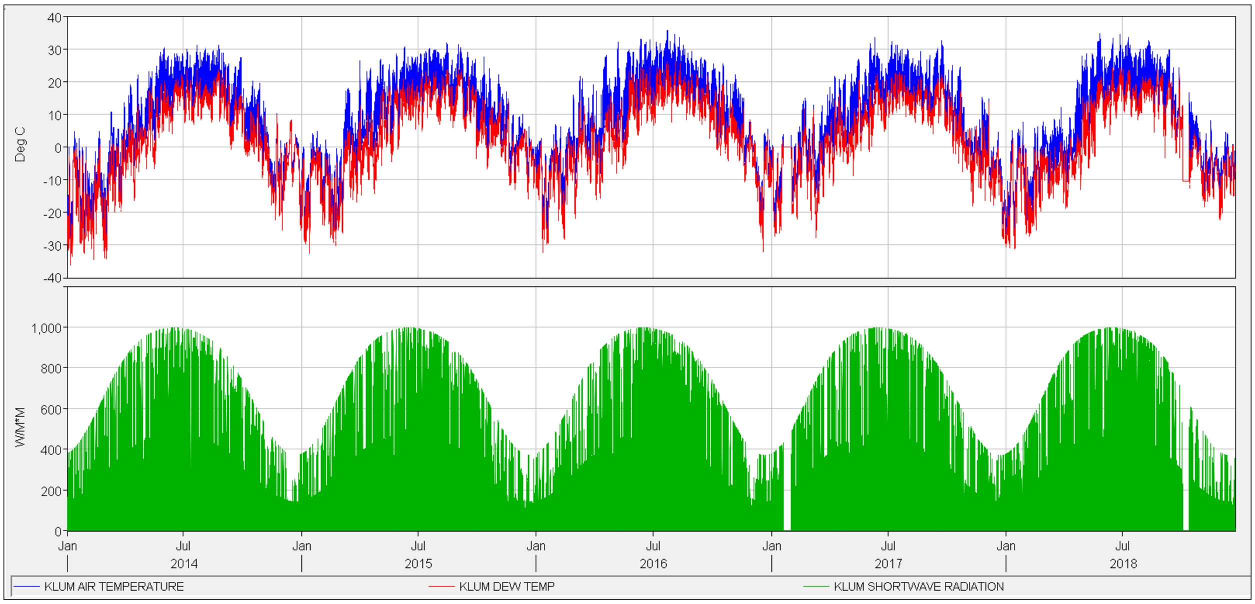

Figure 31. 2014-2018 Hourly Air Temperature (blue), Dew Point Temperature(red) and Shortwave Radiation (green)reported from Menomonie Municipal Airport-Score Field (KLUM).

4 CE-QUAL-W2 Model Performance

4.1 In-Pool Data

The model was calibrated using 2015-2018 summer observed in-pool data collected at five stations (TL1, TL2, TL3, TL4 and TL5) for Tainter Lake and two stations (ML1 and ML5) for Lake Menomin (Figure 1). Table 2 lists the location, station number, and water quality constituents used for comparisons with computed data. Most of the grab samples were collected roughly every two-weeks during the summer starting in 2016 using a 1-m integrated surface sampler (Ref. 1). In addition to grab samples, in situ profile data were also collected at 1-m increments at each station for water temperature (Deg C), specific conductivity (uS/cm), dissolved oxygen (mg/l), pH and a Secchi (m) measurement.

Table 2. Tainter and Menomin Lake sampling stations and water chemistry variable list. AlkPAct = alkaline phosphatase activity.

Station	Coordinates		Total P	SRP	Chla	TKN	NHx	NOx	Phyto ID	Microcystin	AlkPAct
	North	West	(mg/L)	(mg/L)	(mg/L)	(mg/L)	(mg/L)	(mg/L)			(ug/g min)
Tainter Lake 1 (TL 1)	44.9889	-91.8361	X	X	X	X	X	X			
Tainter Lake 2 (TL 2)	44.9822	-91.8603	X	X	X	X	X	X			
Tainter Lake 3 (TL 3)	44.9657	-91.8783	X	X	X	X	X	X			
Tainter Lake 4 (TL 4)	44.9536	-91.8917	X	X	X	X	X	X			
Tainter Lake 5 (TL 5)	44.9384	-91.8913	X	X	X	X	X	X	X	X	X
Menomin Lake 1 (ML 1)	44.8808	-91.9239	X	X	X	X	X	X			
Menomin Lake 5 (ML 5)	44.9332	-91.8879	X	X	X	X	X	X	X	X	X

4.2 Model Calibration / Validation Approach

Water quality modeling is still very much an art with numerous parameters available for adjustment during model development (Ref. 4). For this Red Cedar W2 model, the calibration strategy was to use four years of monitoring data (2015-2018) to estimate a single set of pertinent hydraulic and water quality parameters that:

1) Minimizes the differences in computed and observed data for the simulated time-period of interest (May-Oct) and
2) Maximizes the model's predictive accuracy for testing a wide range of scenarios aimed at limiting cyanobacteria growth.

For minimizing the differences in computed and observed data the Red Cedar W2 model results were assessed using graphical techniques (observed vs. modeled profiles and time series graphs) as well as statistical measures. The statistical measures used to verify model simulated results as compared to observed water quality data include mean absolute error (MAE), percent bias (PBIAS), and the relative percent error (Rel%Err). The equations used to calculate these metrics are listed below.

MAE is a measure of the average magnitude of deviation of the simulated results to the observed data and is defined as:

$$MAE = \sum_{i=1}^{n} \frac{|O_i - S_i|}{n}$$

where O represents observed values and S represents model simulated values.

PBIAS measures the average tendency of the simulated results to be larger or smaller than the observed data (Refs. 6 and 7). The optimal value of PBIAS is 0%, with low values indicating an unbiased model simulation. Positive values indicate that the model has an underestimation bias, and negative values indicate that the model has an overestimation bias (Refs. 6 and 7). PBIAS is calculated based on the following equation:

$$\text{PBIAS} = \left[\frac{\sum_{i=1}^{n}(O_i - S_i) \times (100)}{\sum_{i=1}^{n}(O_i)}\right]$$

Rel%Err is the average of the differences between observed values and simulated values relative to the observed value and is reported as a percentage. It is a measure of the average relative deviation of the simulated results to the observed values. The optimal value of Rel%Err is 0%. Positive values indicate that the model generally underestimates the observed data, and negative values indicate that the model generally overestimates the observed data. Rel%Err is calculated using the following equation:

$$Rel\%Err = 100 \times \frac{\left(\sum_{i=1}^{n} \frac{(O_i - S_i)}{O_i}\right)}{n}$$

Table 3 shows the MAE calibration targets, which were based on targets used for a 2016 CE-QUAL-W2 model developed for the Wisconsin River TMDL (Ref. 7). An emphasis was put on MAE as the primary calibration statistic. PBIAS and Rel%Err were used to further inform the calibration. Statistics were calculated at all of the monitoring sites for each observed data point. The 2014-2018 average MAE was then computed for each location and for each reservoir. Meeting calibration targets at each individual location was not expected, but analysis by individual station provides further insight into model response and potential adjustments to improve the calibration. In applying the target, the goal of the calibration is to be at or below these error values for each parameter.

Table 3 Calibration Targets for Model State Variables

Primary Calibration State Variables	**Mean Absolute Error**
Temperature	1°C
Total Phosphorus	0.02 mg/L
Orthophosphate	0.01 mg/L
Dissolved Oxygen	2 mg/L
Secondary Calibration State Variables	**Mean Absolute Error**
Total Organic Carbon	5 mg/L
Chlorophyll a	4 µg/L
Total Kjeldahl Nitrogen	0.4 mg/L
Ammonia Nitrogen	0.03 mg/L
Nitrate and Nitrite	0.1 mg/L

In order to develop a model that is best suited for predictive simulations of future scenarios, one set of calibration parameters that best represent all the years (2015-2018) of observed data was selected and the model was run continuously. Even though modeling continuously goes against the standard of validating the model through separate calibration and verification years, a calibrated continuous model should better reproduce a wider variation in behavior between all the years. Having a single set of calibrated parameters will undoubtedly miss simulating certain hydrologic or meteorological conditions that may be captured better with a different set of parameter values, but a lot more confidence can be placed in the model's ability to reproduce behavior for the "right" reasons than if the model were calibrated for one year and verified for another year (Ref. 4). Regardless, uncertainty in predicting future water quality conditions is inevitable no matter what calibration strategy is used due to epistemic sources of uncertainty, such as errors in the model structure, input data, and model parameter values (Ref. 5).

The CE-QUAL-W2 model was applied to continuously simulate the period from January 5, 2014, through October 30, 2018. The model calibration focused on summer conditions after 2015 when most of the data collection began. Because the model was not calibrated to winter conditions, W2's ice formation routine was not used. 2014 was considered a model spin-up period, therefore initial water quality conditions were not important. The model was calibrated to observed temperature and dissolved oxygen profile data and 1-m integrated water quality grab samples for the entire 2015–2018 dataset concurrently. The calibration consisted of adjusting a range of parameters over the course of numerous model simulations.

4.2.1 Flow/Water Surface Elevation

Reservoir pool elevation data were obtained from Xcel Energy (Ref 12). The water surface elevations were characterized by run-of-the-river (ROR) operations for the two reservoirs that allow a maximum pool operation range of only 0.5 ft. Figure 32 and Figure 33 shows computed elevations that are well matched to the mean of the observed values, but with a bit more bounce for Tainter Lake and a little too flat for Lake Menomin. Figure 34 shows the relatively short residence times seen on Tainter Lake and Lake Menomin. If hourly inflow data and measured discharge readings from the dams were available, matching the sudden changes in elevation on the two reservoirs would likely improve.

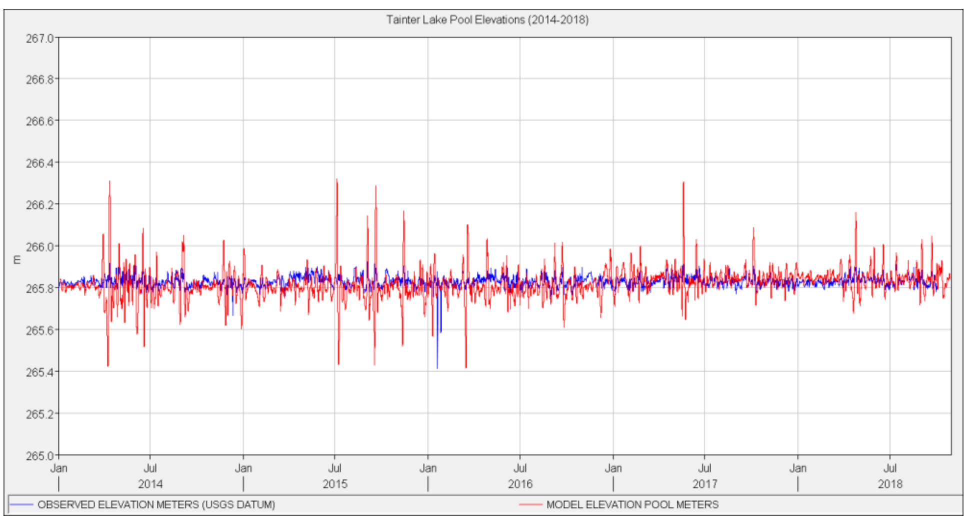

Figure 32. Observed (blue) and computed (red) water surface elevations for Tainter Lake. Mean absolute error (MAE) =0.06 m, Percent bias (PBIAS) = 0.0071, Relative % Error (Rel%Err) = 0.0071 and Count = 41328

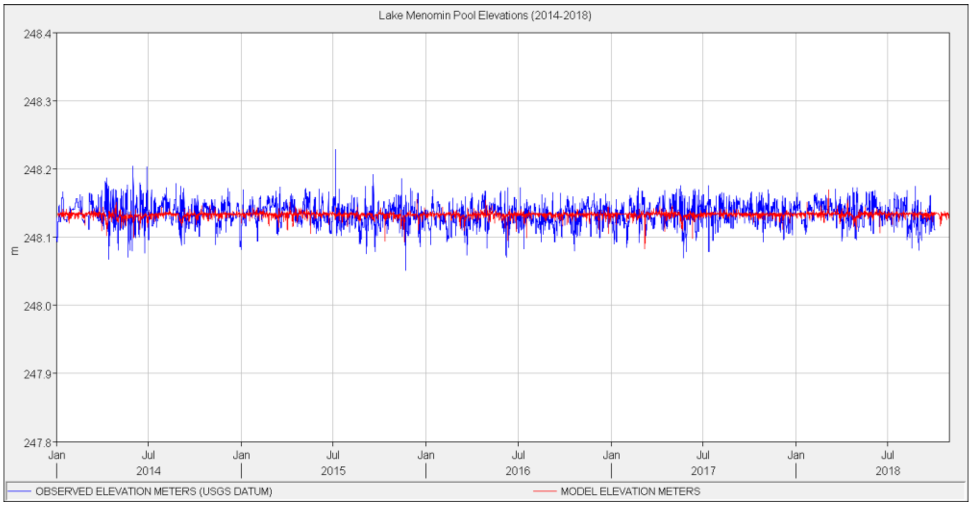

Figure 33. Observed (blue) and computed (red) water surface elevations for Tainter Lake. Mean absolute error (MAE) =0.013 m, Percent bias (PBIAS) = -0.0001, Relative % Error (Rel%Err) -0.0001and Count = 41328

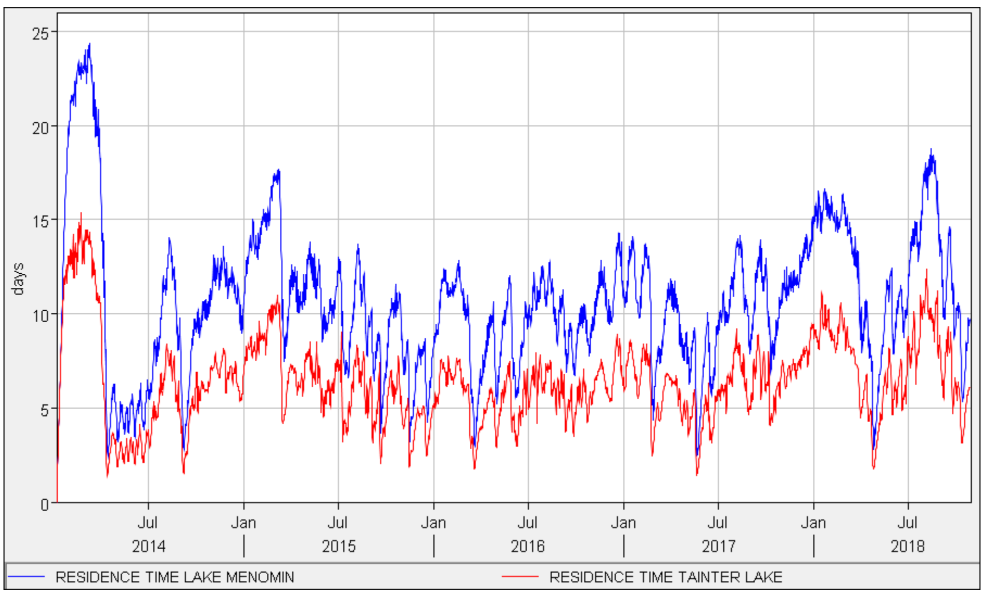

Figure 34. Modeled residence times for Tainter Lake (red) and Tainter Lake + Lake Menomin (blue).

4.2.2 Water Temperature

Table 4 presents the relevant coefficients used in calibrating temperature along with model default values and the final calibrated values. Observed and computed temperature profiles for TL5 are shown in Figure 35 thru Figure 39. Computed temperatures are generally in good agreement with observed temperatures for all dates and stations on Tainter lake and Lake Menomin and overall and station mean absolute error statistics are inline to the 1 Deg C calibration target (Table 5). Profile comparisons were presented to demonstrate that stratification periods are being simulated by the model in the same general manner as seen by the observed data, but it is clear that some individual profile comparisons are better than others. Figure 40 presents the 2014-2018 simulated surface temperatures at ML1 versus observed temperatures and Figure 41 – 46 presents the 2014-2018 simulated temperatures at ML5 versus observed temperatures at increasing depth. These time-series comparisons demonstrate that the model is reproducing the magnitude and timing of the reservoirs' seasonal temperature patterns.

Table 4. Temperature calibration values

Temperature Calibration Coefficients	Variable	Default	Calibrated
Horizontal eddy viscosity (m2/s)	AX	1.0	1.0
Horizontal eddy diffusivity (m2/s)	DX	1.0	1.0
Bottom frictional resistance	MANN		0.03
Fraction of solar radiation absorbed at water surface	BETA	0.45	0.35
Solar radiation extinction - detritus	EXH2O	0.25	0.25
Solar radiation extinction - algae	EXA	0.2	0.2
Wind-sheltering coefficient	WSC	0.7-1.0	1.0
Sediment Temperature (Deg C)	TSED	10	8
Heat lost to sediments that is added back to water	TSEDF	1	1

Table 5. Mean absolute error (MAE) for temperature

<table>
<tr><th colspan="6">Temperature Mean Absolute Error (Deg C)</th></tr>
<tr><th>Tainter Lake</th><th>TL1</th><th>TL2</th><th>TL3</th><th>TL4</th><th>TL5</th></tr>
<tr><td>0.75</td><td>0.85</td><td>0.74</td><td>0.64</td><td>0.74</td><td>0.79</td></tr>
<tr><th>Lake Menomin</th><th colspan="2">ML1</th><th colspan="3">ML5</th></tr>
<tr><td>1.1</td><td colspan="2">0.91</td><td colspan="3">1.13</td></tr>
</table>

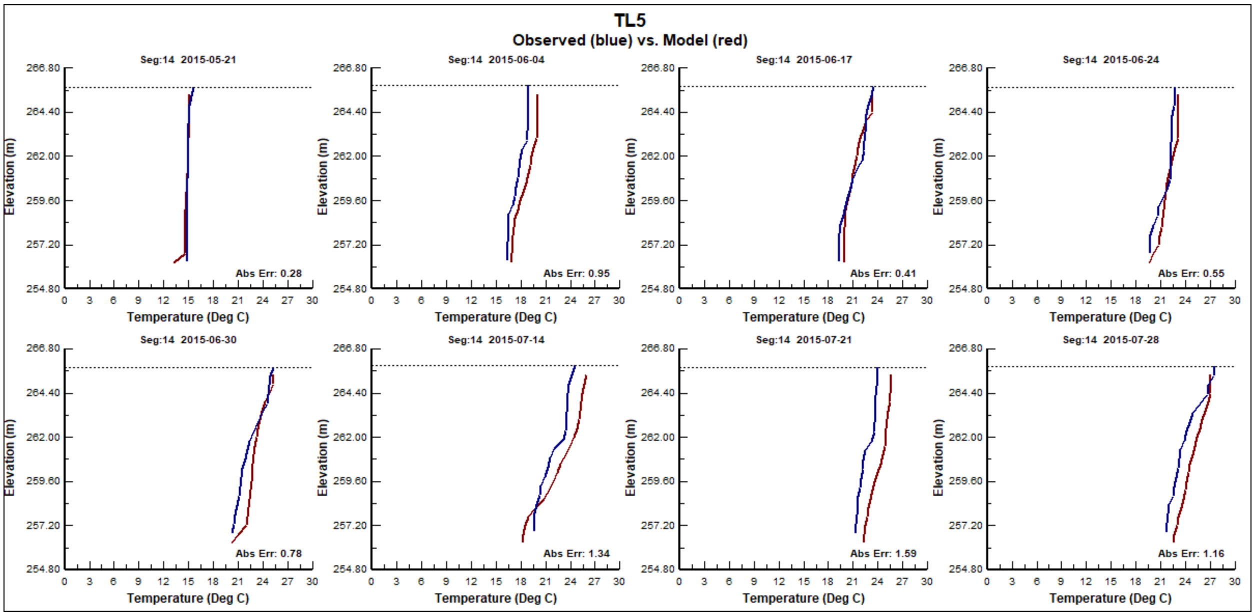

Figure 35. Computed versus observed temperatures at station TL5

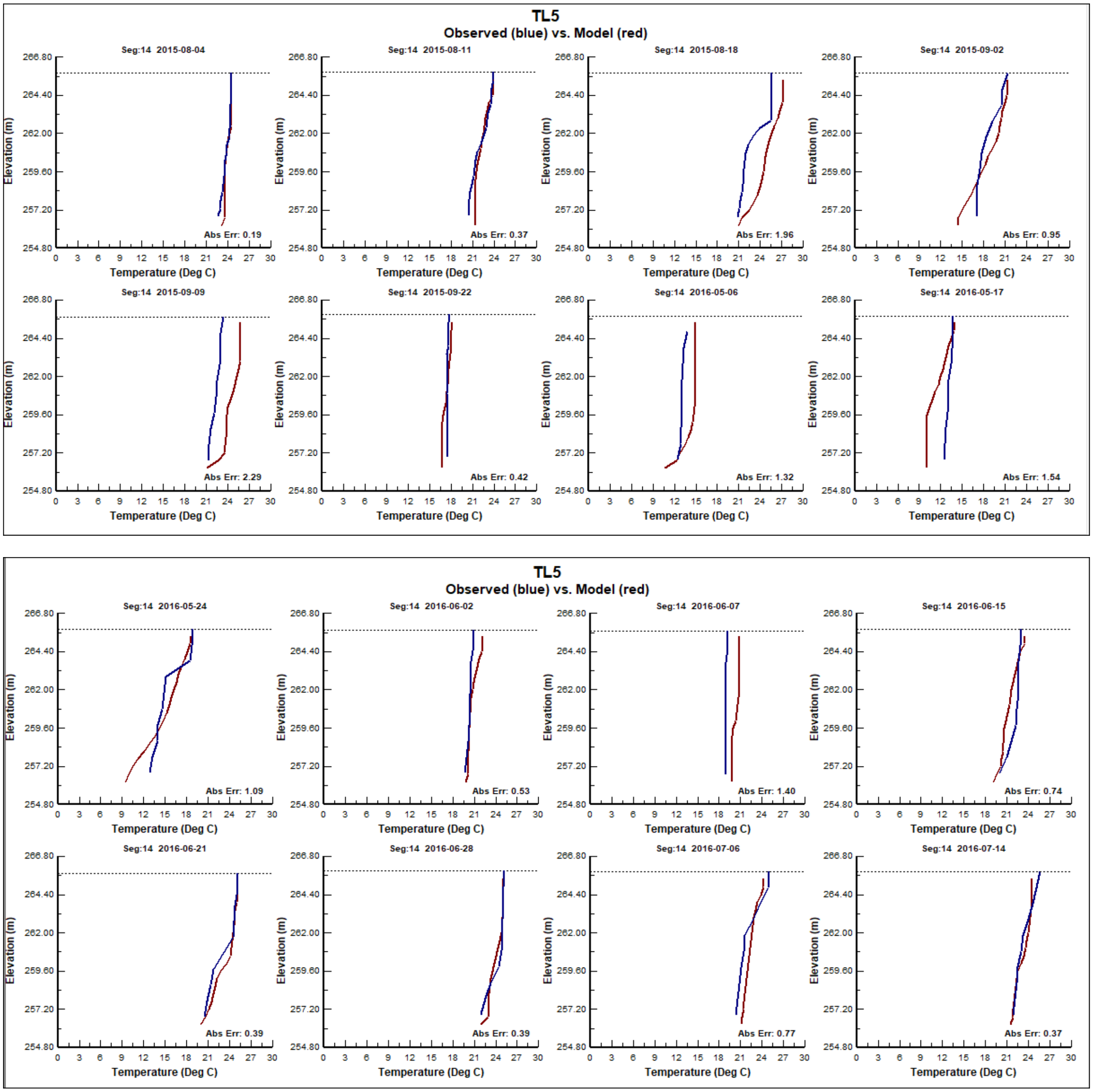

Figure 36 Computed versus observed temperatures at station TL5. Cont.

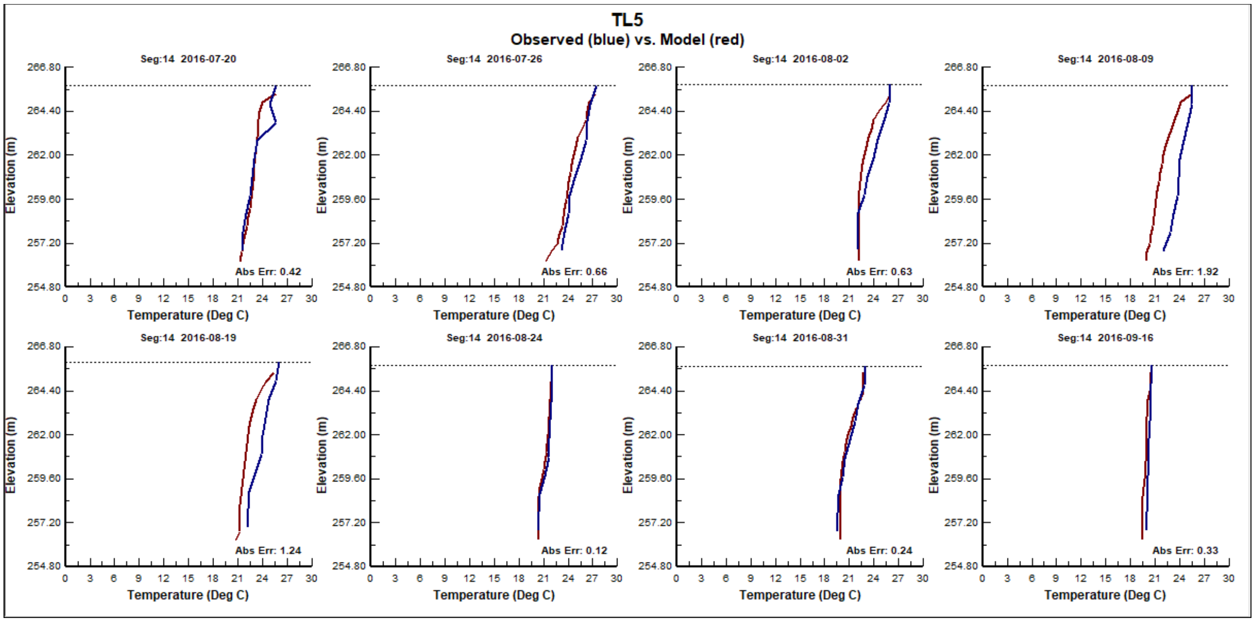

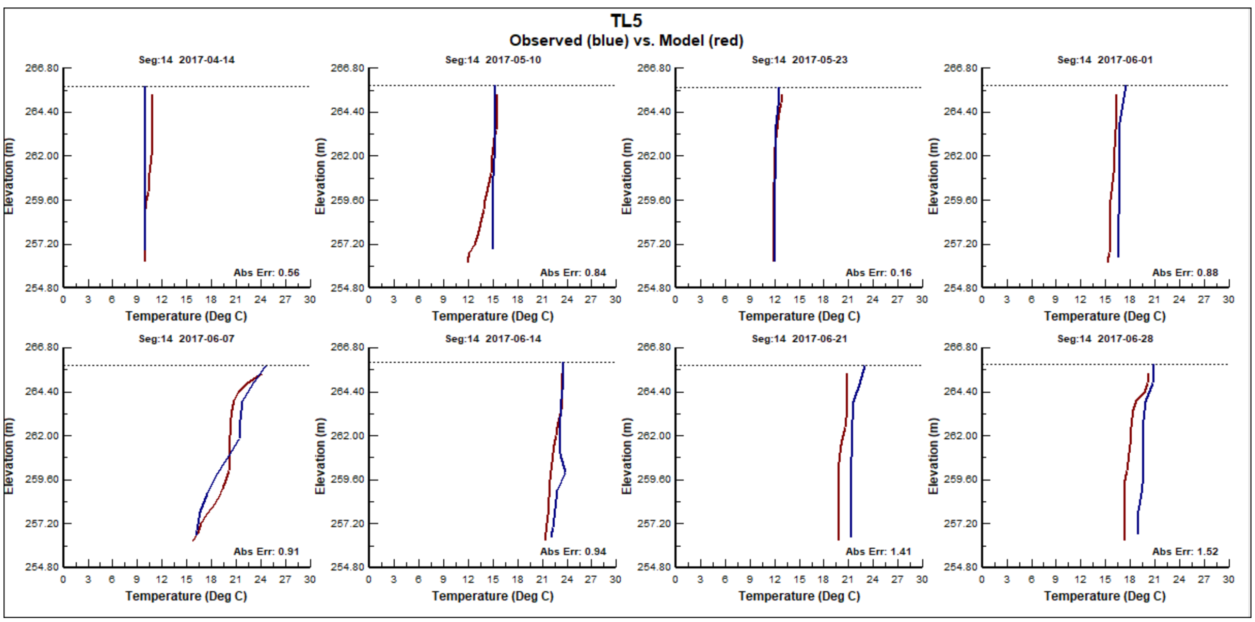

Figure 37 Computed versus observed temperatures at station TL5. Cont.

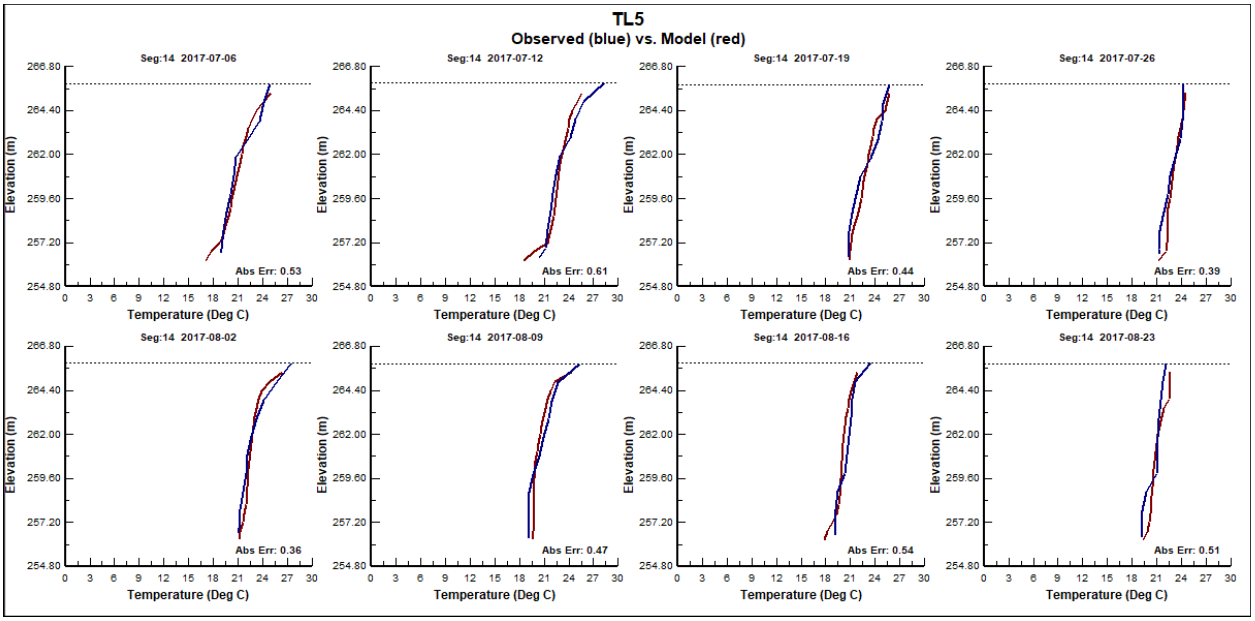

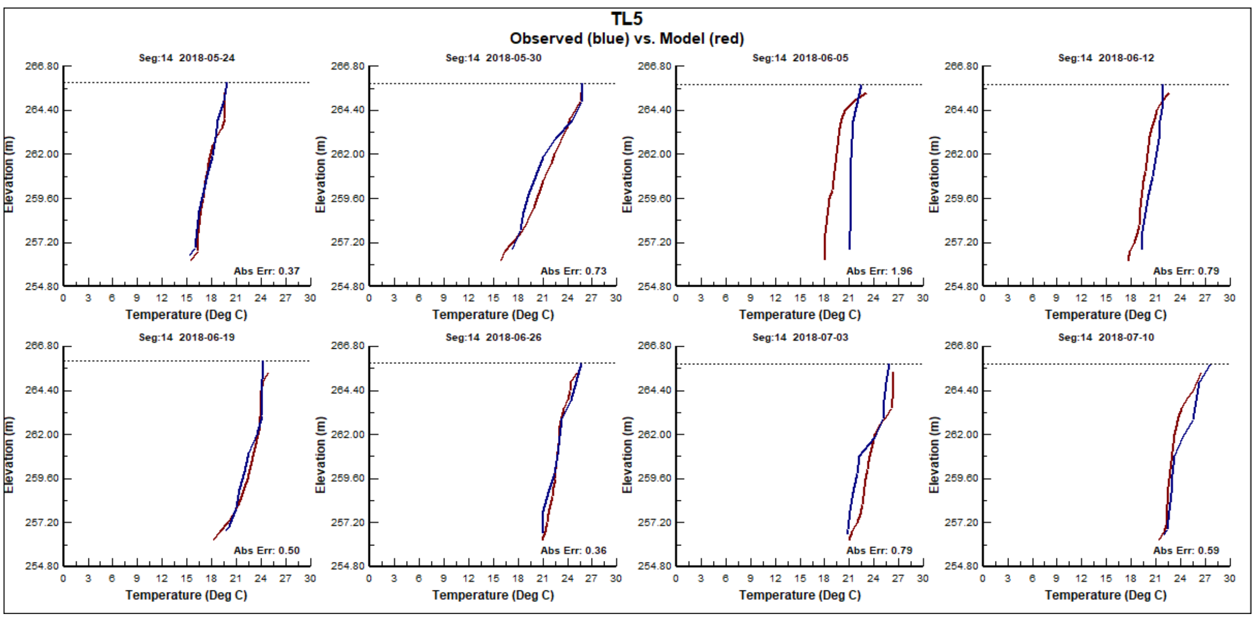

Figure 38 Computed versus observed temperatures at station TL5. Cont.

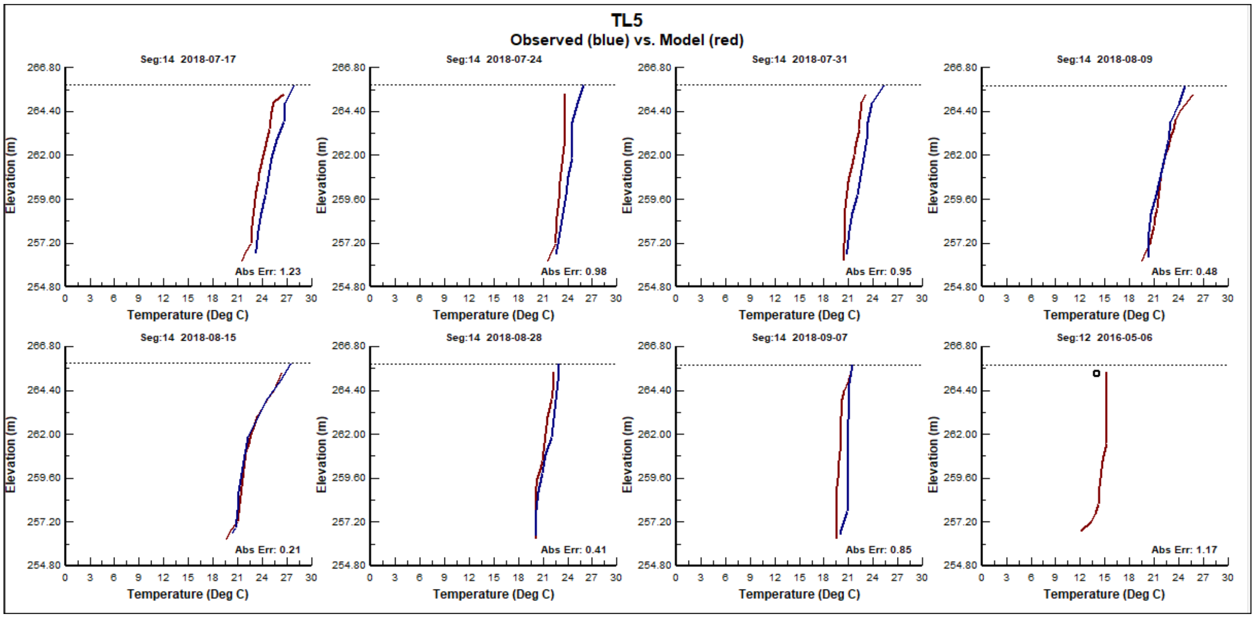

Figure 39 Computed versus observed temperatures at station TL5. Cont.

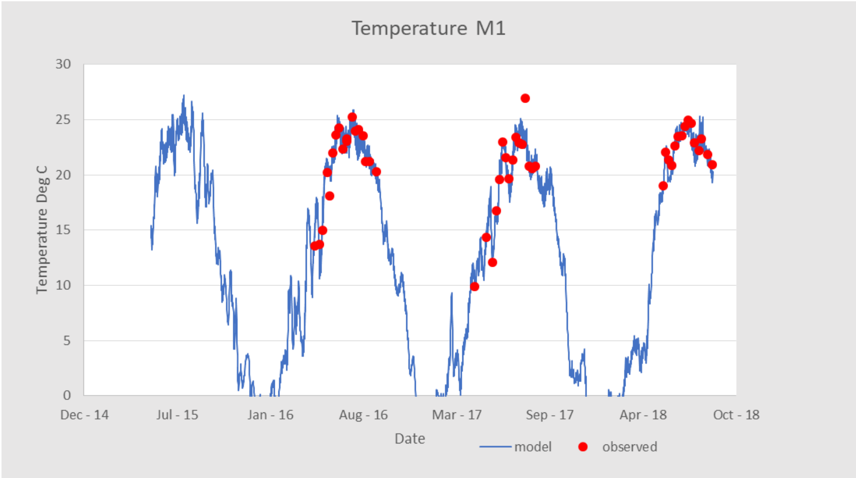

Figure 40. Computed versus observed surface temperatures at station ML1, MAE = 0.91, PBIAS = 2.3, Rel%Err = 2.1.

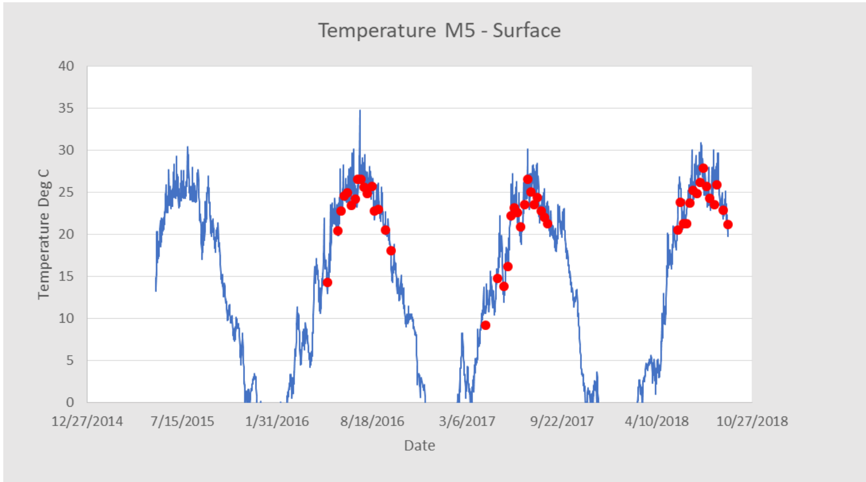

Figure 41 Computed versus observed temperatures at station ML5 – surface

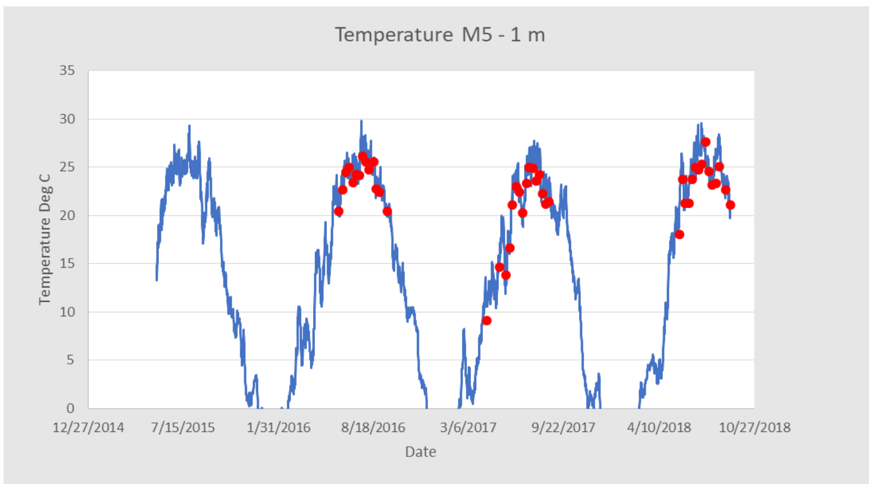

Figure 42 Computed versus observed temperatures at station ML5 – 1m

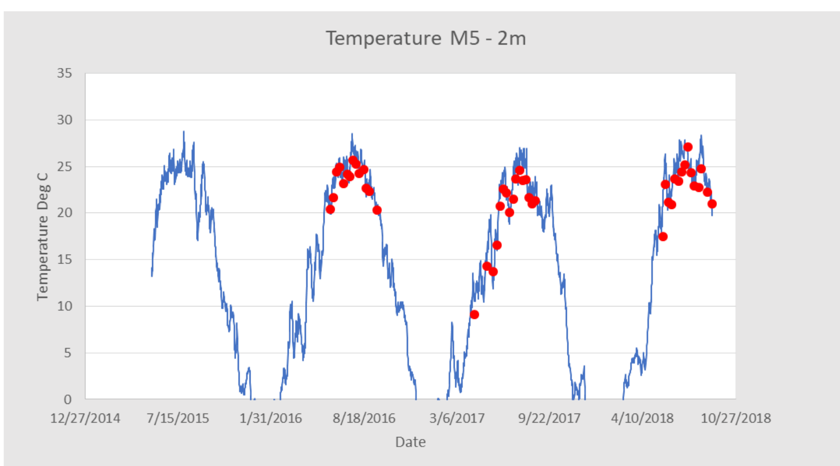

Figure 43 Computed versus observed temperatures at station ML5 – 2m

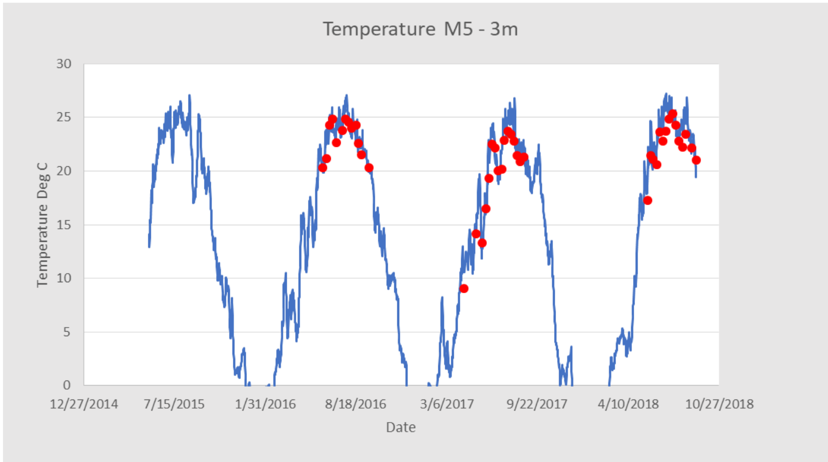

Figure 44 Computed versus observed temperatures at station ML5 – 3m

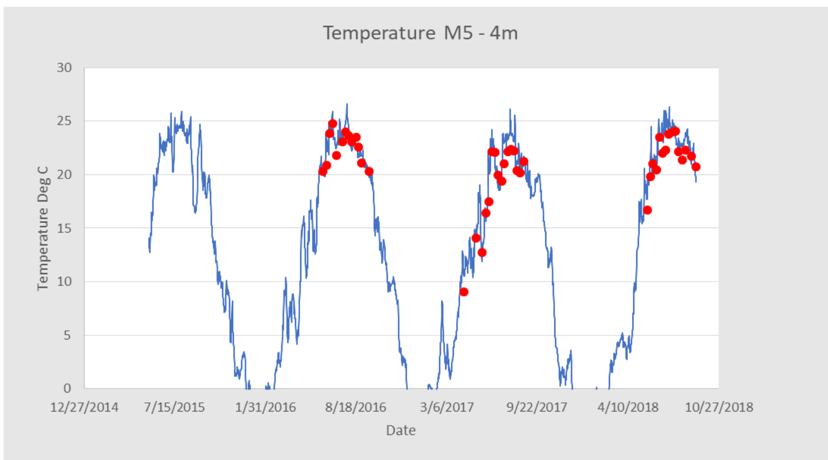

Figure 45 Computed versus observed temperatures at station ML5 – 4m

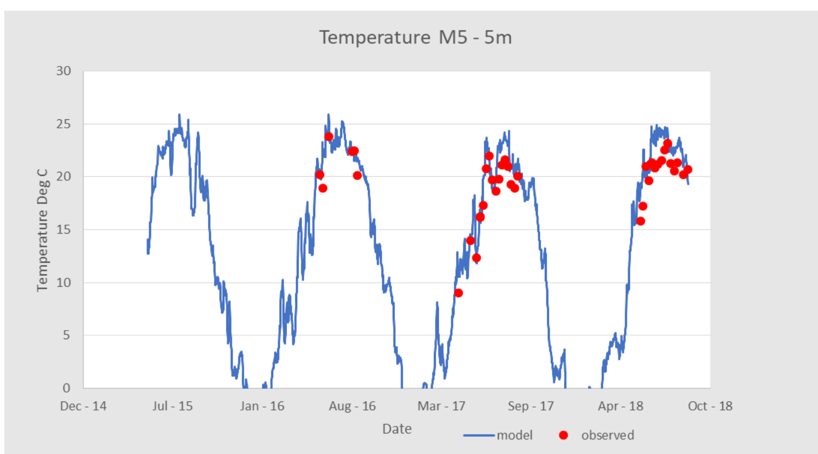

Figure 46 Computed versus observed temperatures at station ML5 – 5m

4.2.3 Water Quality Calibration

The Red Cedar W2 model was calibrated for nutrients (phosphorus and nitrogen), algae, and dissolved oxygen in an iterative cycle due to their interrelated nature. Phosphorus and nitrogen are needed for algae growth and the decay of algae excretion and algal biomass after their death are significant sources of nutrients in natural waters. Key factors controlling dissolved oxygen concentrations in the water column are increases through algal photosynthesis and its removal during algal respiration and biotic decay. Important coefficients that were adjusted during model calibration were algal temperature multipliers to simulate timing and magnitude of the three groups of algae (diatoms, greens and bluegreens), algal production rates related to light and nutrient sensitivity, nitrification rate and also nitrate decay rate. But especially critical in this system that has relatively short residence times were algal growth rates. For Tainter Lake and Lake Menomin, algal groups that can reproduce faster than they are flushed downstream can get a foothold and multiply during times of adequate nutrient and temperature conditions. All applicable model coefficients for calibrating water quality for the Red Cedar W2 model are listed in Tables 6, 7, 8, and 9.

4.2.3.1 Algae

Algal groups representing diatoms, green algae, and blue-green algae are included in the Red Cedar River model. The W2 model simulates algal groups and their interaction using user defined parameters to control growth or limitation. These algal rates were adjusted from initial values to final values reflective of typical literature values for the growth and loss characteristics of each algal group and to improve the calibration. Algal half-saturation for nitrogen limited growth (AHSN) was adjusted from 0.014 g/m3 to 0 g/m3 for the blue-green algal functional group to effectively allow for nitrogen-fixation under the assumption that a significant fraction of the blue-green algal forms are capable of nitrogen fixation.

Algae data were only collected at the surface (1-m) at TL5 and ML 5. Consequently, calibration was limited to the where the algae data were collected. Overall, the model was able to capture the surficial algal trends fairly well; however, at TL5 the model under predicted the first bluegreen peak value in 2016 and at ML5, the model didn't capture the third bluegreen peak value in 2016 or the late summer reemergence of diatoms seen in 2018 (Figure 47 and Figure 48). These discrepancies might be due a combination of poorly specified boundary conditions or localized impacts that could be occurring that are diminished in the model due to lateral averaging. In addition, the different dominant phytoplankton groups will have different growth, mortality, respiration, excretion, and settling rates and different light and nutrient growth rate half-saturation constants over time (Ref.4), which is not captured in this multi-year model that can only use a singular set of calibrated parameter values.

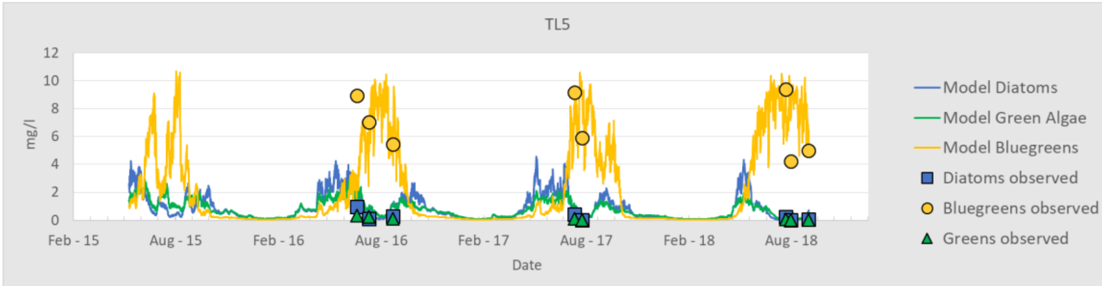

Figure 47. Surface observed algal biomass versus modeled algal biomass at station TL5

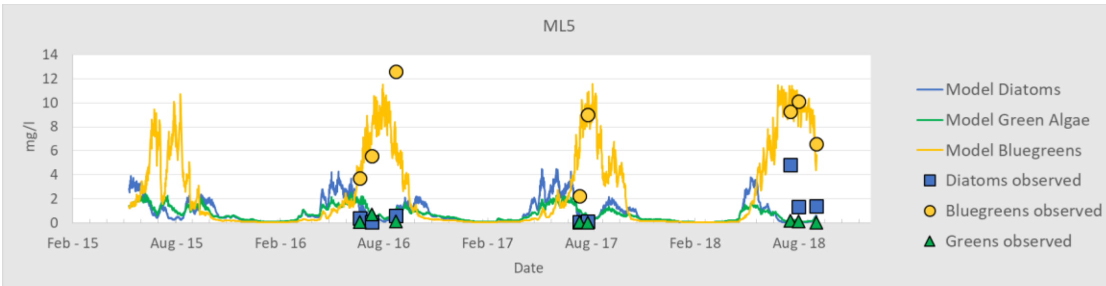

Figure 48. Surface observed algal biomass versus modeled algal biomass at station ML5.

Table 6. Water quality calibration coefficients

Algal Rates and Constants Parameter Description	**ID**	**Diatoms**	**"Green"**	**"Bluegreens"**
Maximum algal growth rate, 1/day	AG	1.5	1.2	1.5
Maximum algal respiration rate, 1/day	AR	0.04	0.04	0.04
Maximum algal excretion rate, 1/day	AE	0.05	0.05	0.05
Maximum algal mortality rate, 1/day	AM	0.1	0.1	0.08
Algal settling rate, 1/day	AS	0.3	0.2	0
Algal half-saturation for phosphorus limited growth, g/m	AHSP	0.003	0.003	0.003
Algal half-saturation for nitrogen limited growth, g/m	AHSN	0.014	0.014	0
Light saturation intensity at maximum photosynthetic rate, W/m	ASAT	100	100	100
Lower temperature for algal growth, DegC	AT1	10	10	10
Lower temperature for maximum algal growth, DegC	AT2	15	20	23
Upper temperature for maximum algal growth, DegC	AT3	22	25	30
Upper temperature for algal growth, DegC	AT4	28	30	40
Fraction of algal growth rate at AT1	AK1	0.1	0.1	0.1
Fraction of maximum algal growth rate at AT2	AK2	0.99	0.99	0.99
Fraction of maximum algal growth rate at AT3	AK3	0.99	0.99	0.99
Fraction of algal growth rate at AT4	AK4	0.1	0.1	0.1
Stoichiometric equivalent between algal biomass and phosphorus	ALGP	0.005	0.005	0.005
Stoichiometric equivalent between algal biomass and nitrogen	ALGN	0.08	0.08	0.08
Stoichiometric equivalent between algal biomass and carbon	ALGC	0.45	0.45	0.45
Ratio between algal biomass and chlorophyll- a	ALCHLA	0.15	0.25	0.07333
Fraction of algal biomass that is converted to particulate organic matter	ALPOM	0.8	0.8	0.8
Equation number for algal ammonium preference (1 or 2)	ALEQN	2	2	2
Algal half saturation constant for ammonium preference	ANPR	0.01	0.01	0.01
Oxygen equivalent for organic matter for algae growth	O2AR	1.1	1.1	1.1
Oxygen equivalent for organic matter for algae respiration	O2AG	1.4	1.4	1.4

Table 7. Organic matter calibration coefficients

Organic Rates and Constants Parameter Description	Model ID	Tainter	Menomin
Dissolved Organic Matter			
Labile DOM decay, 1/day	LDOMDK	0.05	0.05
Labile to refractory decay rate, 1/day	RDOMDK	0.001	0.001
Maximum refractory decay rate, 1/day	LRDDK	0.05	0.05
Particulate Organic Matter			
Labile POM decay rate, 1/day	LPOMDK	0.08	0.08
Labile to refractory decay rate, 1/day	RPOMDK	0.001	0.001
Maximum refractory decay rate, 1/day	LRPDK	0.01	0.01
Settling rate, m/day	POMS	0.1	0.1
Organic Matter Stoichiometry			
Fraction P	ORGP	0.005	0.005
Fraction N	ORGN	0.08	0.08
Fraction C	ORGC	0.45	0.45
Organic Rate Multipliers			
Lower Temperature for OM decay	OMT1	4	4
Upper Temperature for OM decay	OMT2	25	25
Fraction of OM decay at OMT1	OMK1	0.1	0.1
Fraction of OM decay at OMT2	OMK2	0.99	0.99

Table 8. Nutrients calibration coefficients

Nutrient Rates and Constants Parameter Description	Model ID	Tainter	Menomin
Phosphorus			
Sediment release rate	PO4R	0.01	0.01
Ammonium			
Sediment release rate	NH4R	0.001	0.001
Ammonium decay rate, 1/day	NH4DK	0.265	0.265
Ammonium rate multipliers			
Lower temperature for ammonium decay	NH4T1	5	5
Upper temperature for ammonium decay	NH4T2	25	25
Fraction of nitrification rate at NH4T1	NH4K1	0.1	0.1
Fraction of nitrification rate at NH4T2	NH4K2	0.99	0.99
Nitrate			
Nitrate decay rate	ORGP	0.005	0.005
Nitrate sediment diffusion rate	ORGN	0.08	0.08
Fraction NO3 diffused converted to SedORGN	ORGC	0.45	0.45
Nitrate Rate Multipliers			
Lower Temperature for nitrate decay	NO3T1	4	4
Upper Temperature for nitrate decay	NO3T2	25	25
Fraction of denitrification rate at NO3T1	NO3K1	0.1	0.1
Fraction of denitrification rate at NO3T2	NO3K2	0.99	0.99

Table 9. Sediment calibration coefficients

SOD Rates and Constants Parameter Description	Model ID	Tainter	Menomin
Sediment			
Fraction SOD	FSOD	1	1
Zero order SOD, g/m^2/day	SOD	1	1
First order sediment decay	SEDC	ON	ON
SOD rate multipliers			
Lower temperature for sediment decay	SODT1	4	4
Upper temperature for sediment decay	SODT2	25	25
Fraction of sediment rate at SODT2	SODK1	0.1	0.1
Fraction of sediment rate at SODT2	SODK2	0.99	0.99

4.2.3.2 Chlorophyll a

Once the model was adjusted to adequately reproduce algal growth, observed chlorophyll a data was used to estimate appropriate ratios of chlorophyll a to algal biomass (ALCHLA) for each algal group. Ratios of 0.15, 0.25, and 0.07333 were used to generate the chlorophyll a concentrations presented in Figure 49 for Tainter Lake and Figure 50 for Lake Menomin for diatoms, “greens” and cyanobacteria, respectively. As seen in Figures 49 and 50, simulated surface chlorophyll values match a general pattern of the timing and magnitude of observed concentrations, but individual comparisons are often off the mark. In addition to errors in estimating daily boundary conditions from bi-monthly sampling, simulated and observed chlorophyll a discrepancies are probably a result of the W2 model requiring the use of a static chlorophyll a to algal biomass ratio, where in reality this ratio may fluctuate depending on species abundance and environmental conditions. Table 10 summarizes the performance of the model relative to chlorophyll a simulation. The consistent negative Rel%Err values indicate that the model generally overestimates the observed data and the MAE is above the desired target listed in Table 3.

Table 10. Chlorophyll a calibration statistics.

Chlorophyll a calibration statistics	TL1	TL2	TL3	TL4	TL5	**Tainter Lake**	ML1	ML5	**Lake Menomin**
Mean absolute error (MAE) =	21.66	35.59	32.61	31.49	39.60	**32.19**	20.92	40.60	**31.07**
Percent bias (PBIAS) =	-22.80	-13.42	7.66	-8.03	-2.40	**-5.44**	-11.36	-23.34	**-19.55**
Relative % Error (Rel%Err) =	-84.07	-88.99	-79.28	-93.91	-92.26	**-87.68**	-79.41	-91.72	**-85.76**

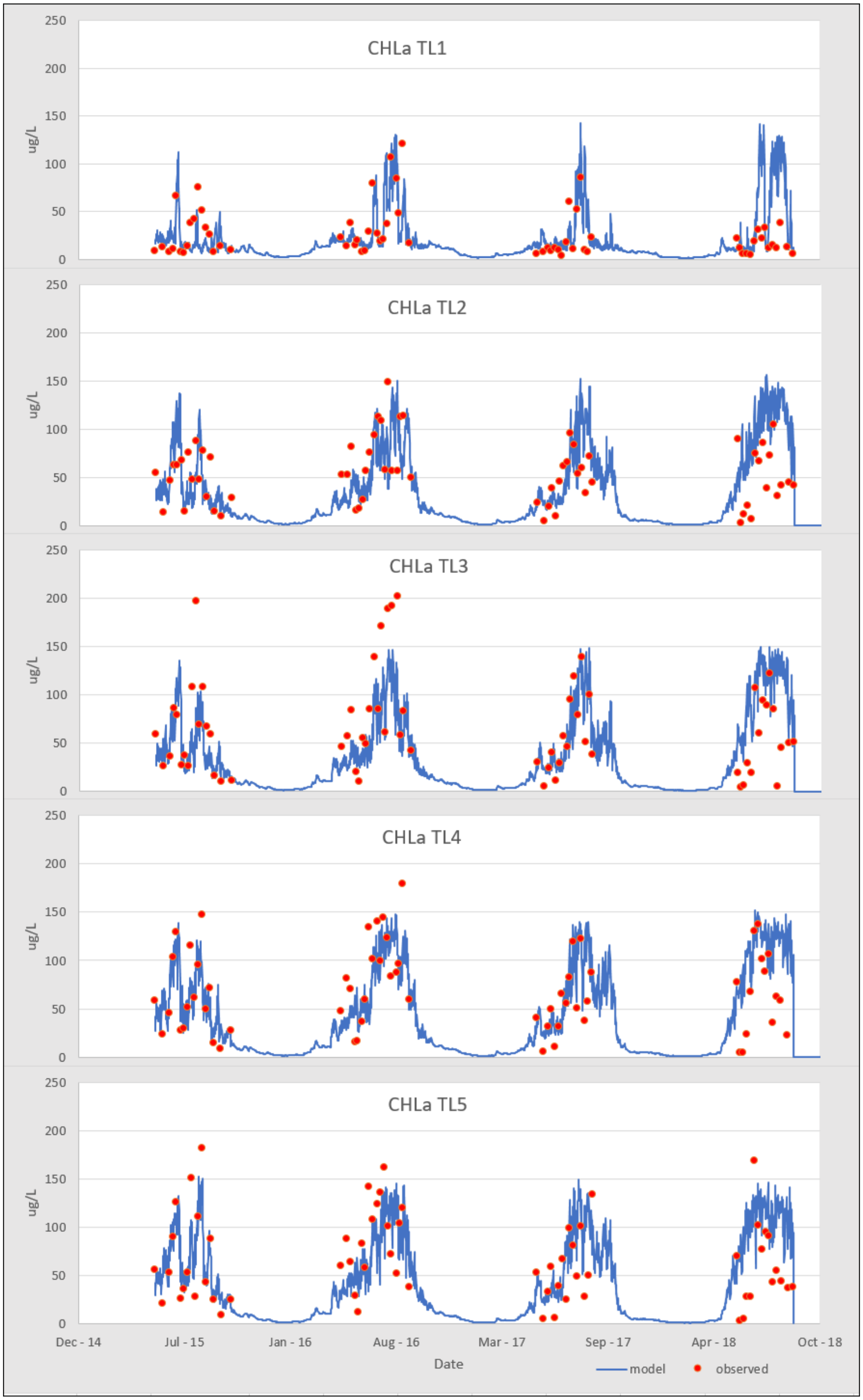

Figure 49. Tainter Lake 1-m observed chlorophyll a (red) versus model chlorophyll a (blue) based on estimated chlorophyll a to algal biomass ratios (ALCHLA).

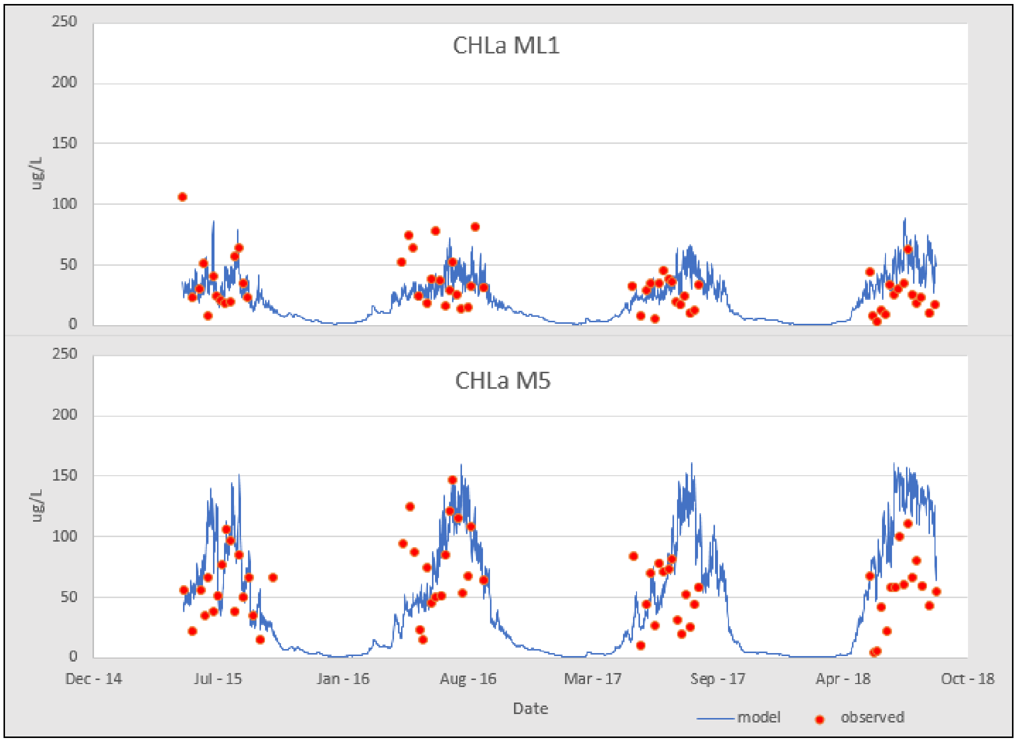

Figure 50. Lake Menomin 1-m observed chlorophyll a (red) versus model chlorophyll a (blue) based on estimated chlorophyll a to algal biomass ratios (ALCHLA).

4.2.3.3 Nutrients

Likewise to chlorophyll a, observed nutrient data were only collected at the surface using a 1-m integrated sampling tube. Even though not having profile data limited nutrient calibration to the surface, routine secchi disk measurements of around 1-m suggested that the critical zone for algal growth was limited by light to the top 1-m.

Phosphorus calibration was mostly focused on achieving a good match between simulated and observed dissolved phosphorus (phosphate), which is the phosphorus fraction used for algal growth. Particulate phosphorus is not available for algal growth unless it first cycles to the dissolved form through chemical or biological means. In the W2 model, a portion of particulate phosphorus is converted to dissolved phosphorus via microbial decomposition of organic matter (LPOM). Also included in the model is the anoxic release of some dissolved phosphorus from inorganic particulate phosphorus though the zero-order SOD routine. Only aluminum-bound phosphorus and other tightly bound phosphorus compounds remain largely unavailable for algal growth (RPOM). Observed total phosphorus (TP) measurements, which includes all forms of phosphorus, had a target MAE of 0.02 mg/l. Model performance for phosphate and total phosphorus are shown in Figure 51 and Figure 53 for Tainter Lake and Figure 52 and Figure 54 for Lake Menomin, respectively.

Surficial ammonium (NH4) and nitrate/nitrite (NO3/NO2) calibration was performed using the default W2 model's decay and nitrification rates and sediment release rates. As long as the model has reasonable boundary conditions and is correctly simulating algal processes (growth, excretion, respiration and mortality), the default settings for nitrogen seem to work well. Model performance for ammonium and nitrate/nitrite are shown in Figure 55 and Figure 57 for Tainter Lake and Figure 56 and Figure 58 for Lake Menomin, respectively.

Table 11 presents the calibration statistics for nutrients. The resulting MAEs for phosphate (PO4) for Tainter Lake was 0.015 mg/l and 0.014 mg/L for Lake Menomin, which were both very close to the calibration target value of 0.01 mg/L. Total phosphorus (TP), ammonium (NH4), and nitrate/nitrite (NO3/NO2) MAEs were all a bit above the calibration targets (Table 3), but total kjeldahl nitrogen (TKN) (Figure 59 and Figure 60) and total organic carbon (TOC) (Figure 61 and Figure 62) met the calibration objectives.

Table 11. Calibration statistics for nutrients.

Nutrient (MAE calibration target)	Statistic	TL1	TL2	TL3	TL4	TL5	Tainter Lake	ML1	ML5	Lake Menomin
PO4 (0.01 mg/l)	MAE	0.019	0.015	0.015	0.014	0.013	0.015	0.018	0.010	0.014
	PBIAS	11.06	-7.21	-13.35	-3.29	-15.94	-2.23	-32.90	-28.35	-31.41
	*R*el%Err	3.27	-6.69	-63.94	-249.3	-291.78	-121.68	-59.09	-134.67	-96.88
TP (0.02 mg/l)	MAE	0.046	0.028	0.029	0.022	0.022	0.029	0.016	0.025	0.021
	PBIAS	32.31	20.56	22.87	14.74	13.21	21.61	8.45	5.36	6.88
	*R*el%Err	29.79	15.71	19.21	9.47	6.94	16.27	4.06	-6.57	-1.42
NH4 (0.03 mg/l)	MAE	0.06	0.05	0.06	0.06	0.07	0.06	0.08	0.06	0.07
	PBIAS	43.71	3.43	10.77	-19.80	-34.23	13.40	34.32	-35.37	9.74
	*R*el%Err	34.85	0.19	1.78	-34.50	-105.21	-37.50	0.74	-2.54	-39.35
Nitrate/Nitrite (0.1 mg/l)	MAE	0.30	0.40	0.47	0.53	0.53	0.45	0.27	0.45	0.36
	PBIAS	-12.39	-38.79	-49.05	-54.80	-57.46	-39.75	-23.29	-48.46	-29.85
	*R*el%Err	-21.42	-55.64	-107.46	-108.83	-95.81	-77.83	-26.88	-36.49	-44.38
TKN (0.4 mg/l)	MAE	0.28	0.31	0.33	0.29	0.35	0.31	0.18	0.54	0.36
	PBIAS	6.78	-14.24	7.96	-15.39	-29.66	-8.94	-4.72	-36.61	-22.71
	*R*el%Err	-6.48	-32.36	-12.12	-34.60	-24.45	-27.20	-13.37	-30.67	-45.87
TOC (5 mg/l)	MAE	1.83	1.42	1.43	2.03	1.32	1.61	1.80	3.39	1.61
	PBIAS	31.28	7.13	12.62	13.31	-1.37	12.30	34.96	-15.76	9.67
	*R*el%Err	29.37	5.02	9.52	1.81	-4.89	1.64	32.13	-19.84	6.14

4.2.3.4 Dissolved Oxygen

Dissolved oxygen is challenging to correctly calibrate due to the many processes that affect the concentration. Moreover, even if a particular set of calibration values provides reasonable results, there can be uncertainty that it was done for the right reason. Sources of oxygen in the model are from inflows, surface exchange and mixing, and algal photosynthesis. Oxygen is lost through the decomposition of organic matter in the sediment (SOD), decomposition of organic matter in the oxic water column (BOD), and outflow from the reservoirs. The calibration approach for the Red Cedar model focused on using as many default settings for unmeasured parameters and only changing necessary parameter values within reasonable limits. The main calibration adjustment after inflows and algal growth were estimated was changing SOD values. Even though each segment in the model can have its own specific SOD values, without observed data, it was decided to use a 1 g/m^2/day SOD for all segments. The SOD is a zero-order sediment compartment that provides organic sediment contributions to nutrients and dissolved oxygen demand that does not vary over time except as a result of temperature dependence of the decay rate. Combining the SOD with the first-order sediment compartment (SED), which accounts for sediment accumulation, a satisfactory dissolved oxygen calibration was achieved. It is important to note, even though SED can predict some effects of changes of allochthonous material loading, there is no release of phosphorus or other diagenesis products when overlying water is anoxic since this sediment compartment is labile, oxic decay of organics on the sediment surface (Ref. 4). Plots showing simulated versus observed DO profiles are provided in Figure 63 through Figure 66 for TL5, and MAE statistics is presented in Table 12.

Table 12. Dissolved Oxygen MAE statistics for Tainter Lake and Lake Menomin.

Dissolved Oxygen Mean Absolute Error (mg/L)					
Tainter Lake	**TL1**	**TL2**	**TL3**	**TL4**	**TL5**
1.93	1.99	2.04	1.99	1.90	1.90
Lake Menomin	**ML1**			**ML5**	
2.0	1.08			2.18	

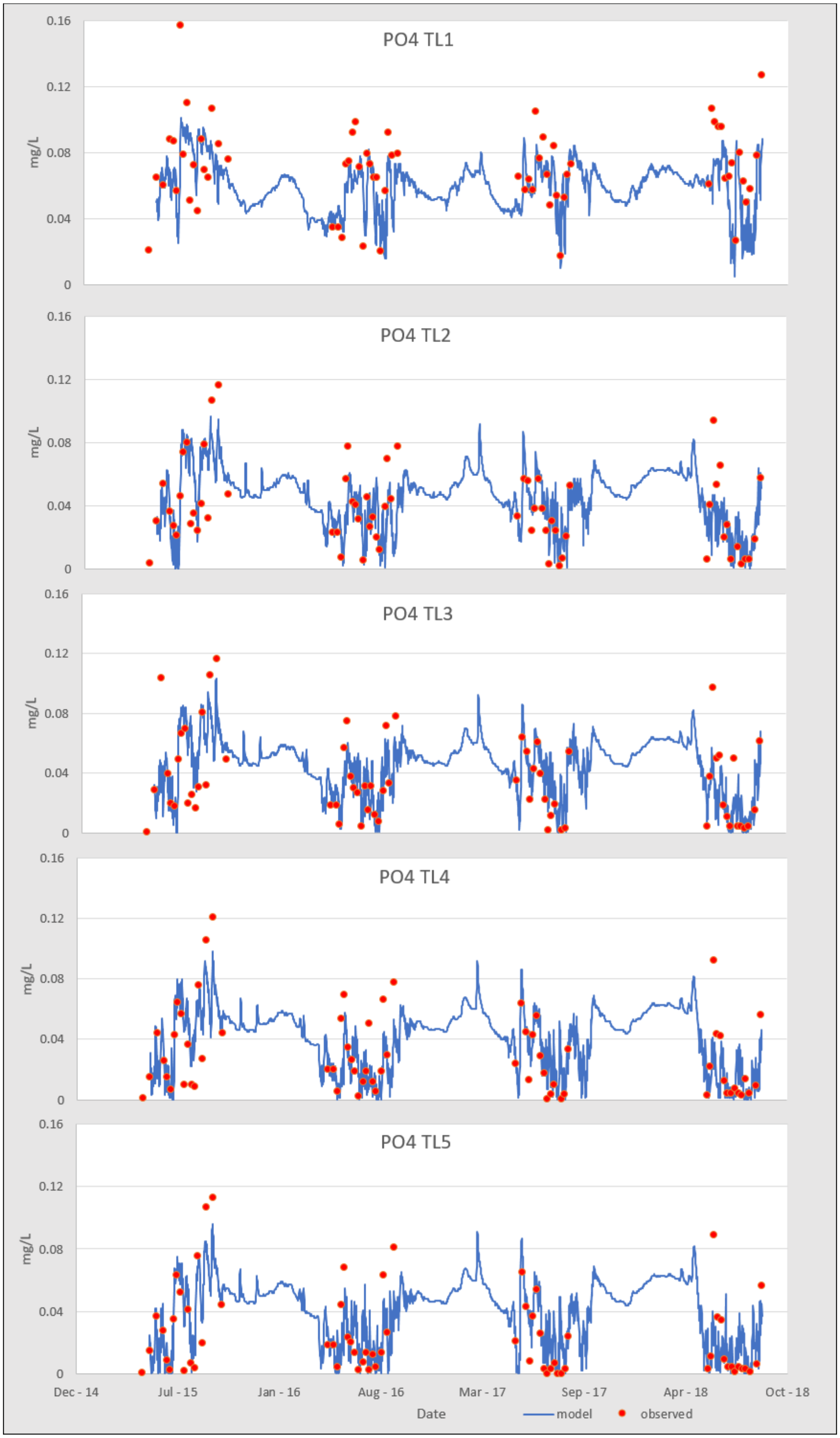

Figure 51. Tainter Lake (TL5) 1-m phosphate calibration, model (blue) vs. observed SRP (red).

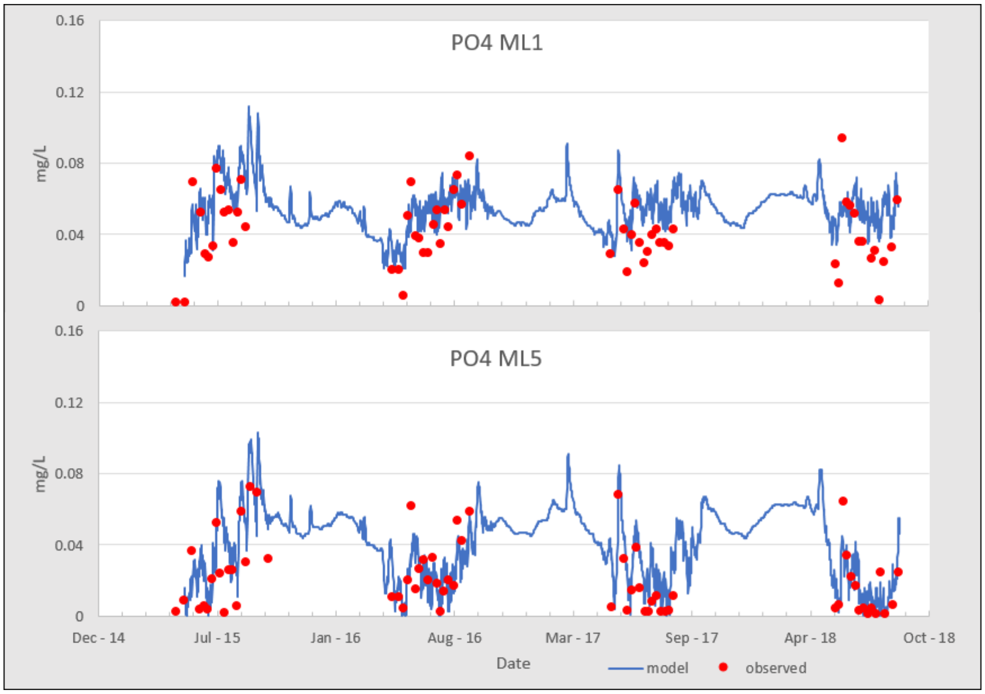

Figure 52. Lake Menomin (ML5) 1-m phosphate calibration, model (blue) vs. observed SRP (red).

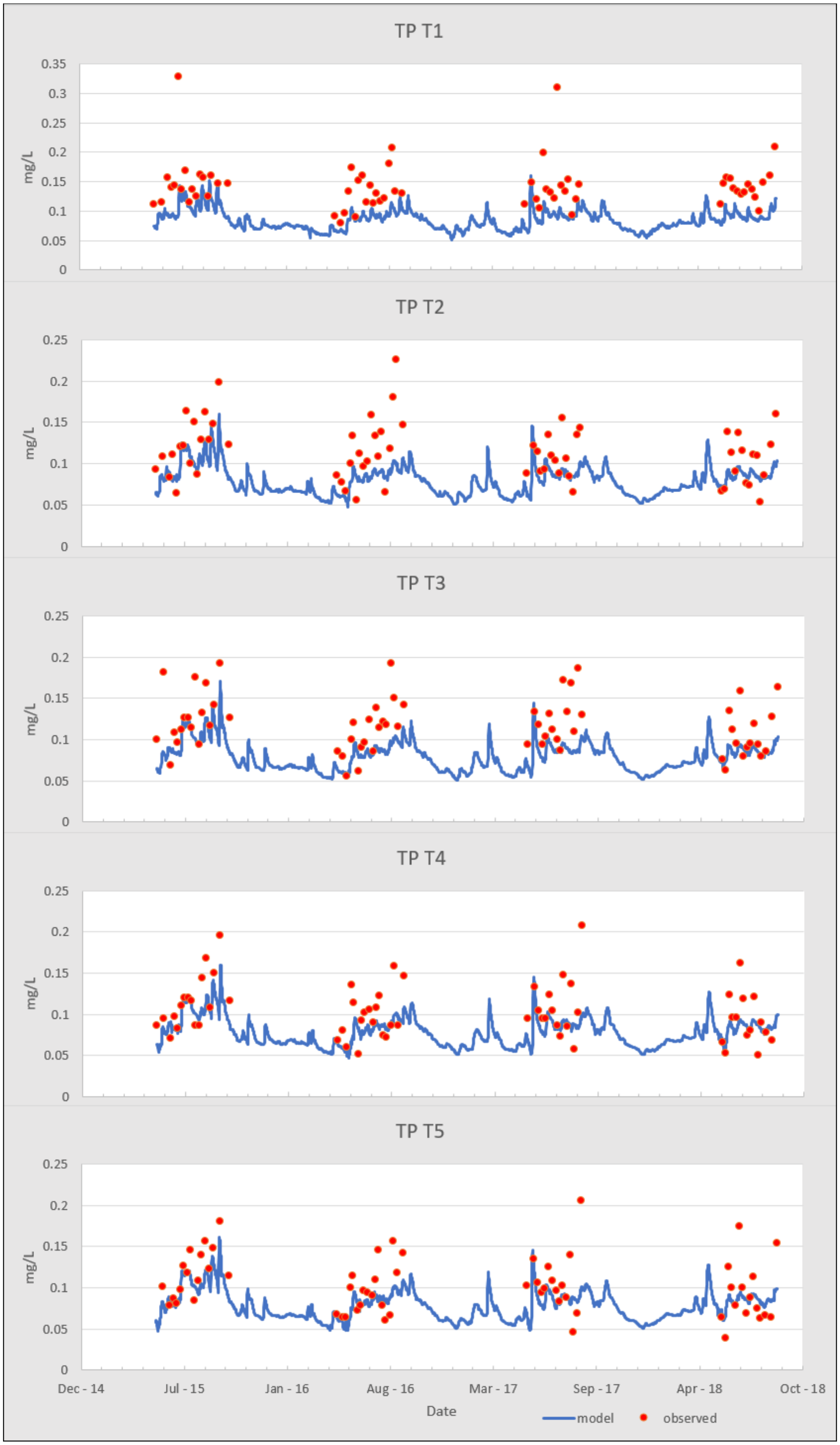

Figure 53. Tainter Lake (TL5) 1-m total phosphorus (TP) calibration, model (blue) vs. observed (red).

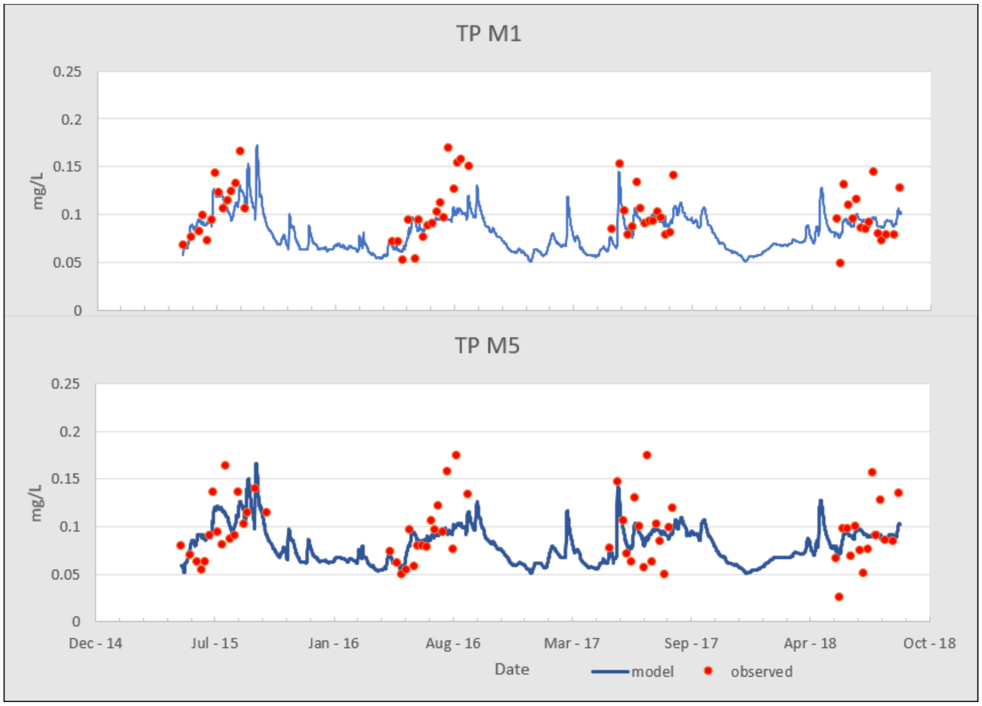

Figure 54. Lake Menomin (ML5) 1-m total phosphorus (TP) calibration, model (blue) vs. observed (red).

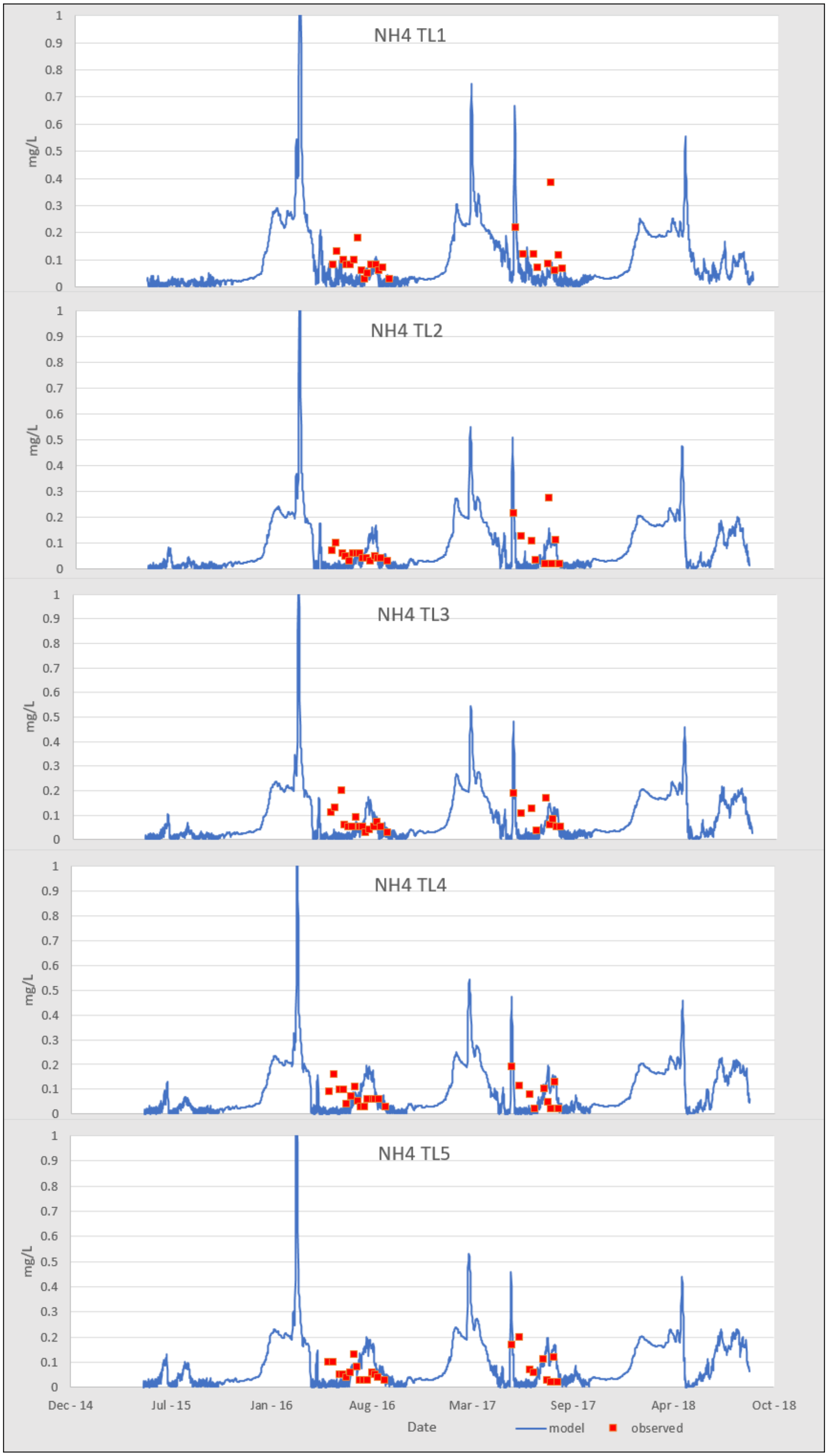

Figure 55. Tainter Lake (TL5) 1-m ammonium (NH4) calibration, model (blue) vs. observed (red).

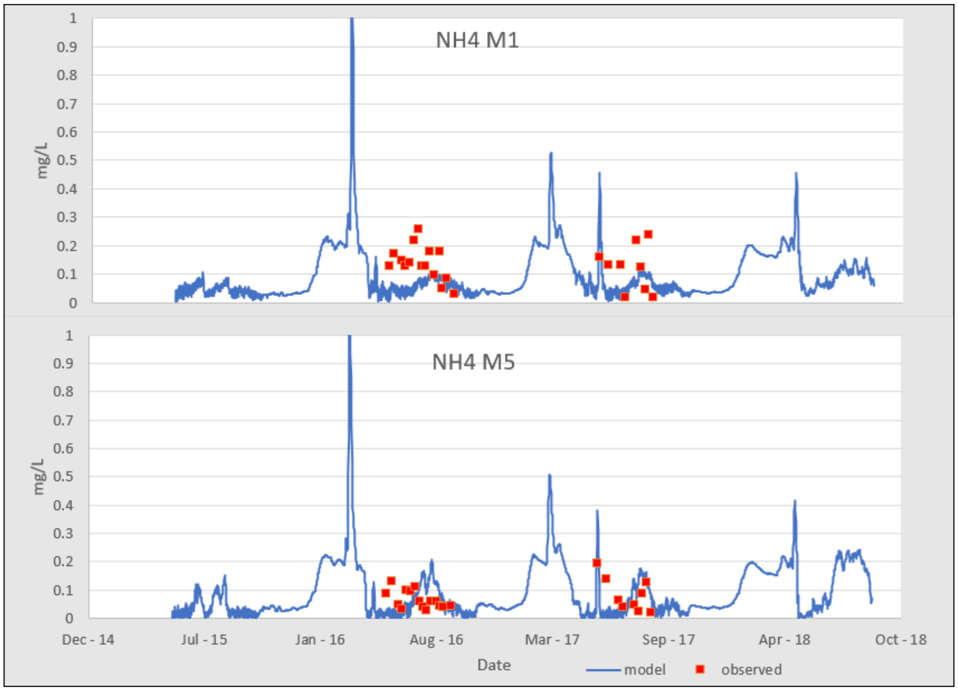

Figure 56. Lake Menomin (ML5) 1-m ammonium (NH4) calibration, model (blue) vs. observed (red).

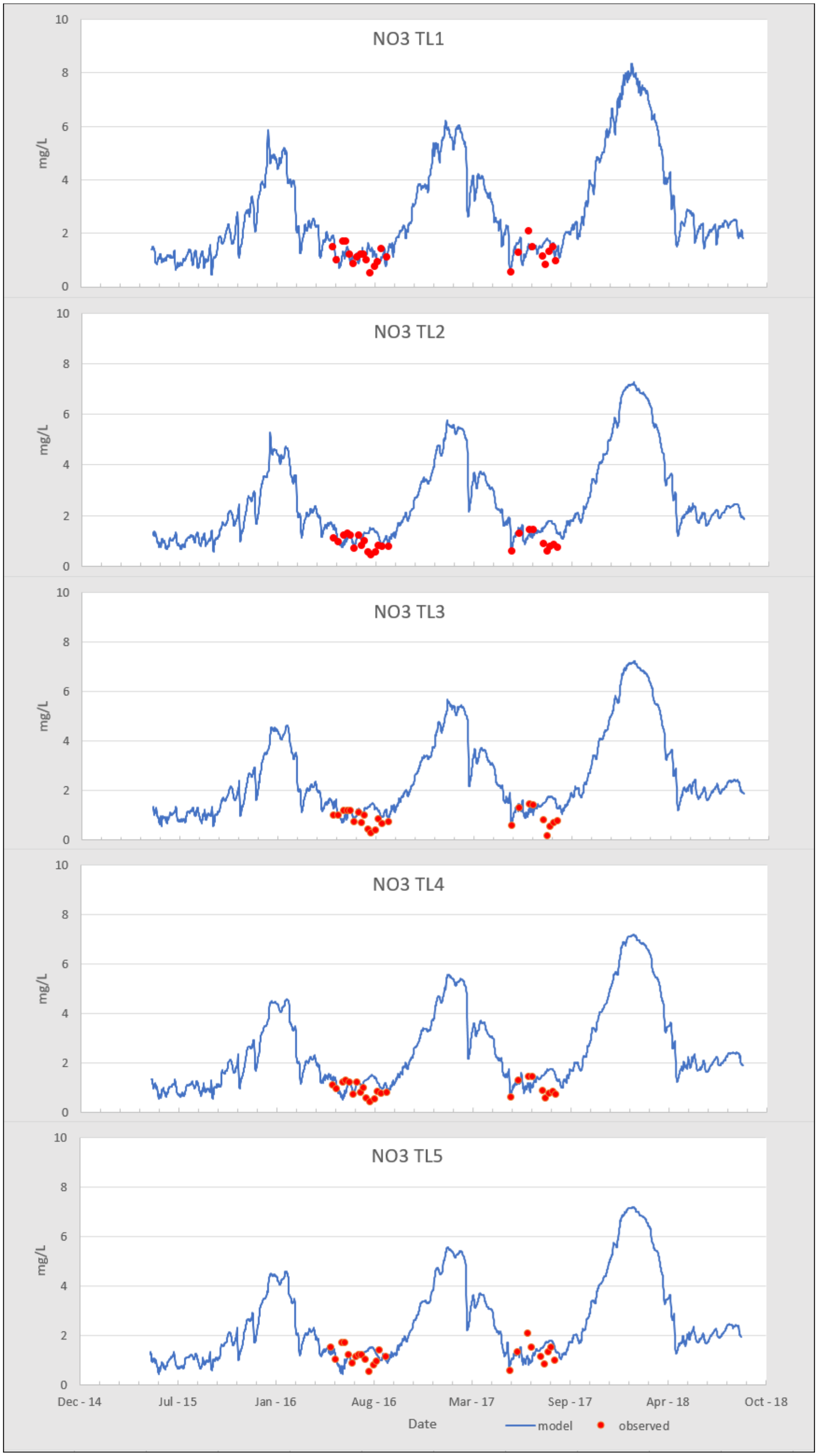

Figure 57. Tainter Lake (TL5) 1-m nitrate/nitrite (NO3/NO2) calibration, model (blue) vs. observed (red).

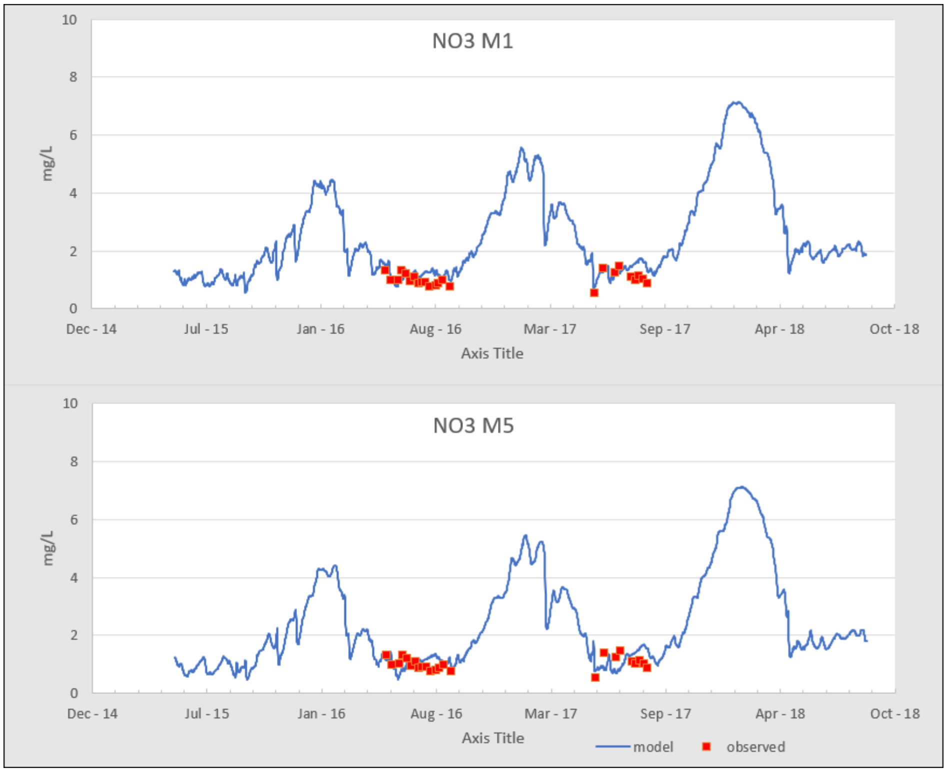

Figure 58. Lake Menomin (ML5) 1-m nitrate/nitrite (NO3/NO2) calibration, model (blue) vs. observed (red).

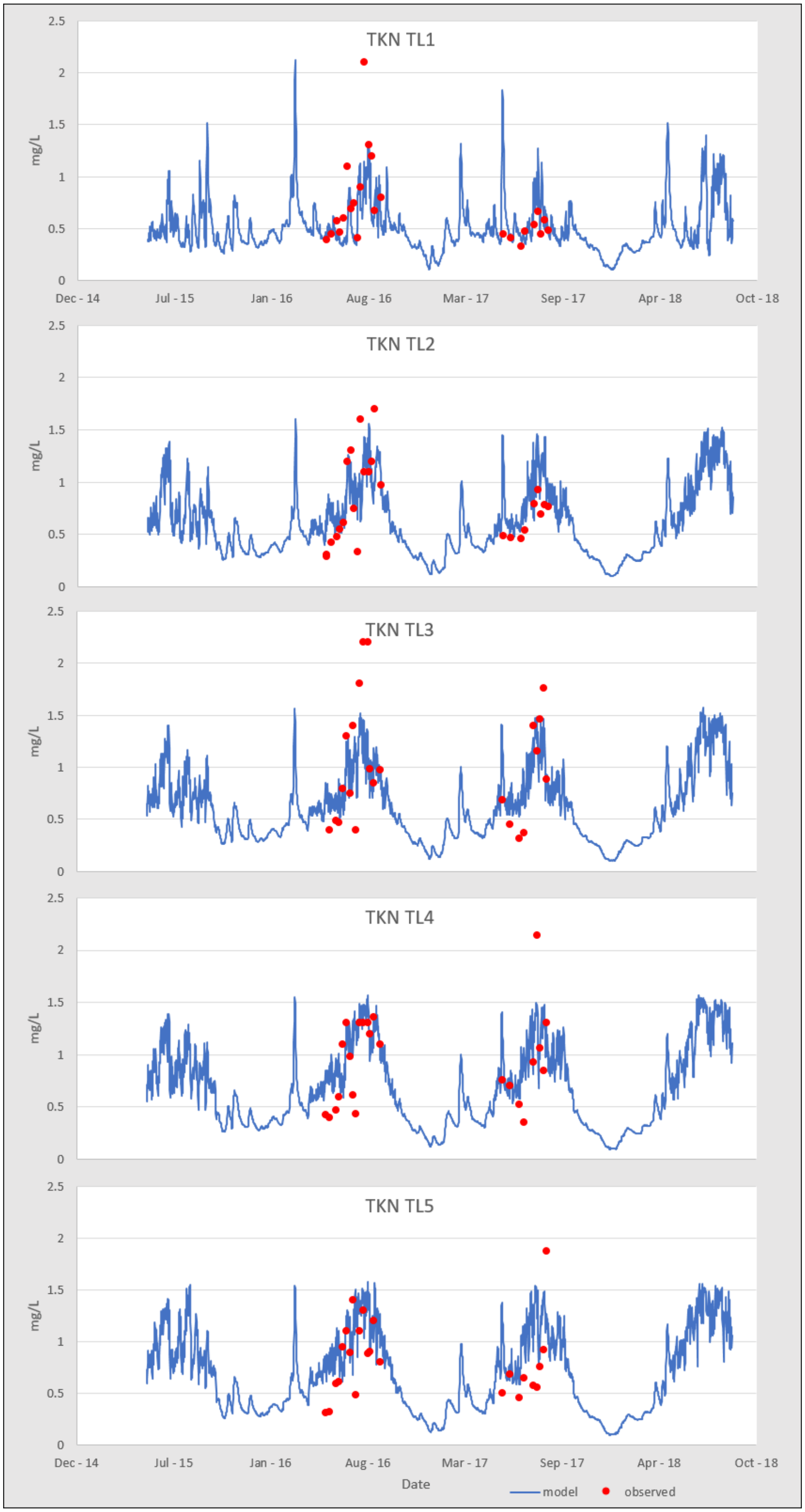

Figure 59. Tainter Lake (TL5) 1-m total kjeldahl nitrogen (TKN) calibration, model (blue) vs. observed (red).

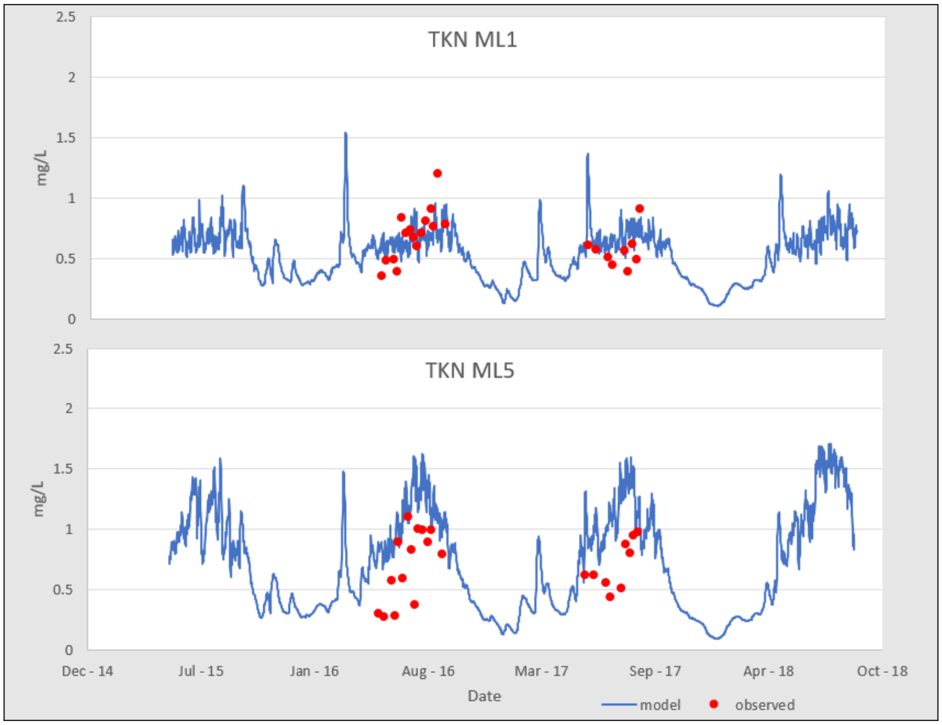

Figure 60. Lake Menomin (ML5) 1-m total kjeldahl nitrogen (TKN) calibration, model (blue) vs. observed (red).

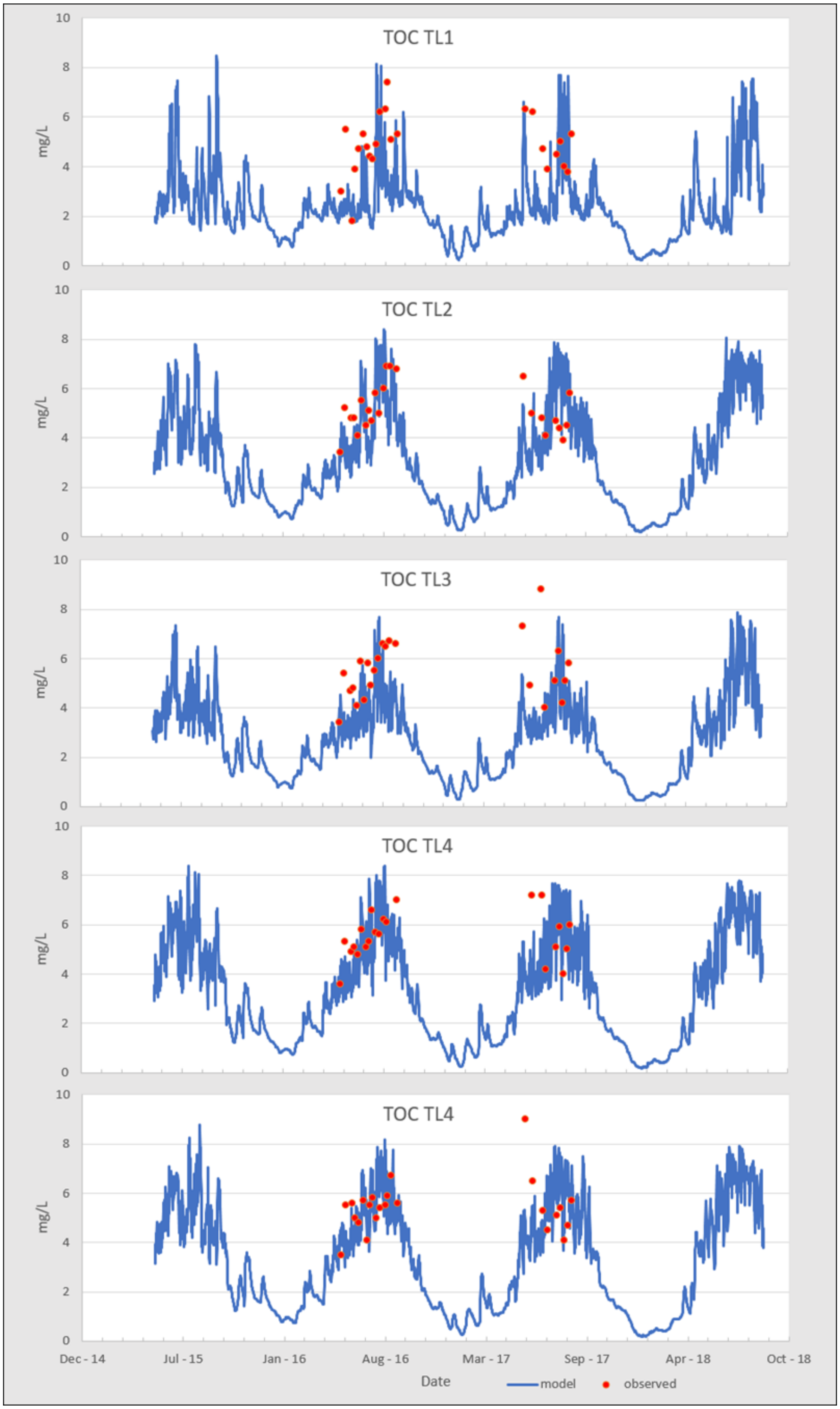

Figure 61. Tainter Lake (TL5) 1-m total organic carbon (TOC) calibration, model (blue) vs. observed (red).

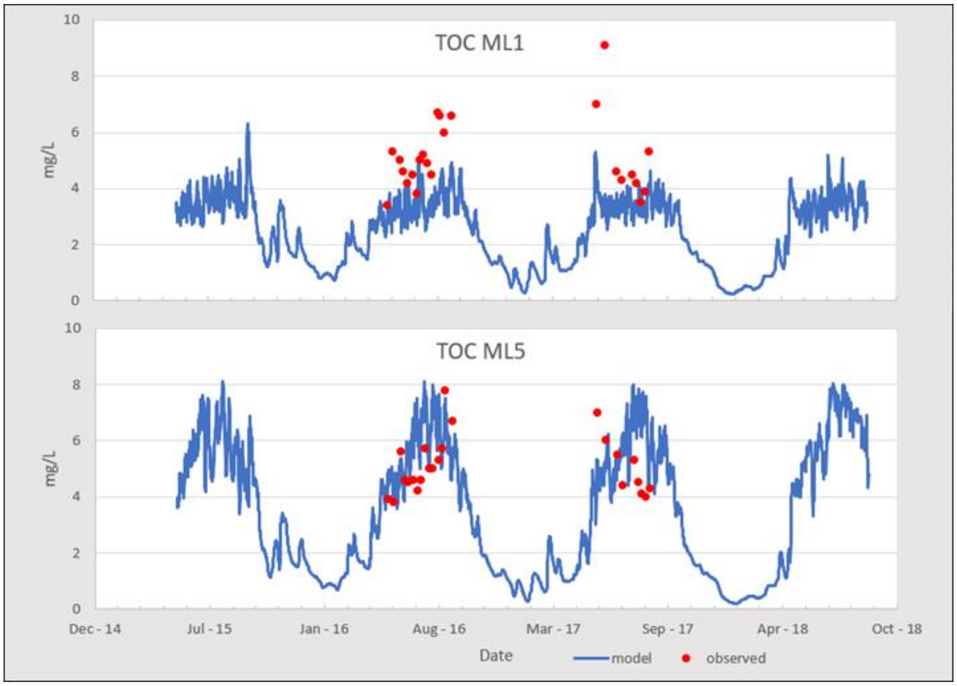

Figure 62. Lake Menomin (ML5) total organic carbon (TOC) calibration, model (blue) vs. observed (red).

.

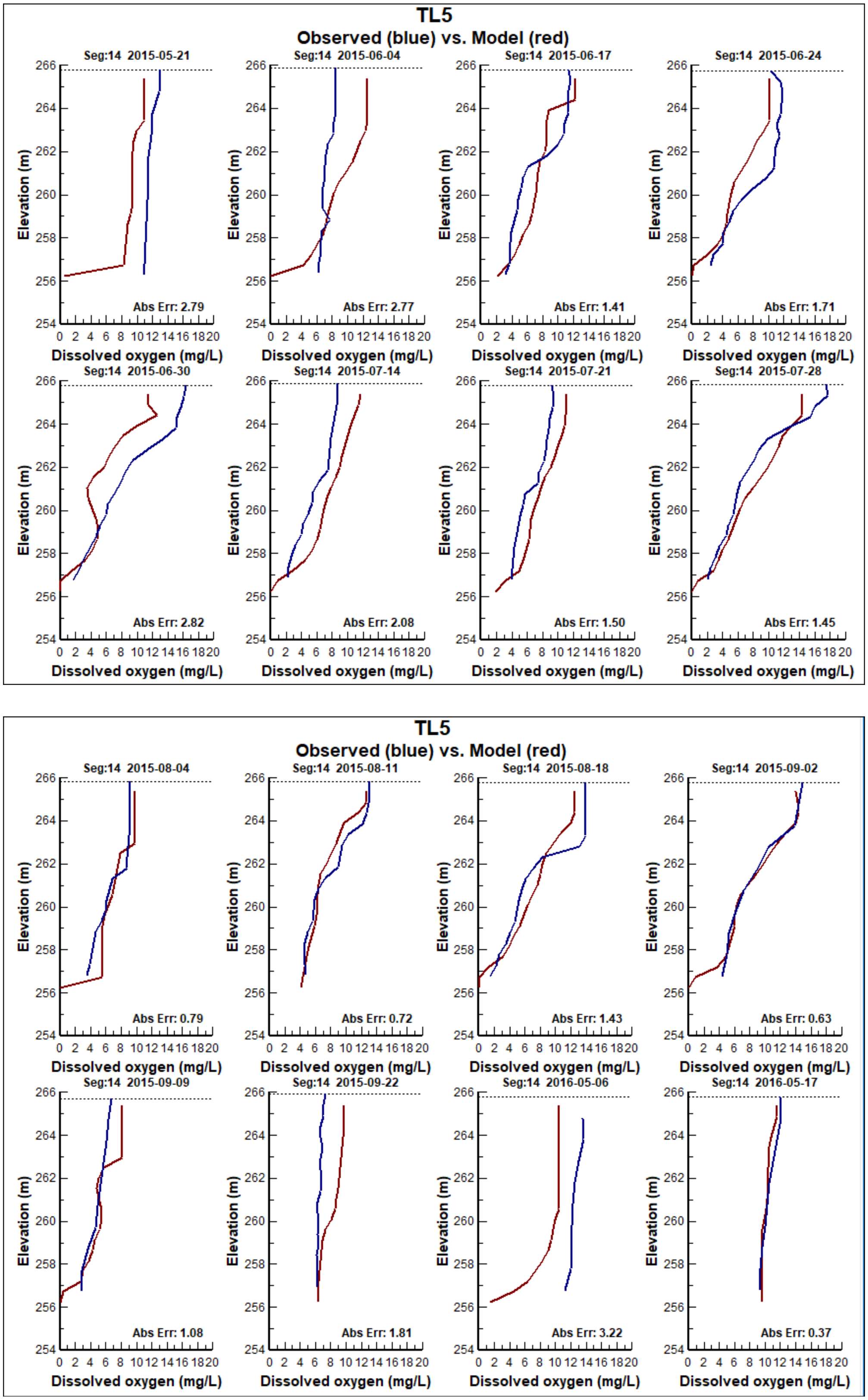

Figure 63. Observed (blue) vs model (red) dissolved oxygen profiles at TL5.

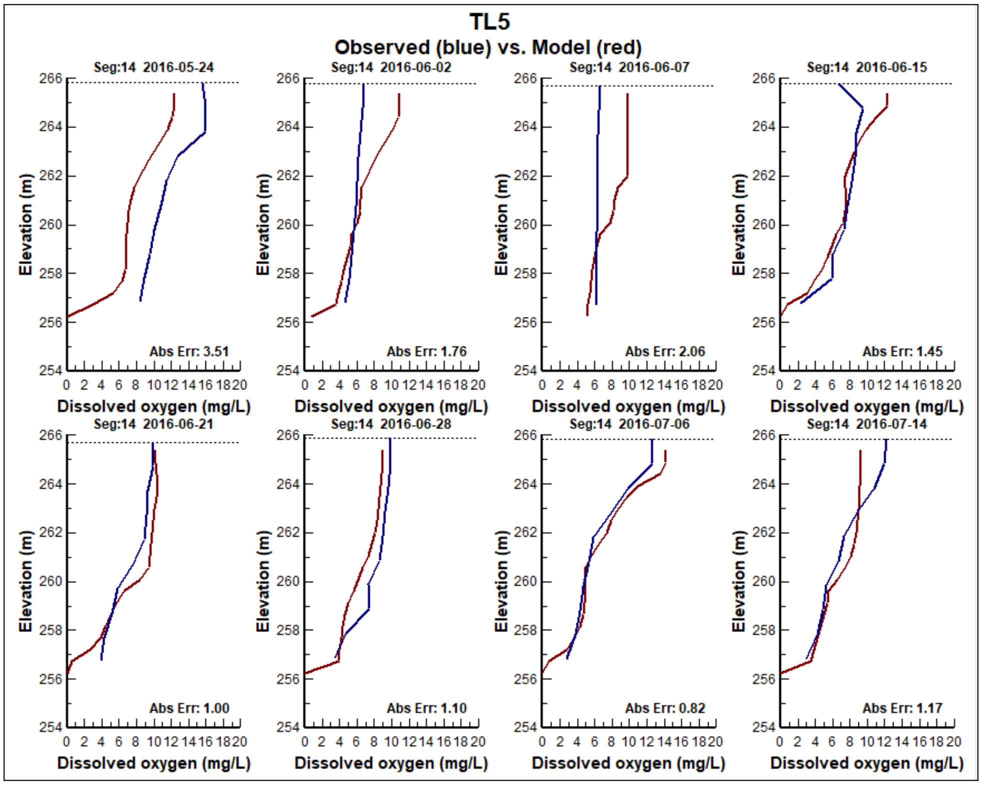

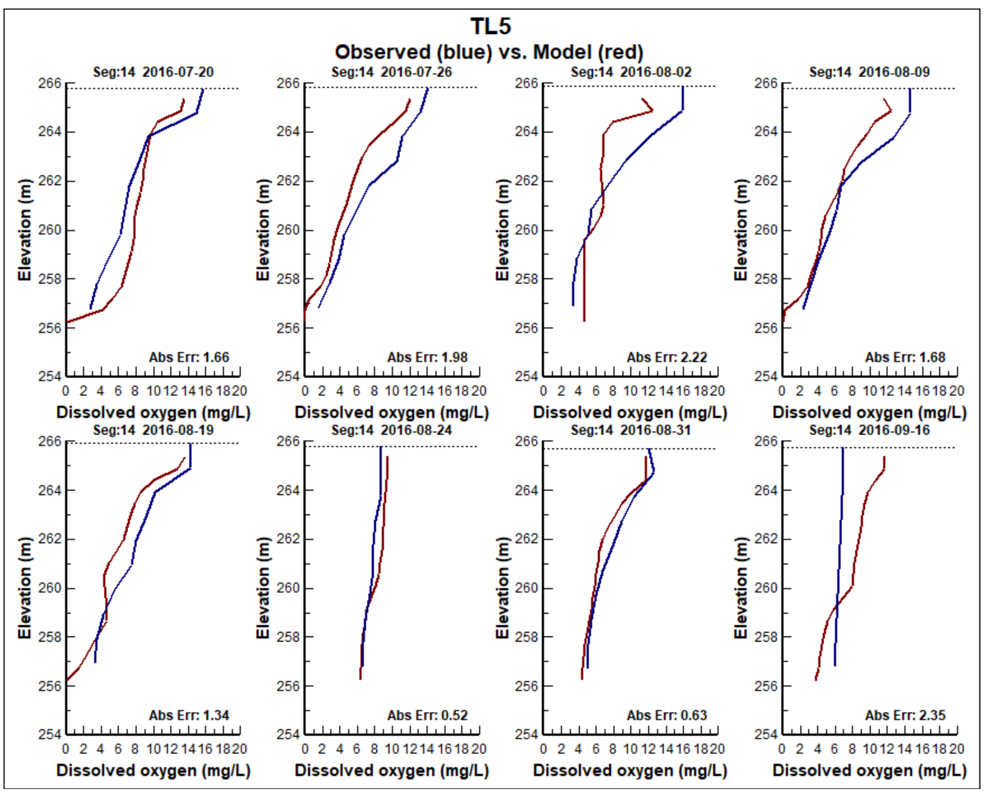

Figure 64. Observed (blue) vs model (red) dissolved oxygen profiles at TL5.Cont.

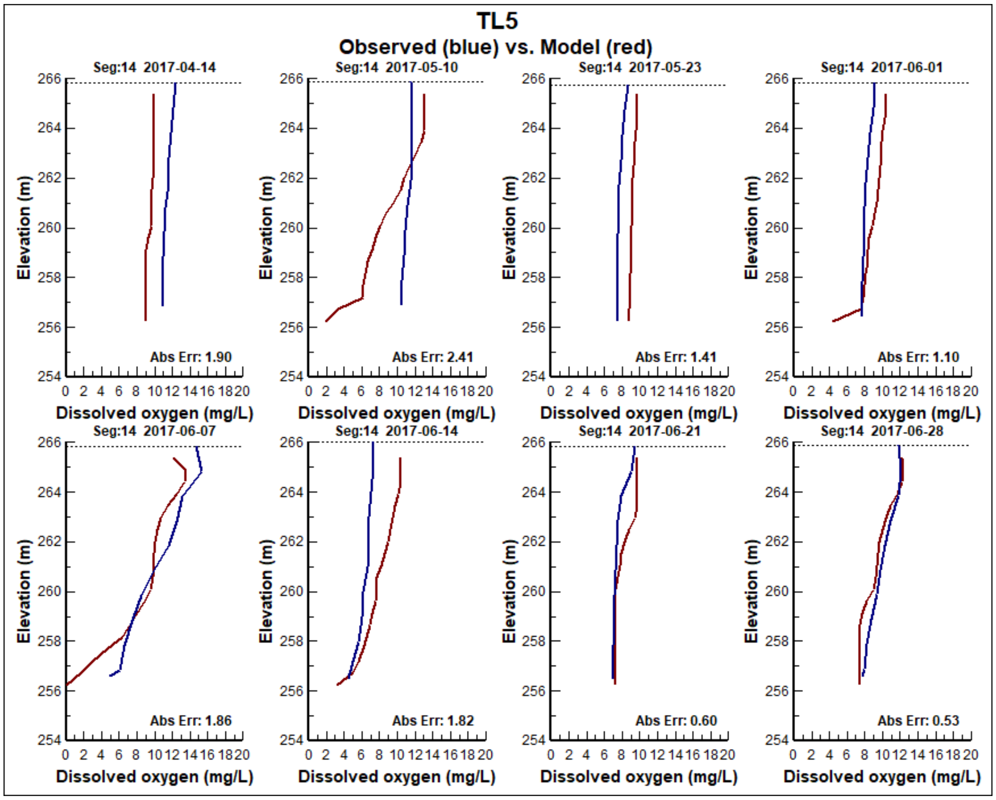

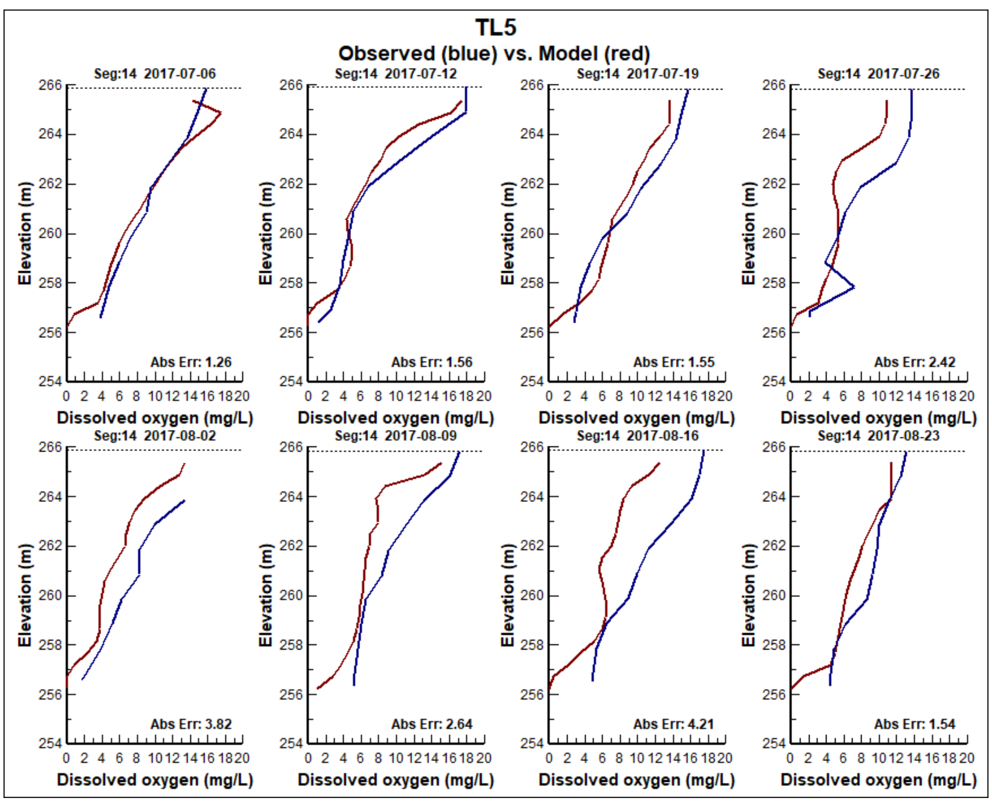

Figure 65. Observed (blue) vs model (red) dissolved oxygen profiles at TL5.Cont.

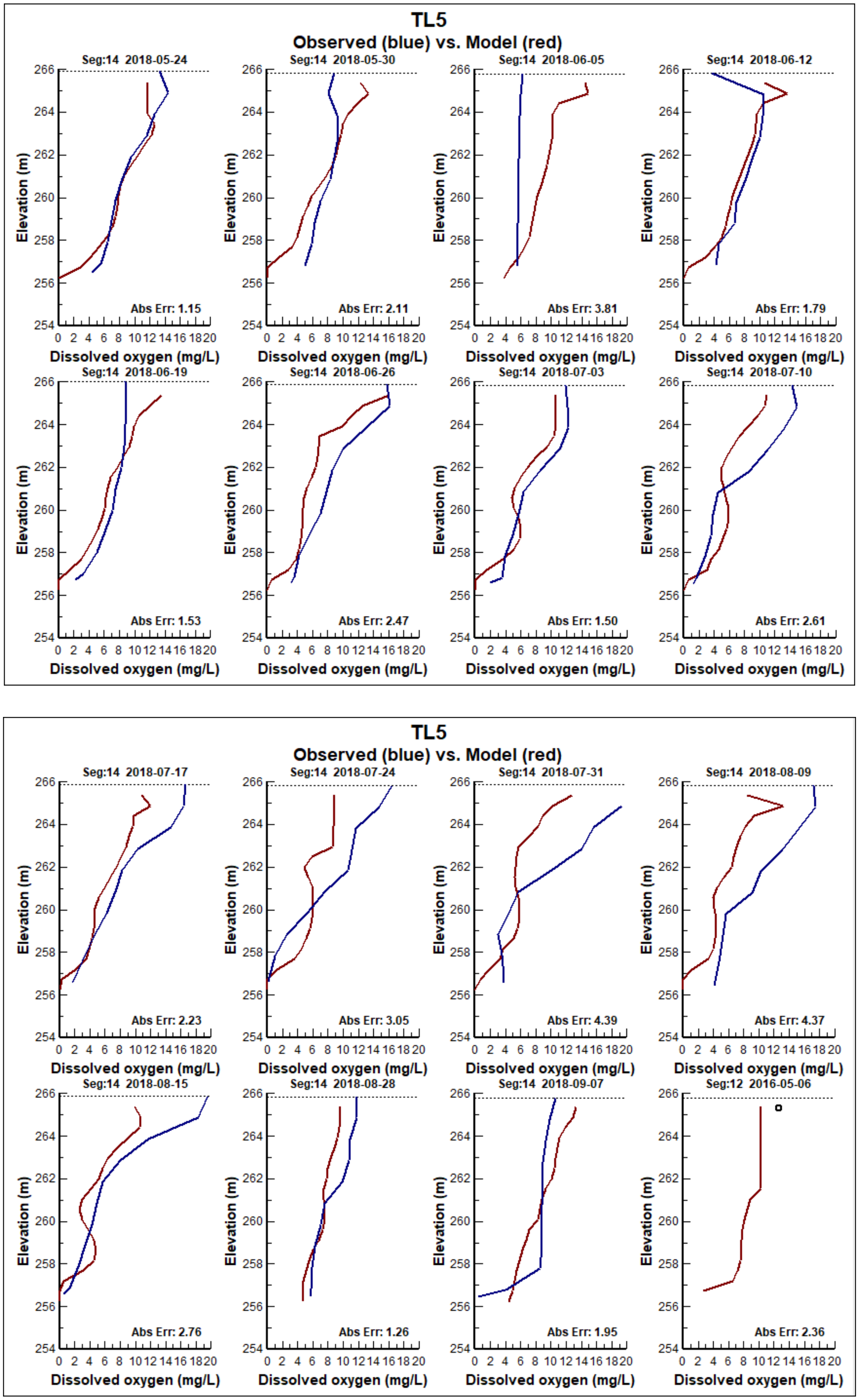

Figure 66. Observed (blue) vs model (red) dissolved oxygen profiles at TL5.Cont.

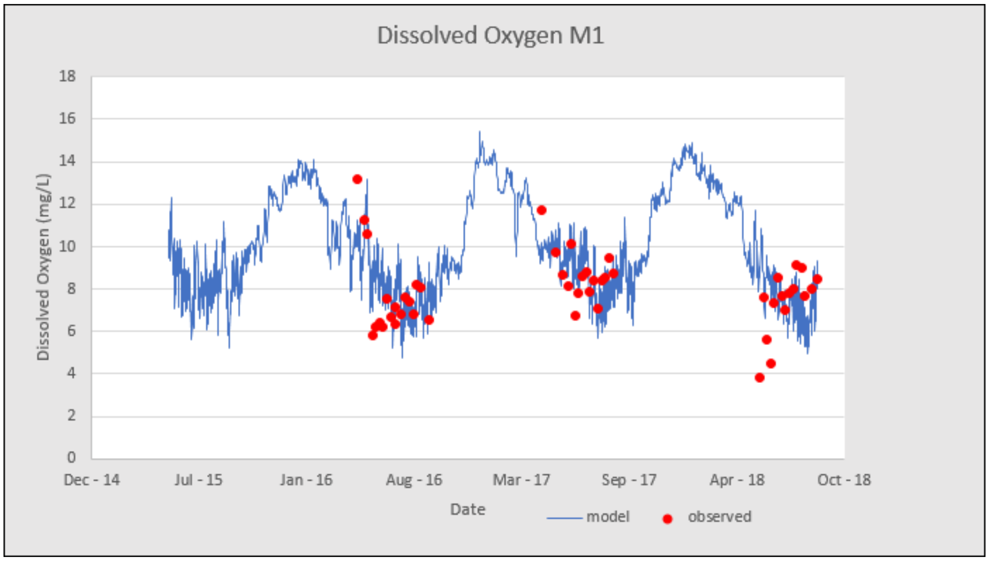

Figure 67. Observed (red) vs model (blue) dissolved oxygen at ML1 (1-m).

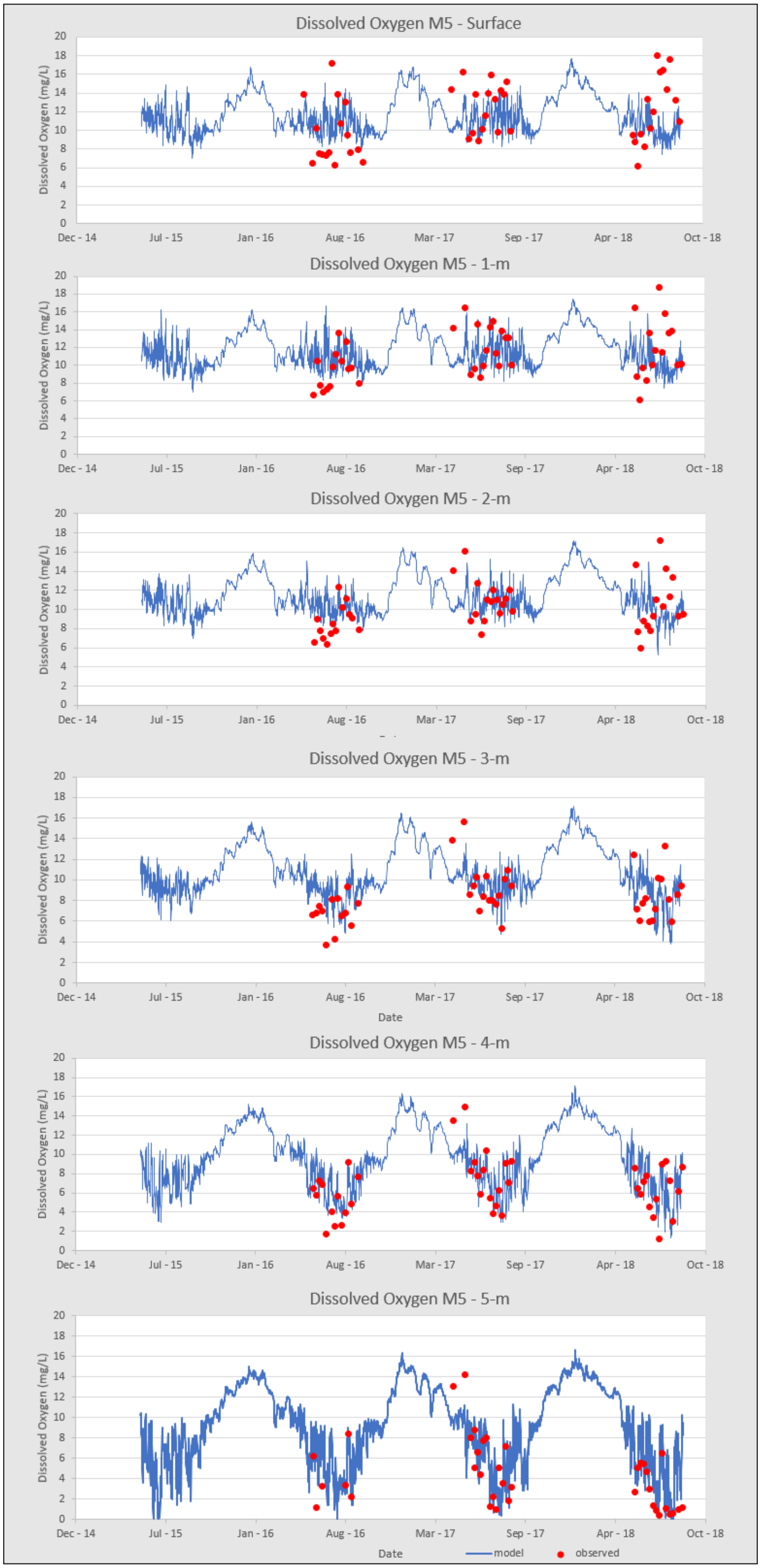

Figure 68. Observed (red) vs model (blue) dissolved oxygen at ML5.

5 Limitations

1) Additional observed data at a finer time interval would help validate the model calibration. Boundary conditions were estimated from several different methods, including loading calculations, temperature models and dissolved oxygen assumptions. In addition, discharge flows from the hydroelectric dams were not directly measured and discharge elevations were estimated between penstock and tainter gate sill elevations based on monthly maintenance records. Hourly inflow, temperature and water quality data plus better information on dam discharges for an additional summer would be ideal to verify the model calibration.

2) The model was calibrated using water years that were all above average for the basin based on the gaged period of records. Not having low flow conditions available during model calibration may make any conclusions drawn from loading scenarios during longer residence times less reliable.

3) Due to the lack of a direct linkage between organic matter loading and SOD and benthic nutrient flux, the model in its present stage is not suitable for predicatively evaluating the long-term impact of load reductions on SOD. However, due to the relatively short residence times normally seen on these two reservoirs, internal loading of nutrients is not considered a major factor in algal growth.

4) The water quality model is built based on a laterally averaged 2-D framework, therefore, the model is not capable of simulating the possible localized water quality change. However, it can be used to evaluate the overall consequence of watershed development or several “what if” scenarios.

6 Conclusions

A CE-QAUL-W2 model was developed for the Red Cedar River for Tainter Lake and Lake Menomin, two west central Wisconsin reservoirs that are very nutrient-rich and have frequent and severe nuisance algal blooms and low transparency. The focus of this calibration was to select reasonable coefficients that capture the major driving forces of cyanobacteria growth (e.g., nutrients, residence time, temperature) to allow for better prediction of reservoir responses to loading reducing scenarios that are needed to refine TMDL goals.

7 Acknowledgements

Special thanks to: Bill James at UW Stout for data collection and helping with model development, Zhonglong Zhang at USACE-ERDC for help estimating boundary conditions and model setup, Sean

Hartnett at UW Eau Claire for providing DEM data for Tainter Lake and Lake Menomin and Matthew Miller at Xcel Energy for providing structure, operational and water surface elevation data for the Cedar Falls and Menomonie hydroelectric power projects.

8 References

1) James WF. 2018. Limnological Conditions in Tainter and Menomin Reservoirs: Interim Report 2018
2) La Liberte P, Oldenburg P, Schreiber K, Voss K, Simonson D, Bartilson K, & Clayton N. 2012. Phosphorus Total Maximum Daily Loads (TMDLs) Tainter Lake and Lake Menomin Dunn County, Wisconsin – 31 May 2012. Wisconsin Department of Natural Resources. https://dnr.wi.gov/water/wsSWIMSDocument.ashx?documentSeqNo=73903997
3) Walker, William W. 1999 Simplified Procedures for Eutrophication Assessment and Prediction: User Manual Instruction Report W-96-2 USAE Waterways Experiment Station, Vicksburg, Mississippi (Revision of 1996 document) http://el.erdc.usace.army.mil/products.cfm?Topic=model&Type=watqual
4) Cole, T.M., Wells S.A. 2016. CE-QUAL-W2: A Two-Dimensional, Laterally Averaged, Hydrodynamic and Water Quality Model, Version 4.0, Department of Civil and Environmental Engineering, Portland State University, Portland, OR. http://www.cee.pdx.edu/w2/.
5) McIntyre, N. 2004. Analysis of uncertainty in river water quality modelling, PhD thesis, Department of Civil and Environmental Engineering, Imperial College London. http://www3.imperial.ac.uk/pls/portallive/docs/1/7253966.PDF (accessed 11 April 2019).
6) Gupta, H. V., Sorooshian, S., & Yapo, P. O. 1999. Status of automatic calibration for hydrologic models: Comparison with Multilevel Expert Calibration. Journal of Hydrologic Engineering, 4(2), 135−143.
7) Moriasi, D. N., Arnold, J. G., Van Liew, M. W., Bingner, R. L., Harmel, R. D., & Veith, T. L. 2007. Model evaluation guidelines for systematic quantification of accuracy in watershed simulations. Transactions of the ASABE, 50(3), 885−900.
8) Limnotech. 2016. CE-QUAL-W2 Lake Response Modeling of Petenwell and Castle Rock Reservoirs for the Wisconsin River TMDL.
9) Porter, D. W., Gibbs, B. P., Jones, W. F., Huyakom, P. S., Hamm, L. L., & Flash, C. P. 1999. Data fusion modeling for groundwater systems. J. Contam. Hydrol., 42, 303–335
10) AQUAVEO. 2015. Water modeling solutions (WMS) V10.1 User Manual www.aquaveo.com.
11) Edinger, J.E., Buchak E.M. 1975. A Hydrodynamic, Two-Dimensional Reservoir Model: The Computational Basis, prepared for US Army Engineer Division, Ohio River, Cincinnati, Ohio. [as cited in Cole and Wells 2003]
12) M. Miller, Fall 2018. Personal communication, Xcel Energy, Eau Claire, WI.
13) Washington State Department of Ecology. 2011. Response temperature: a simple model of water temperature. Greg Pelletier, Washington State Department of Ecology. Olympia, Washington. Retrieved from http://www.ecy.wa.gov/programs/eap/models.html
14) Edinger, J.E., Brady, D.K. and Geyer, J.C., 1974. Heat exchange and transport in the environment. EPRI publication no. 74-049-00-3, Electric Power Research Institute, Palo Alto, CA.

15) Walker, W.W., 1996. Simplified procedures for eutrophication assessment and prediction: User manual, Chapter 2 FLUX: U.S. Army Corp of Engineers, Water Operations Technical Support Program, Instruction report W-96-2, p. 2-1 to 2-61.
16) Weiss, R.F., 1970. The solubility of nitrogen, oxygen and argon in water and seawater: Deep-Sea Research, vol. 17, p. 721-735. (Also online at http://water.usgs.gov/owq/rfweiss.paper.pdf.)
17) Schindler, D.W. 1971. Food Quality and Zooplankton Nutrition, J. of Animal Ecology, Vol 40, pp 598-595.
18) Vollenweider, R.A. 1968. Scientific Fundamentals of the Eutrophication of Lakes and Flowing Waters, with Particular Reference to Nitrogen and Phosphorus as Factors in Eutrophication, Tech. Rept. OECD, DAS/CSI/68.27, Paris, France.
19) Myrbo A. (2012) Carbon Cycle in Lakes. In: Bengtsson L., Herschy R.W., Fairbridge R.W. (eds) Encyclopedia of Lakes and Reservoirs. Encyclopedia of Earth Sciences Series. Springer, Dordrecht.
20) U.S. Army Corps of Engineers. 1999, January. Water Quality Modeling of Lake Monroe Using CE-QUAL-W2. Miscellaneous Paper EL-99-1, 13.